Geometry Processing & Discrete Shells

Behrend Heeren

July 26, 2017

Contents

Preface These notes have been written to prepare the lecture course *Geometry Processing & Discrete Shells* which I taught at the Institute for Numerical Simulation, University of Bonn, in summer term 2017 . Sec. 0 and Sec. 1 are based on the geometry processing textbook by Mario Botsch *et al*. [BKP$^+$10]. Sec. 2 is related to the notation and curriculum of the elementary differential geometry textbook by Christian Bär [Bär00]. Large parts of Sec. 3 are based on the PhD thesis of Max Wardetzky [War06] whose main results have been published in [HPW06]. Furthermore, we briefly summerize the results by Cohen-Steiner and Morvan [CSM03] and introduce a triangle-averaged discrete shape operator [Hee11, HRWW12]. Sec. 4 starts with an introduction to $3D$ elasticity, as it can be found in several works by Philippe G. Ciarlet and coworkers, *cf*. *e.g*. [Cia88, Cia00, Cia05, CM08]; parts of this section are also based on the elasticity chapter in [Bra07a] and the section on bending problems in [Bar15]. Finally, the seminal papers on Γ-convergence for a membrane model [LDR95, LDR96] and for a bending model [FJM02a, FJM02b, FJMM03], respectively, are introduced to derive a dissimilarity measure between two shells. Sec. 5 then finally introduces the concept of shape spaces and in particular the variational time-discretization and geodesic calculus proposed by Rumpf and Wirth [WBRS09, RW13, RW15] as well as its applications on the space of discrete shells [HRWW12, HRS$^+$14, HRS$^+$16].
Many paragraphs and figures in this manuscript have been adopted from my PhD thesis [Hee16]. There is no guarantee for correctness, however, if you find any mistakes or typos please let me know.

Behrend Heeren, July 2017

0 Introduction

First, 3D acquisition technology, such as

- computer tomography,
- MRI,
- $3D$ laser scanning,
- ultrasound,
- radar,

enable higly accurate digitalization of complex (geometric) $3D$ objects.

Second, numerous (scientific) disciplines rely on analysis and processing of such geometric data, e.g.

- neuroscience / medicine
- mechanical engineering
- material sciences
- architecture
- geo-exploration and urban modeling
- entertainment (animation, computer games etc.)

e.g. to understand geometric structures and enable/facilitate new scientific discoveries.

Third, revolution in digital manufacturing technology (e.g. $3D$ printing), novel materials and robotic production will soon allow the automated creation of complex, fully functional physical objects from a digital design plan.

Geometry processing closes the gap between acquisition of raw geometric data and production based on geometric models. Here we focus on data describing the surface/boundary of compact three-dimensional solids, which are digitally represented as polygon meshes (e.g. triangle meshes).

Typical problems in *geometry processing* are for instance

- smoothing and filtering of data (e.g. removal of topological and geometric errors, noise removal)
- surface reconstruction and parametrization (to apply mesh-based algorithms)
- remeshing (to increase mesh quality)
- model repair (remove artefacts like holes)
- simplification and approximation (reduction of complexity)
- deformation, modeling and interactive design

The primal focus of this course is the mathematical foundation of *deformations and modeling tasks (animation)* of complex geometric objects represented as triangle meshes. In particular, we are interested in dynamics i.e. deformation paths and nontrivial motions. Hence we assume we are already given a nice triangulation (parametrization) without topological errors, geometrical noise or mesh artefacts. To enable efficient algorithms we build on state-of-the-art *simplification and approximation* techniques to design a *hierarchical/multiresolution method*.

The main focus of this course will be:

- local geometry: geometric quantities on a single discrete surface (i.e. triangle mesh), in particular the notion of discrete curvature, and a convergence analysis thereof
- physics: nonlinear deformations based on a physically sound thin shell model and a corresponding discrete analgon (discrete shells)
- global geometry and dynamics: deformation paths and navigation in the space of discrete shells which is considered as a Riemannian manifold

1 Surface representations

The common definition of a surface in the context of computer graphics applications is

"an orientable, compact, continuous $2D$ manifold embedded in $3D$, which might be closed or not".

Intuitively, a surface can be understood as the boundary (or part of the boundary) of a non-degenerate $3D$ solid. Here, non-degenerate means that the solid does not have any infinitesimal thin parts or features, such that the surface properly separates interior and exterior of the solid. We will give a precise mathematical definition later.

1.1 Implicit vs. explicit representations

There are two major classes of surface representations: explicit (or parametric) and implicit surfaces.

Parametric surfaces are defined by a vector-valued parametrization function

$$f : \Omega \subset \mathbb{R}^2 \to \mathbb{R}^3 \,,$$

that maps a two-dimensional domain $\Omega \subset \mathbb{R}^2$ to the surface

$$\mathcal{S} = f(\Omega) \,.$$

Implicit surfaces are defined as the zero-levelset of a scalar valued function

$$F : \mathbb{R}^3 \to \mathbb{R} \,,$$

such that

$$\mathcal{S} = \{x \in \mathbb{R}^3 \,:\, F(x) = 0\} \,.$$

Example (Torus, $0 < r < R$)

$$f(\theta, \phi) = \begin{pmatrix} (R + r\cos\theta)\cos\phi \\ (R + r\cos\theta)\sin\phi \\ r\sin\theta \end{pmatrix} \,, \quad (\theta, \phi) \in \Omega = [0, 2\pi)^2 \,,$$
$$F(x, y, z) = (x^2 + y^2 + z^2 + R^2 - r^2)^2 - 4R^2(x^2 + y^2) \,.$$

Note: For more complex shapes it is often necessary to split the domain into several patches (consistent/smooth transition has to be guaranteed, cf. definition of a manifold).

Regularity In most applications, the first step in generating a reasonable surface representation is to establish *continuity*. A parametric surface $\mathcal{S}$ (subject to the parametrization function f) is *locally manifold* at a point $p \in \mathcal{S}$ if there is $\epsilon > 0$ such that the pre-image of $B_\epsilon(p) \cap \mathcal{S}$ under f is an open ball in $\Omega \subset \mathbb{R}^2$. In other words, this means that (the neighbourhood of) p is *topologically equivalent (homeomorphic) to a disk* — the latter definition also applies to implicit surfaces.
Except for a well-defined set of sharp feature-curves and -corners, a surface should be smooth in general. Mathematically, this is measured by the the regularity of f resp. F, i.e. a surface is of class C^k if $f \in C^k(\Omega)$ resp. $F \in C^k(\mathbb{R}^3)$. In applications, one often requires an even stricter property than smoothness, namely *fairness*. Here not only the continuity of the derivatives is considered but also their magnitudes and variations. However, there is no rigorous definition of the aesthetic concept of fairness. Usually, a (discrete) surface is considered as fair if the curvature (or its variation) is globally minimized.

The two representations (i.e. parametric vs. implicit) have almost complementary strengths and weaknesses. These become obvious if we investigate the performance of typical geometric operations, e.g.

- evaluation, e.g. compute surface normals (e.g. for rendering)
- (spatial) queries, e.g. inside/outside or signed distance queries
- modification, e.g. of geometry or topology

Common criteria are usually *efficiency* and *robustness* of these operations.

Parametric surfaces

+ reduction of many $3D$ problems on the surface to $2D$ problems in the parameter domain
+ capture finest geometric details
+ easy to sample (e.g. sample points or normals for rendering)
+ efficient shape editing possible, e.g. by composition of $f : \Omega \to \mathbb{R}^3$ with some deformation $\phi : \mathbb{R}^3 \to \mathbb{R}^3$
- generating a parametric surface representation can be very complex, since the parameter domain has to match the topological and metric structure of the surface
- change of topology expensive (re-parametrization), since topology of parameter domain is equivalent to the topology of the surface (parametrization is continuous and injective!)
- inside/outside resp. signed distance queries are expensive
- detection of self-collision is hard

Implicit surfaces

+ no holes as long as F is continuous
+ no geometric self-intersections
+ as surface is zero-level isosurface, (signed) distance queries are easy to answer (e.g. inside/outside queries)
+ well-suited for construction of complex geometric objects (Boolean operations applied to geometric primitives)
- geometric detail resolution depends on voxel-size
- generate sample points, rendering and texture mapping etc. is relatively difficult
- surface modification and shape editing

In this course: parametric surfaces (due to applications considered here!)

1.2 Approximation power

A natural choice for parametrizing functions are polynomials, because they can be evaluated by elementary arithmetic operations. Furthermore, due to the Weierstrass Theorem, each smooth function can be approximated by a polynomial up to any desired precision (on a compact domain). From Taylor's theorem we know that a smooth function on a compact interval of length h can be approximated by a polynomial of degree p such that the approximation error behaves like $O(h^{p+1})$. As a consequence, there are two possibilities to improve the accurancy of the approximation: one can either raise the degree of the polynomial (p-refinement) or partition the domain in small patches, i.e. use more segments for the approximation (h-refinement).
In *Geometry Processing* applications one usually prefers h-refinement. With the today's computer architecture, processing a large number of of simple objects is often easier and more efficient that processing a smaller number of more complex objects. This leads to the somewhat extremal choice of C^0 piecewise linear surface representations, i.e. polygonal meshes, which have become the widely established standard in geometry processing.
Hence we consider $p = 1$ and $h \to 0$, i.e. we are dealing with an approximation power of $O(h^2)$ which is controlled by second-order information of the surface, i.e. curvature bounds.

1.3 Examples of parametric representations

Example 1 (Subdivision surfaces) Starting from a coarse *control mesh* $\mathcal{S}_0$ with vertices $c_1, \dots, c_n \in \mathbb{R}^3$, a sequence of meshes $\mathcal{S}_1, \mathcal{S}_2, \dots$ with growing complexity is generated by applying so-called subdivision rules.

Loop subdivision algorithm (for triangle meshes): For $n = 1, 2, \dots$:

- topological update: each triangle of $\mathcal{S}_{n-1}$ is divided into four congruent triangles by adding a new vertex on each edge midpoint of $\mathcal{S}_{n-1}$
- geometric update: compute new positions for all vertices in $\mathcal{S}_n$ by local average operations

Theorem: $\mathcal{S}_n$ converges to a surface $\mathcal{S}_\infty$ that is C^2 except for a finite set of points where it is C^1.

Furthermore, $\mathcal{S}_\infty$ can be parametrized over $\mathcal{S}_0$ by means of (cubic) spline functions $\phi_i : \Omega \subset \mathbb{R}^2 \to \mathbb{R}$, i.e.

$$f(u, v) = \sum_{i=1}^{n} c_i \phi_i(u, v) \,,$$

where $(u, v) \in \mathbb{R}^2$ are barycentric coordinates. Note, that the support of ϕ_i is the face 2-ring of the ith vertex. This representation allows for an intuitive control of the limit surface by picking and dragging the control points $c_i \in \mathbb{R}^3$. Hence subdivision surfaces (and related concepts) are popular for shape editing and Computer Aided Design (CAD) as it is used e.g. in vehicle manufacturing.

Adaptivity: each basis function $\phi_i = \phi_i^0$ on the control mesh $\mathcal{S}_0$ can be written as a linear combination of refined basis functions $\{\phi_j^k\}_j$ belonging to $\mathcal{S}_k$, $k > 0$. That means we have

$$\phi_i(u, v) = \sum_j \alpha_{ij}^k \phi_j^k(u, v)$$

with certain scalar weights α_{ij}^k. This inherent hierarchical structure allows for highly efficient algorithms.

However, subdivision techniques are restricted to meshes with so-called *semi-regular subdivision connectivity*, i.e. one has to assume that the given triangle mesh has been obtained by such a subdivision process. Furthermore, as the limit surface is smooth, the treatment of boundaries and feature creases is difficult.

Further references on subdivision surfaces: Course notes SIGGRAPH 2000 [SZ00]; subdivision FEM and simulations [COS00, CO01, CSA+02, DSB07, CL11, JMPR16]; implementation [Sta99, SZ00, BLZ00, GKS02]

Example 2 (Unstructured triangle meshes) In contrast to subdivision surfaces unstructured triangle meshes allow for arbitrary connectivities. Furthermore, geometric details, feature creases etc can be represented easily, hence unstructured meshes provide a higher flexibility and still allow for efficient surface processing.

A triangle mesh $\mathcal{M}_h$ consists of geometric and topological components, whereas the latter one can be represented by a graph structure, i.e. we have a set of vertices

$$\mathcal{V} = \{v_1, \dots, v_n\}$$

and a set of triangular faces

$$\mathcal{F} = \{f_1, \dots, f_m\} \subset \mathcal{V} \times \mathcal{V} \times \mathcal{V} \,.$$

Based on $\mathcal{V}$ and $\mathcal{F}$ one can deduce a set of edges

$$\mathcal{E} \subset \mathcal{V} \times \mathcal{V} \,.$$

The geometric embedding of a triangle mesh is given by a mapping

$$E : \mathcal{V} \to \mathbb{R}^3 \,, \quad E(v_i) = X_i \,.$$

An important topological quality of the mesh is whether or not it is a (discrete) 2-manifold. This is the case if it contains neither non-manifold edges nor non-manifold vertices nor self-intersections.
The famous *Euler formula* states an interesting relation between the number of vertice, faces and edges in a closed and connected (but otherwise unstructured) mesh:

$$\chi_{\mathcal{M}_h} := |\mathcal{V}| + |\mathcal{F}| - |\mathcal{E}| = 2(1-g)\,, \tag{1.1}$$

where g is here the genus of the surface (intuitively, the genus counts the number of handles of a surface). Since for most applications g is small, one can neglect the left hand side. Furthermore, as each edge is incident to two faces and each face has three edges, we have $3|\mathcal{F}| = 2|\mathcal{E}|$ and one can deduce the following mesh statistics:

- the number of triangles is twice the number of vertices, i.e. $|\mathcal{F}| \approx 2\,|\mathcal{V}|$,
- the number of edges is three times the number of vertices, i.e. $|\mathcal{E}| \approx 3\,|\mathcal{V}|$,
- the average vertex valence (number of incident edges) is 6.

In this course: unstructured meshes!

2 Differential geometry of parametric surfaces

In this chapter we gather basic properties of parametric surfaces $\mathcal{S} \subset \mathbb{R}^3$. For further reading we refer to [Bär00, dC76] (*cf*. also third chapter in [BKP+10]).

Definition 2.1. (Regular surface) The set $\mathcal{S} \subset \mathbb{R}^3$ is a *regular surface* if for each $p \in \mathcal{S}$ there is an $\epsilon > 0$, an open set $\Omega \subset \mathbb{R}^2$ and a smooth mapping $x : \Omega \to \mathbb{R}^3$, such that

(i) $x(\Omega) = \mathcal{S} \cap B_\epsilon(p)$ and $x : \Omega \to \mathcal{S} \cap B_\epsilon(p)$ is a homeomorphism.

(ii) The Jacobi matrix $D_\xi x \in \mathbb{R}^{3,2}$ has rank 2 for each $\xi \in \Omega$.

Remark: In the following we will assume that ϵ is large enough such that $\mathcal{S} \cap B_\epsilon(p) = \mathcal{S}$, *i.e*. there is a global *parametrization* $x : \Omega \to \mathcal{S}$.

Let us consider some $\xi = (\xi_1, \xi_2) \in \Omega$ and let $p = x(\xi) \in \mathcal{S}$. Then we define

$$T_p\mathcal{S} = \{\, \dot\gamma(0) \,|\, \gamma : (-1,1) \to \mathcal{S},\ \gamma(0) = p\} \,.$$

Note that by the same definition we have

$$T_\xi\Omega = \{\dot\alpha(0) \,|\, \alpha : (-1,1) \to \Omega,\ \alpha(0) = \xi\} = \mathbb{R}^2 \,.$$

If we consider $\alpha : (-1,1) \to \Omega$ with $\alpha(0) = \xi$ and $\gamma_\alpha := x \circ \alpha$ we have $\dot\gamma_\alpha(0) = Dx\dot\alpha(0)$ and get

$$T_p\mathcal{S} = Dx\, T_\xi\Omega = \operatorname{span}\{\partial_{\xi_1} x(\xi), \partial_{\xi_2} x(\xi)\} \,.$$

In the following, we will denote the tangent vectors

$$V_i = \partial_i x(\xi) = \partial_{\xi_i} x(\xi) = \frac{\partial x(\xi)}{\partial \xi_i} = Dx e_i, \quad i = 1, 2 \,,$$

as *canonical basis* of $T_p\mathcal{S}$, where $e_1, e_2 \in \mathbb{R}^2$ are the standard basis vectors of $\mathbb{R}^2$.

2.1 First and second fundamental forms

Definition 2.2 (First fundamental form)**.** The first fundamental form in $p \in \mathcal{S}$ is given by

$$g_p : T_p\mathcal{S} \times T_p\mathcal{S} \to \mathbb{R}, \quad g_p(U, V) := \langle U, V\rangle_{\mathbb{R}^3} \,.$$

After choosing a basis of $T_p\mathcal{S}$—here and in the following the canonical basis (V_1, V_2)—we can represent g_p by a symmetric, positive-definite matrix $g = g_\xi \in \mathbb{R}^{2,2}$ with

$$g_{ij} = g_p(V_i, V_j) = \langle V_i, V_j\rangle_{\mathbb{R}^3} \,, \tag{2.1}$$

i.e. we have $g = Dx^T Dx$. The pull-back of g_p to the parameter domain $\Omega \subset \mathbb{R}^2$ is defined as

$$g_\xi(u, v) = g_p(Dx\, u, Dx\, v) = u^T g v \,, \quad u, v \in T_\xi\Omega = \mathbb{R}^2 \,.$$

Geometrically, the first fundamental form is necessary to measure on the surface, *e.g*. to determine lengths of curves or angles between tangent vectors. Let $\gamma_\alpha = x \circ \alpha$ be as above, then the length of γ_α is defined as

$$\mathcal{L}[\gamma_\alpha] = \int_{-1}^{1} |\dot\gamma_\alpha(t)| \,\mathrm{d}t = \int_{-1}^{1} \sqrt{\langle Dx\dot\alpha(t), Dx\dot\alpha(t)\rangle_{\mathbb{R}^3}}\,\mathrm{d}t = \int_{-1}^{1} \sqrt{\langle Dx^T Dx\dot\alpha(t), \dot\alpha(t)\rangle_{\mathbb{R}^3}}\,\mathrm{d}t \,,$$

where we actually have $Dx = Dx(\alpha(t))$.

To simplify notation, we will often drop the index and write $g = g_p$ or $g = g_\xi$, respectively. In particular, g refers to the bilinear form as well as to its representative matrix in $\mathbb{R}^{2,2}$. Note that $g \in \mathbb{R}^{2,2}$ is invertible, since $\mathcal{S} \subset \mathbb{R}^3$ is assumed to be regular.

For some $A \subset \Omega$ and for some function $\varphi : \mathcal{S} \to \mathbb{R}$ we have

$$\int_{x(A)} \varphi \, \mathrm{d}a = \int_A (\varphi \circ x)(\xi) \sqrt{\det g_\xi} \, \mathrm{d}\xi \,,$$

and in particular for $\varphi \equiv 1$ we get

$$\mathrm{vol}(x(A)) = \int_A \sqrt{\det g_\xi} \, \mathrm{d}\xi \,.$$

Differentiation For a function $\varphi : \mathcal{S} \to \mathbb{R}$ we define the differential $d_p\varphi$ as a linear form acting on tangent vectors $V \in T_p\mathcal{S}$ as directional derivative, i.e.

$$d_p\varphi(V) := \frac{d}{dt}\varphi(\gamma(t))\Big|_{t=0}$$

for an arbitrary curve $\gamma : (-1, 1) \to \mathcal{S}$ with $\gamma(0) = p$ and $\dot\gamma(0) = V$. For a vector-valued deformation $\phi : \mathcal{S} \to \mathbb{R}^3$ the definition above holds for each component of $\phi = (\phi_1, \phi_2, \phi_3)$. In particular, $d_p\phi$ defines a linear map between the tangent spaces, i.e.

$$d_p\phi : T_p\mathcal{S} \to T_{\phi(p)}\phi(\mathcal{S}) \,.$$

Definition 2.3 (Normal field)**.** Let $S^2 \subset \mathbb{R}^3$ be the 2-dimensional unit sphere. The (unit) normal field of $\mathcal{S}$ is a mapping $n : \mathcal{S} \to S^2$ with $n(p) \perp T_p\mathcal{S}$ for all $p \in \mathcal{S}$. We say that $\mathcal{S}$ is orientable if there is a continuous normal field. In particular, as $\mathrm{rank}(Dx) = 2$, we will write

$$n(p) = (n \circ x)(\xi) = \frac{x_{,1} \times x_{,2}}{|x_{,1} \times x_{,2}|}(\xi) \,.$$

Definition 2.4. (Shape operator) Let $\mathcal{S} \subset \mathbb{R}^3$ be regular and orientable, $p \in \mathcal{S}$. The shape operator $S_p : T_p\mathcal{S} \to T_p\mathcal{S}$ at p is the linear mapping defined via $S_p(U) = d_p n(U)$ for $U \in T_p\mathcal{S}$.

Remark: As $T_{n(p)}S^2 = n(p)^\perp = T_p\mathcal{S}$ the shape operator S_p is indeed an endomorphism on $T_p\mathcal{S}$.

Definition 2.5. (Second fundamental form) Let $\mathcal{S} \subset \mathbb{R}^3$ be regular and orientable, $p \in \mathcal{S}$. The second fundamental form $h = h_p$ is the bilinear form on $T_p\mathcal{S}$ associated with S_p, *i.e.*

$$h_p(U, V) := g_p(S_pU, V) \,, \quad U, V \in T_p\mathcal{S} \,.$$

The corresponding matrix representation $h = h_\xi \in \mathbb{R}^{2,2}$ is given by

$$h_{ij} = h_p(V_i, V_j) = g_p(S_pV_i, V_j) = \langle d_p n \, \partial_i x, \partial_j x\rangle_{\mathbb{R}^3} = \langle \partial_i(n \circ x), \partial_j x\rangle_{\mathbb{R}^3} \,. \tag{2.2}$$

Note that since $n(p) \perp T_p\mathcal{S}$ we have

$$0 = \partial_{\xi_i}\Big(g_p(n \circ x, \partial_j x)\Big) = g_p\left(\partial_i(n \circ x), \partial_j x\right) + g_p\left((n \circ x), \partial_i\partial_j x\right) = h_p(V_i, V_j) + g_p\left((n \circ x), \partial^2_{ij} x\right) \,,$$

hence $h \in \mathbb{R}^{2,2}$ is symmetric and we have

$$h_{ij} = -\langle n \circ x, \partial^2_{ij} x\rangle_{\mathbb{R}^3} \,.$$

Finally, we can represent the (symmetric) matrix $h \in \mathbb{R}^{2,2}$ by

$$h = Dn^T Dx \,, \quad Dn = \left[\frac{\partial n(p)}{\partial \xi_1}, \frac{\partial n(p)}{\partial \xi_2}\right] \in \mathbb{R}^{3,2} \,.$$

If we write S_p in the canonical basis (V_1, V_2), *i.e.*

$$S_pV_i = \sum_{k=1}^{2} s_{ki} V_k$$

for $i = 1, 2$, the coefficient matrix $s = s_\xi \in \mathbb{R}^{2,2}$ is the representation of S_p in the parameter domain. Since

$$h_{ij} = g_p(S_p V_i,\, V_j) = g_p\Big(\sum_{k=1}^{2} s_{ki} V_k,\; V_j\Big) = \sum_{k=1}^{2} s_{ki}\; g_p\Big(V_k, V_j\Big) = \sum_{k=1}^{2} s_{ki} g_{kj},$$

we get $h = s^T g$, i.e. due to the symmetry of g and h we have

$$s_\xi = g_\xi^{-1} h_\xi \,. \tag{2.3}$$

Remark on notation: S_p denotes either the endomorphism on $T_p\mathcal{S}$ or the corresponding matrix $S_p \in \mathbb{R}^{3,3}$, whereas $s \in \mathbb{R}^{2,2}$ denotes the matrix representation of S_p in the canonical basis.

Since g and h are symmetric forms on $T_p\mathcal{S}$ we get for $U, V \in T_p\mathcal{S}$

$$g_p(S_p U, V) = h_p(U, V) = h_p(V, U) = g_p(S_p V, U) = g_p(U, S_p V)\,,$$

which means that S_p is symmetric with respect to the metric. Hence S_p and thus s_ξ diagonalize in an orthonormal basis.

Definition 2.6. (Curvatures) The eigenvalues κ_1, κ_2 of s_ξ are denoted as principal curvatures of $\mathcal{S}$ in $p = x(\xi)$. The mean curvature in p is defined as the sum $H_p = \operatorname{tr} s_\xi = \kappa_1 + \kappa_2$ and the Gaussian curvature in p as the product $K_p = \det s_\xi = \kappa_1 \cdot \kappa_2$.

Note that $\det S_p = 0$ since there is no normal variation in normal direction, hence the eigenvalues of S_p are given by $0, \kappa_1, \kappa_2$.

The *normal curvature* of $p \in \mathcal{S}$ in some direction $U \in T_p\mathcal{S}$ is defined as

$$\kappa_p(U) = \frac{h_p(U, U)}{g_p(U, U)}\,.$$

Intuitively, $\kappa_p(U)$ describes the curvature of a curve $\gamma : I \subset (-1, 1) \to \mathcal{S}$ with $\gamma(0) = p$ and $\gamma(I) = \mathcal{S} \cap (T_p\mathcal{S})^\perp$ at $t = 0$. If one obeys the ordering convention $\kappa_1 \le \kappa_2$, one can show that

$$\kappa_1 = \min_{U \in T_p\mathcal{S}} \kappa_p(U)\,, \quad \kappa_2 = \max_{U \in T_p\mathcal{S}} \kappa_p(U)\,.$$

2.2 The relative shape operator

Later, we aim at measuring differences between two (discrete) surfaces up to rigid body motions. That means, if $\mathcal{S} \subset \mathbb{R}^3$ is a parametric surface and $\phi : \mathcal{S} \to \mathbb{R}^3$ is a deformation, we aim at quantifying the *dissimilarity* of $\mathcal{S}$ and $\tilde{\mathcal{S}} := \phi(\mathcal{S})$ up to rigid body motions.

Theorem 2.7 (The Fundamental Theorem of Surfaces)**.** *Congruent parametric surfaces in $\mathbb{R}^3$ have the same first and second fundamental forms. Conversely, two parametric surfaces in $\mathbb{R}^3$ with the same first and second fundamental forms are congruent.*

Hence the theorem above suggests to measure differences of first fundamental forms g and $\tilde{g}$ as well as second fundamental forms h and $\tilde{h}$ of $\mathcal{S}$ and $\tilde{\mathcal{S}}$, respectively. First, it is easy to see that $g = \tilde{g}$ if $D\phi^T D\phi = \mathbb{1}$. Indeed, if $x : \Omega \to \mathbb{R}^3$ is a parametrization of $\mathcal{S}$ then $\tilde{x} = \phi \circ x$ is a parametrization of $\tilde{\mathcal{S}}$, and hence $\tilde{g} = D\tilde{x}^T D\tilde{x} = Dx^T D\phi^T D\phi Dx$. Second, since the shape operator represents the second fundamental form in the metric, one often penalizes deviations in the shape operator. Furthermore, if $g = \tilde{g}$ then $h = \tilde{h}$ iff. $s = \tilde{s}$, cf. (2.3). In the most general setup one aims at comparing the embedded shape operators $S_p : T_p\mathcal{S} \to T_p\mathcal{S}$ and $\tilde{S}_{\tilde{p}} : T_{\tilde{p}}\tilde{\mathcal{S}} \to T_{\tilde{p}}\tilde{\mathcal{S}}$, for an arbitrary point $p \in \mathcal{S}$ and $\tilde{p} = \phi(p)$. However, since these operators live on different tangent spaces one defines:

Definition 2.8. (Pulled-back shape operator) The pulled-back shape operator $S_p^*[\phi] : T_p\mathcal{S} \to T_p\mathcal{S}$ is given by

$$g_p\left(S_p^*[\phi]U,\, V\right) = h_{\phi(p)}\left(D\phi U,\, D\phi V\right)\,, \quad \forall U, V \in T_p\mathcal{S}\,. \tag{2.4}$$

Definition 2.9. (Relative shape operator) The *relative shape operator* $S_p^{\text{rel}}[\phi]$ is defined as the pointwise difference, *i.e.*

$$S_p^{\text{rel}}[\phi] : T_p\mathcal{S} \to T_p\mathcal{S}\,, \quad S_p^{\text{rel}}[\phi] := S_p - S_p^*[\phi]\,. \tag{2.5}$$

The matrix representations $s_\xi^*[\phi] \in \mathbb{R}^{2,2}$ and $s_\xi^{\text{rel}}[\phi] \in \mathbb{R}^{2,2}$ of $S_p^*[\phi]$ and $S_p^{\text{rel}}[\phi]$, respectively, are given by

$$s_\xi^*[\phi] = g_\xi^{-1}\tilde{h}_\xi\,, \quad s_\xi^{\text{rel}}[\phi] = s_\xi - s_\xi^*[\phi] = g_\xi^{-1}(h_\xi - \tilde{h}_\xi)\,. \tag{2.6}$$

Remark: The fundamental theorem of surfaces provides a *geometric* argument why to measure differences in first and second fundamental forms. Later, we will also consider a *physical* justification.

2.3 Differential operators

For a (differentiable) function $f : \Omega \subset \mathbb{R}^d \to \mathbb{R}$, the gradient is defined by

$$\langle \nabla f(x), W\rangle_{\mathbb{R}^d} = \frac{d}{dt} f(x+tW)\Big|_{t=0} \quad \forall W \in T_x\Omega = \mathbb{R}^d\,.$$

Now consider a function $f : \mathcal{S} \subset \mathbb{R}^3 \to \mathbb{R}$. For a $p = x(\xi)$ we have $\nabla_{\mathcal{S}} f(p) \in T_p\mathcal{S}$. If we represent $\nabla_{\mathcal{S}} f$ in the canonical basis, i.e. $\nabla_{\mathcal{S}} f(p) = \sum_i v_i V_i = Dxv$ for some $v = v_f \in \mathbb{R}^2$, we have the implicit definition

$$g_\xi(v,w) = \frac{d}{dt}\tilde{f}(\xi+tw)\Big|_{t=0} = \langle \nabla\tilde{f}(\xi),\, w\rangle_{\mathbb{R}^2} \quad \forall w \in T_\xi\Omega\,.$$

where we used the notation $\tilde{f} = f \circ x : \Omega \subset \mathbb{R}^2 \to \mathbb{R}$. Hence we have $v = v_f = g_\xi^{-1}\nabla\tilde{f}$ and hence

$$\nabla_{\mathcal{S}} f = Dx\, g^{-1}\nabla(f\circ x)\,. \tag{2.7}$$

For a (differentiable) vector field $w : \Omega \subset \mathbb{R}^d \to \mathbb{R}^d$, the divergence $\operatorname{div} w$ fulfills

$$\int_\Omega \operatorname{div} w \cdot \varphi \,\mathrm{d}x = -\int_\Omega \langle w, \nabla\varphi\rangle_{\mathbb{R}^d}\,\mathrm{d}x \quad \forall \varphi \in C_0^\infty(\Omega)\,.$$

Now we consider a vector field w on $\mathcal{S}$. As ussual, $w(p) \in \mathbb{R}^2$ represents the coefficients w.r.t. the canonical basis, *i.e.* the embedded vector field is given by $p \mapsto \sum_{i=1}^2 w_i(p)V_i(p)$ with $\sum_{i=1}^2 w_i(p)V_i(p) \in T_p\mathcal{S}$. Analogously, we consider $\tilde{w} = w \circ x$ as being a vector field on Ω. Let $\varphi \in C_0^\infty(\mathcal{S})$ such that $\tilde{\varphi} = \varphi \circ x \in C_0^\infty(\Omega)$ and $v_{\tilde{\varphi}} = g^{-1}\nabla\tilde{\varphi} \in T_\xi\Omega$. Then

$$\int_\Omega \operatorname{div}_{\mathcal{S}}\tilde{w}\cdot\tilde{\varphi}\sqrt{\det g_\xi}\,\mathrm{d}\xi := -\int_\Omega g_\xi(\tilde{w}, v_{\tilde{\varphi}})\sqrt{\det g_\xi}\,\mathrm{d}\xi = -\int_\Omega \langle \tilde{w}, \nabla\tilde{\varphi}\rangle_{\mathbb{R}^2}\sqrt{\det g_\xi}\,\mathrm{d}\xi = \int_\Omega \operatorname{div}\big(\sqrt{\det g_\xi}\tilde{w}\big)\cdot\tilde{\varphi}\,\mathrm{d}\xi\,,$$

where we have used integration by parts in the last step. Since this is supposed to hold for all test functions we get

$$(\operatorname{div}_{\mathcal{S}} w)\circ x = \frac{1}{\sqrt{\det g}}\operatorname{div}\Big(\sqrt{\det g}\,(w\circ x)\Big) = \frac{1}{\sqrt{\det g}}\sum_{i=1}^2 \partial_{\xi_i}\Big(\sqrt{\det g_\xi}\,(w\circ x)(\xi)\Big)\,.$$

Definition 2.10. (Laplace-Beltrami operator) For some function $f : \mathcal{S} \to \mathbb{R}$, the *Laplace-Beltrami operator* is given by $\Delta_{\mathcal{S}} f = \operatorname{div}_{\mathcal{S}}\nabla_{\mathcal{S}} f$, i.e.

$$(\Delta_{\mathcal{S}} f)\circ x = \frac{1}{\sqrt{\det g}}\sum_{i=1}^2 \partial_{\xi_i}\Big(\sqrt{\det g_\xi}\sum_{j=1}^2 g^{ij}\partial_{\xi_j}(f\circ x)(\xi)\Big)\,,$$

where we have used the notation $\sum_j g_{ij}g^{jk} = \delta_{ik}$.

Theorem 2.11. *Let* $\mathrm{id} : \mathcal{S} \to \mathbb{R}^3$ *the identity mapping (or the embedding), i.e.* $\mathrm{id}(p) = p$ *for all* $p \in \mathcal{S}$*, then we have*

$$(\Delta_{\mathcal{S}}\mathrm{id})(p) = -H(p)\,n(p)\,, \tag{2.8}$$

where $H(p) \in \mathbb{R}$ *is the mean curvature in* p*.*

2.4 Intrinsic vs. extrinsic surface quantities

Definition 2.12. (Isometric surfaces) A differentiable mapping $\phi : \mathcal{S} \to \tilde{\mathcal{S}}$ between two surfaces $\mathcal{S} \subset \mathbb{R}^3$ and $\tilde{\mathcal{S}} \subset \mathbb{R}^3$ is a local isometry, if for each $p \in \mathcal{S}$ the differential $d_p\phi : T_p\mathcal{S} \to T_{\phi(p)}\tilde{\mathcal{S}}$ is a linear isometry with respect to the first fundamental forms, i.e.

$$g_p(V, W) = \tilde{g}_{\phi(p)}\Big(d_p\phi(V),\, d_p\phi(W)\Big) \quad \forall V, V \in T_p\mathcal{S}\,.$$

If a local isometry $\phi : \mathcal{S} \to \tilde{\mathcal{S}}$ is bijective we say that ϕ is an *isometry*. If there is an isometry $\phi : \mathcal{S} \to \tilde{\mathcal{S}}$, then the two surfaces $\mathcal{S}, \tilde{\mathcal{S}}$ are said to be *isometric*.

A quantity of a surface, *e.g.* some function $f_{\mathcal{S}} : \mathcal{S} \to \mathbb{R}$, is said to be *intrinsic*, if it is not distorted under local isometries, *i.e.* we have $f_{\mathcal{S}} = f_{\tilde{\mathcal{S}}} \circ \phi$ for every local isometry $\phi : \mathcal{S} \to \tilde{\mathcal{S}}$. Otherwise, a surface quantity is said to be *extrinsic*.

Remark: An intrinsic quantity only depends on the first fundamental form.

Obviously, the first fundamental form is intrinsic, as well as the Laplace-Beltrami operator. However, mean curvature (and thus also the principle curvatures) is an *extrinsic* quantity, as, for example, $H \equiv 0$ for the plane but $H \equiv 1$ for the cylinder, whereas plane and cylinder are locally isometric. Likewise, the second fundamental form as well as the shape operator are also extrinsic quantities. However, the Gaussian curvature is *not* extrinsic:

Theorem 2.13 (Theorema egregium (Gauss))**.** *The Gaussian curvature is an intrinsic invariant of a surface.*

This implies that the sphere cannot be unfolded onto a flat plane without distorting the distances, i.e. a sphere and a plane are not isometric, even locally. This fact is of enormous significance for cartography: it implies that no planar (flat) map of Earth can be perfect, even for a portion of the Earth's surface.

Later, we want to quantify distortions induced by isometric deformations. The results above imply that this can be done by measuring differences in shape operators (in a suitable matrix norm) or, even simpler, differences in mean curvature. On the other hand, measuring differences in Gaussian curvature does not make sense due to Gauss' theorem. Hence a particular focus will be on deriving a discrete notion of mean curvature whereas the discrete notion of Gaussian curvature is less important.

Nevertheless, an important property of Gaussian curvature of an surface is the relation to its topology as stated in the Gauss-Bonnet theorem:

Theorem 2.14 (Theorem of Gauss-Bonnet)**.** *For a compact, orientable, closed surface $\mathcal{S} \subset \mathbb{R}^3$ we have*

$$\int_{\mathcal{S}} K \,\mathrm{d}a = 2\pi \cdot \chi_{\mathcal{S}}\,,$$

where the Euler-characteristic $\chi_{\mathcal{S}} \in \mathbb{N}$ is given as $\chi_{\mathcal{S}} = 2(1-g)$, where g denotes the genus of the surface here.

Since $\mathcal{S}$ can be approximated to arbitrary precision by some triangle mesh $\mathcal{M}_h = (\mathcal{V}, \mathcal{F}, \mathcal{E})$, the Euler formula (1.1) implies

$$\int_{\mathcal{S}} K \,\mathrm{d}a = 2\pi\,(\,|\mathcal{V}| + |\mathcal{F}| - |\mathcal{E}|\,)\,. \tag{2.9}$$

We will see that a fundamental (even defining) property in the derivation of a discrete Gaussian curvature is that this theorem holds on discrete surfaces as well.

3 Discrete Differential Geometry

Differential and geometric quantities defined on a surface require the surface to be sufficiently smooth, e.g. the definition of curvatures requires the existence of second derivatives. Since polygonal meshes are piecewise affine and globally only of class C^0, many of the concepts presented in Sec. 2 can not be applied directly. However, usually a discrete surface (i.e. a polygonal mesh) is assumed to be an approximation of a smooth surface. Hence one aims to compute approximations of differential and geometric properties of the smooth surface directly from the mesh data. This leads to the derivation of discrete equivalents of the geometric notions of classical differential geometry. In particular, the study of the discrete equivalents themselves defines a new and active mathematical field, namely *Discrete Differetial Geometry (DDG)*.

Discrete differential geometry aims to develop discrete equivalents of the geometric notions and methods of classical differential geometry. [...] It can be said to have arisen from the observation that when a notion from smooth geometry (such as the notion of a minimal surface) is discretized properly, the discrete objects are not merely approximations of the smooth ones, but have special properties of their own which make them form in some sense a coherent entity by themselves. [...] The discrete theory would seem to be the more fundamental one: The smooth theory can always be recovered as a limit, while there seems to be no natural way to predict from the smooth theory which discretizations will have the nicest properties. Oberwolfach report 2006

The behavior of physical systems is typically described by a set of continuous equations using tools such as geometric mechanics and differential geometry to analyze and capture their properties. For purposes of computation one must derive discrete (in space and time) representations of the underlying equations. Researchers in a variety of areas have discovered that theories, which are discrete from the start, and have key geometric properties built into their discrete description can often more readily yield robust numerical simulations which are true to the underlying continuous systems: they exactly preserve invariants of the continuous systems in the discrete computational realm. Such theories make up the nascent field of discrete differential geometry Discrete Differential Geometry: An Applied Introduction [DGSW08]

Guiding principles of DDG:

- **Weak/integrated notions** Higher order quantities, such as curvatures, are defined in an integrated or weak sense *e.g.* a discrete Laplace-Beltrami operator is defined as an element in H^{-1}. In particular, on general meshes convergence is mostly shown in a weak or integrated sense, *e.g.* in H^{-1}.
- **Spatial averaging** To get a pointwise evaluation, e.g. at a vertex, one computes the integrated quantity in a neighbourhood of that vertex and divides by the associated area (cf. [MDSB02])
- **Attach quantities to appropriate locations**, i.e. associate physical/geometric quantities at their natural locations, not necessarily at vertices. Here the field of Discrete Exterior Calculus (DEC) is an appropiate tool (not considered here, cf. [DKT08, Hir03, DHLM05]).
- **Discretize theory, not equations!** That means, one aims at a consistent discrete theory. To ensure the existence of fundamental properties (e.g. Gauss-Bonnet), one often uses *top-down* instead of *bottom-up* approaches, e.g. one directly defines a notion of discrete curvature without having a notion of a discrete normal field in the first place.

3.1 Basic notions

As mentioned above, a triangular mesh is uniquely determined by its *geometry* and its *connectivity*. The geometry is described by the embedding $E : \mathcal{V} \to \mathbb{R}^3$, *i.e.* the coordinates of the vertices, and the connectivity is encoded in the set of faces $\mathcal{F} \subset \mathcal{V} \times \mathcal{V} \times \mathcal{V}$ or equivalently in the set of edges $\mathcal{E} \subset \mathcal{V} \times \mathcal{V}$. Note that all further structural properties of the mesh, such as neighbouring relationships, boundary etc., can be derived from $\mathcal{F}$ or $\mathcal{E}$, respectively.

Geometry. If $n \in \mathbb{N}$ denotes the number of vertices in the mesh, we often identify a vertex $X_i = E(v_i)$ with $v_i \in \mathcal{V}$ or with its global index $i \in \{1, \dots, n\}$. Likewise, if $m \in \mathbb{N}$ denotes the number of faces in the mesh, we often identify a face $f_j \in \mathcal{F}$ with its global index $j \in \{1, \dots, m\}$. Moreover, we might represent a face $f = (i_0, i_1, i_2)$ by its embedded triangle $T = T(f)$, i.e.

$$T = T(f) = (E(v_{i_0}),\, E(v_{i_1}),\, E(v_{i_2})) = (X_{i_0},\, X_{i_1},\, X_{i_2}) \quad \subset \mathbb{R}^3 \,. \tag{3.1}$$

Besides its global index $i \in \{1, \dots, n\}$, each vertex $X = X_i$ belongs to at least one face f, hence it has an additional local index $j \in \{0, 1, 2\}$ with respect to f. That means, we sometimes rewrite (3.1) as

$$T = T(f) = \Big(X_0(f), X_1(f), X_2(f)\Big) \quad \subset \mathbb{R}^3 \,. \tag{3.2}$$

Analogously, each edge E of a mesh belongs to at least one face and hence it also has a local index $j \in \{0, 1, 2\}$ with respect to f, *i.e.* $E = E_j(f)$. Moreover, we make use of the convention that an edge with local index j (wrt. face f) connects the nodes with local indices $j - 1$ and $j + 1$ (wrt. face f), where the notation is modulo 3, *i.e.*

$$E_j = X_{j-1} - X_{j+1} \,, \quad j \in \{0, 1, 2\} \bmod 3 \,.$$

That means E_j is opposite X_j in face f, if j is the local index wrt. face f. In the following, it will be clear from the context if we are referring to the global or local index of a vertex or edge, respectively.

Topology. We assume that each mesh is a *two-dimensional discrete manifold*, or (discrete) 2-manifold, in the sense of [DKT08]. This is the case if it contains neither non-manifold edges nor non-manifold vertices nor self-intersections. That means for example, that any pair of triangles either shares one edge or one node or that their intersection is empty. In particular, we do not allow for hanging nodes, *i.e.* nodes that do not belong to any face, or degenerated faces, *i.e.* faces with less than three different nodes.

Orientation. The order of the local indices of nodes within one face determines the orientation of the face and hence of the mesh. Since we only consider (approximations of) orientable surfaces we assume that all local indices are ordered consistently.

Definition 3.1 (Discrete surface)**.** A *discrete surface* is a triangular mesh $\mathcal{M}_h = (\mathcal{V}, \mathcal{F}, \mathcal{E})$ along with an injective embedding $E : \mathcal{V} \to \mathbb{R}^3$, such that $\mathcal{M}_h$ is a discrete 2-manifold which is orientable (*i.e.* has consistent local index ordering).

Remark: A discrete surface is entirely described by the pairing $\mathcal{M}_h = (E(\mathcal{V}), \mathcal{F})$, where $E(\mathcal{V}) \in \mathbb{R}^{3n}$.

Parametrization. We assume that each discrete surface $\mathcal{M}_h$ is parametrized over a reference or parameter domain Ω_h. Yet different from the continuous setting this reference domain is not a connected subset of $\mathbb{R}^2$ but rather an abstract collection of multiple reference triangles as it is often used in the context of subdivision surfaces (*cf.* [Rei95]). Thus each face $f \in \mathcal{F}$ of $\mathcal{M}_h$, with the corresponding embedded/geometric triangle $T = T(f)$ as in (3.1) resp. (3.2) is parametrized over a reference triangle given by the *unit triangle*

$$\omega := (\begin{pmatrix} 0 \\ 0 \end{pmatrix}, \begin{pmatrix} 1 \\ 0 \end{pmatrix}, \begin{pmatrix} 0 \\ 1 \end{pmatrix}) \subset \mathbb{R}^2$$

via an affine mapping $X_f : \omega \to T$, which is defined by

$$X_f(\xi) := X_f(\xi_1, \xi_2) := \xi_1 X_1(f) + \xi_2 X_2(f) + (1 - \xi_1 - \xi_2) X_0(f) \tag{3.3}$$

for the barycentric coordinates $\xi \in \omega$, *i.e.* $\xi = (\xi_1, \xi_2)$ with $0 \le \xi_1, \xi_2 \le 1$ and $\xi_1 + \xi_2 \le 1$. Formally, the reference domain is given by $\Omega_h = \omega \times \mathcal{F}$, a global parametrization via $X : (\xi, i) \mapsto X_{f_i}(\xi)$. Wherever it is possible, we drop the dependence of the local parametrization X on the face f_j in the following and write $X = X_{f_j}$.

Discrete first fundamental form. Let $\mathcal{S} \subset \mathbb{R}^3$ be a regular embedded surface with (local) parametrization $x : \Omega \to \mathcal{S}$ and $\xi \in \Omega$. Following Def. 2.2 resp. (2.1) we can represent the first fundamental form g at some point $x(\xi)$ by the matrix $g_\xi = Dx(\xi)^T Dx(\xi)$. According to (3.3), the local parametrization X of a a discrete surface $\mathcal{M}_h$ is affine, hence its derivative is constant on each triangle $f \in \mathcal{M}_h$, *i.e.*

$$DX|_f = \left(\frac{\partial X_f}{\partial \xi_1}, \frac{\partial X_f}{\partial \xi_2}\right) = \Big[X_1(f) - X_0(f) \,\Big|\, X_2(f) - X_0(f)\Big] = \Big[E_2(f) \,\Big|\, -E_1(f)\Big] \in \mathbb{R}^{3,2} \,. \tag{3.4}$$

Hence the definition of an elementwise constant discrete first fundamental form follows canonically:

$$G_f = (DX|_f)^T DX|_f \in \mathbb{R}^{2,2} \,, \quad f \in \mathcal{F} \,. \tag{3.5}$$

To simplify notation we will often drop the dependence on f and write $G = G_f$. Note that $\det G_f = 0$ iff. f has parallel edges, which is not admissible due to the assumption that $\mathcal{M}_h$ is a discrete 2-manifold. Hence G_f is invertible for each $f \in \mathcal{F}$. Furthermore, we get the following formula for the area $a_f = |T|$ of an embedded triangle:

$$a_f = \int_T \mathrm{d}a = \int_\omega \sqrt{\det G_f}\,\mathrm{d}\xi = \frac{1}{2}\sqrt{\det G_f}\,. \tag{3.6}$$

3.2 Discrete Laplace-Beltrami operator

Definition 3.2 (Weak derivatives)**.** Let $\mathcal{S} \subset \mathbb{R}^3$ a regular surface. Then $u : \mathcal{S} \to \mathbb{R}$ has a weak surface gradient—also denoted by $\nabla_{\mathcal{S}} u$—if

$$\int_{\mathcal{S}} g(\nabla_{\mathcal{S}} u, V)\,\mathrm{d}a = -\int_{\mathcal{S}} \mathrm{div}_{\mathcal{S}} V \cdot u\,\mathrm{d}a\,, \quad \forall\, V \in C_0^\infty(\mathcal{S}, \mathbb{R}^3)\,.$$

More general, let $\beta = (\beta_1, \ldots, \beta_d)$ be a multi-index with $|\beta| = \sum_k \beta_k$ and $\partial^\beta = \partial_1^{\beta_1} \ldots \partial_d^{\beta_d}$. Then $u \in L^2(\mathcal{S})$ has a *weak derivative* $\partial^{(\beta)} u \in L^2(\mathcal{S})$ if

$$\int_{\mathcal{S}} \partial^{(\beta)} u\,\varphi\,\mathrm{d}a = (-1)^{|\beta|} \int_{\mathcal{S}} u\,\partial^\beta \varphi\,\mathrm{d}a\,, \quad \forall \varphi \in C_0^\infty(\mathcal{S})\,.$$

Definition 3.3 (Sobolev spaces on a surface)**.** Let $\mathcal{S} \subset \mathbb{R}^3$ a regular surface, $m \geq 0$. We set

$$H^m(\mathcal{S}) = \{u \in L^2(\mathcal{S}) \mid \exists\, \partial^{(\beta)} u \in L^2(\mathcal{S}) \quad \forall 0 \leq |\beta| \leq m\}\,,$$
$$\|u\|_{m,\mathcal{S}}^2 = \sum_{|\beta| \leq m} \int_{\mathcal{S}} |\partial^{(\beta)} u|^2\,\mathrm{d}a\,.$$

Furthermore, if $\Gamma = \partial\mathcal{S} \neq \varnothing$ we set

$$H_0^m(\mathcal{S}) = \{u \in H^m(\mathcal{S}) \mid u|_\Gamma = 0\}\,,$$

where $u|_\Gamma = 0$ holds in the sense of traces and if $\mathcal{S}$ is closed, *i.e.* $\partial\mathcal{S} = \varnothing$, we set

$$H_0^m(\mathcal{S}) = \{u \in H^m(\mathcal{S}) \mid \int_{\mathcal{S}} u\,\mathrm{d}a = 0\}\,.$$

The dual space of $H^m(\mathcal{S})$ is denoted by $H^{-m}(\mathcal{S})$, *i.e.* we have

$$H^{-m}(\mathcal{S}) = \{\ell : H^m(\mathcal{S}) \to \mathbb{R} \mid \ell \text{ linear}\}\,.$$

Likewise we define $H_0^{-m}(\mathcal{S}) = \{\ell : H_0^m(\mathcal{S}) \to \mathbb{R} \mid \ell \text{ linear}\}$.

Remark: $H^m(\mathcal{S})$ is a Hilbert space for all $m \geq 0$, hence complete and reflexive. We have $H^m \subset L^2 \subset H^{-m}$. Furthermore, due to the Sobolev embedding theorem, we have $H^2(\mathcal{S}) \hookrightarrow C^{0,\alpha}(\mathcal{S})$ which does not hold for $H^1(\mathcal{S})$.

If X is a vector space and X' its dual space the *dual pairing* is defined as

$$\langle x' | x \rangle = \langle x' | x \rangle_{X',X} = x'(x)\,, \quad x' \in X'\,, x \in X\,.$$

For some differentiable vector field $v \in C^2(S, \mathbb{R}^3)$ the divergence theorem (resp. Green's identity) reads

$$\int_{\mathcal{S}} \mathrm{div}_{\mathcal{S}} v\,\varphi\,\mathrm{d}a = -\int_{\mathcal{S}} g(v, \nabla_{\mathcal{S}}\varphi)\,\mathrm{d}a + \int_{\partial\mathcal{S}} \varphi\, g(v, n_s)\,\mathrm{d}s\,, \quad \forall \varphi \in C^1(\mathcal{S})\,.$$

Note that the last term vanishes if $\varphi = 0$ on $\partial\mathcal{S}$. A special case is given by $v = \nabla_{\mathcal{S}} u$ for some differentiable function $u : \mathcal{S} \to \mathbb{R}$. This motivates the following definition:

Definition 3.4 (Weak Laplace-Beltrami)**.** Let $\mathcal{S} \subset \mathbb{R}^3$ a regular surface. Then a weak Laplace-Beltrami operator $\Delta_{\mathcal{S}} : H_0^1(\mathcal{S}) \to H_0^{-1}(\mathcal{S})$ is defined by

$$\langle \Delta_{\mathcal{S}} u | \varphi \rangle := \int_{\mathcal{S}} \Delta_{\mathcal{S}} u\,\varphi\,\mathrm{d}a := -\int_{\mathcal{S}} g(\nabla_{\mathcal{S}} u,\, \nabla_{\mathcal{S}}\varphi)\,\mathrm{d}a\,, \quad \forall \varphi \in H_0^1(\mathcal{S})\,.$$

Remark: For some set $A \subset \mathcal{S}$ a local notion can be defined by

$$\int_A \Delta_{\mathcal{S}} u\,\varphi\,\mathrm{d}a := -\int_A g(\nabla_{\mathcal{S}} u,\, \nabla_{\mathcal{S}}\varphi)\,\mathrm{d}a + \int_{\partial A} \varphi\, g(\nabla_{\mathcal{S}} u, n_s)\,\mathrm{d}s\,, \quad \forall \varphi \in H_0^1(\mathcal{S})\,. \tag{3.7}$$

Linear FEM on a discrete surface. For a triangle mesh $\mathcal{M}_h$ with n vertices we associate the linear FEM space spanned by the nodal hat basis.

Definition 3.5 (Linear FEM space)**.** If $\mathcal{M}_h$ denotes a discrete surface with n vertices we set

$$\mathcal{X}_h = \operatorname{span}\{\phi_1, \dots, \phi_n\}\,, \quad \phi_i(X_j) = \delta_{ij}\,, \quad \phi_i \text{ affine on each face }. \tag{3.8}$$

In particular, $\phi_i \in C^0(\mathcal{M}_h)$ and $\phi_i \in H^1(\mathcal{M}_h)$, hence $\mathcal{X}_n \subset C^0(\mathcal{M}_h)$ and $\mathcal{X}_n \subset H^1(\mathcal{M}_h)$. Furthermore, we make use of the notation $\tilde{\phi}_i = \phi_i \circ X : \Omega_h \subset \mathbb{R}^2 \to \mathbb{R}$.

Intuitively, the steepest ascent direction of a basis function ϕ_i located at some vertex v_i on a triangle $T(f) = (X_i, X_j, X_k)$ is orthogonal to the opposite edge, i.e. E_i, and scales as h_i^{-1}, where h_i is the corresponding height in T w.r.t. E_i. Hence we expect

$$\nabla_h \phi_i\Big|_f := \nabla_{\mathcal{M}_h} \phi_i\Big|_f \sim \frac{1}{h_i} \frac{E_i^\perp}{|E_i|} = \frac{(X_k - X_j)^\perp}{2a_f}\,,$$

since $a_f = \frac{1}{2}\,|E_i|\,h_i$. Note that here and in the following we make use of the convention $V^\perp = V \times N_f$, that means $V^\perp$ is in the tangent plane induced by $T(f) \subset \mathbb{R}^3$. On the other hand, using (2.7) one can indeed verify

$$\nabla_h \phi_i\Big|_f = DX|_f\, G_f^{-1}\, \nabla_{\mathbb{R}^2}(\phi_i \circ X_f) = \frac{(X_k - X_j)^\perp}{2a_f}\,. \tag{3.9}$$

Note that $\nabla_{\mathbb{R}^2}(\phi_i \circ X_f) \in \{(-1,-1)^T, (1,0)^T, (0,1)^T\}$, depending which local index is assigned to ϕ_i within f. By construction, the basis function set fulfills the condition of partition of unity, i.e. for each $\xi \in \Omega_h$ we have $\sum_i \tilde{\phi}_i(\xi) = 1$. That means, on a triangle $T(f) = (X_i, X_j, X_k)$ we have

$$\nabla_h \phi_i\Big|_f + \nabla_h \phi_j\Big|_f + \nabla_h \phi_k\Big|_f = 0\,. \tag{3.10}$$

A discrete function $u : \mathcal{M}_h \to \mathbb{R}$, i.e. a piecewise affine function, can be represented as a vector $(u_i)_i \in \mathbb{R}^n$ with $u_i = u(E(v_i))$ for $i = 1, \dots, n$. For the concatenation $\tilde{u} = u \circ X : \Omega_h \subset \mathbb{R}^2 \to \mathbb{R}$ this yields the representation

$$\tilde{u}(\xi) = \sum_{i=1}^{n} u_i\, \tilde{\phi}_i(\xi)\,. \tag{3.11}$$

Furthermore, (3.11) and (3.10) imply

$$\nabla_h u\Big|_f = \frac{u_j - u_i}{2a_f}(X_i - X_k)^\perp + \frac{u_k - u_i}{2a_f}(X_j - X_i)^\perp\,.$$

Remark: Note that we have omitted the rigorous definition of Sobolev spaces on polyhedral surfaces (*e.g.* discrete surfaces) here. Later, we will introduce a bi-Lipschitz mapping between a smooth surface $\mathcal{S}$ and its polyhedral approxiation $\mathcal{M}_h$. Based on this map, one can identify $H^1(\mathcal{M}_h)$ with $H^1(\mathcal{S})$ since weak differentiablility is preserved under bi-Lipschitz maps (which is a consequence of Rademacher's theorem). For details on the definition and construction of Sobolev spaces on polyhedral surfaces we refer *e.g.* to Sec. 2.2 in [War06].

Next, we derive a weak notion of a discrete Laplace-Beltrami operator using two different approaches. Eventually, we derive a pointwise evaluation by means of *spatial averaging*.

Discrete Laplace-Beltrami & cotan formula from a FEM point of view. If we define the *stiffness matrix* $L \in \mathbb{R}^{n,n}$ by

$$L_{ij} = \int_{\mathcal{M}_h} g\left(\nabla_h \phi_i,\, \nabla_h \phi_j\right) \mathrm{d}a = \int_{\mathcal{M}_h} \langle \nabla_h \phi_i,\, \nabla_h \phi_j \rangle_{\mathbb{R}^3}\, \mathrm{d}a\,,$$

we can define a weak Laplace-Beltrami operator $\Delta_h : \mathcal{X}_h \to (\mathcal{X}_h)'$ via

$$\langle \Delta_h u | v \rangle := -\int_{\mathcal{M}_h} g\left(\nabla_h u,\, \nabla_h v\right) \mathrm{d}a = -\sum_{i,j=1}^{n} u_i v_j \int_{\mathcal{M}_h} g\left(\nabla_h \phi_i,\, \nabla_h \phi_j\right) \mathrm{d}a = -\sum_{i,j=1}^{n} L_{ij} u_i v_j\,, \tag{3.12}$$

where $\bar{u} = (u_i)_i$ and $\bar{v} = (v_j)_j$ are the coefficients (*e.g.* nodal values) of two discrete functions $u, v : \mathcal{M}_h \to \mathbb{R}$.

Next we derive the evaluation of the entries of L. For $i \neq j$ we get

$$L_{ij} = \sum_{f \in \mathcal{F}} \int_{T(f)} \langle \nabla_h \phi_i, \nabla_h \phi_j \rangle_{\mathbb{R}^3} \, \mathrm{d}a = \int_{T_k} \langle \nabla_h \phi_i, \nabla_h \phi_j \rangle_{\mathbb{R}^3} \, \mathrm{d}a + \int_{T_l} \langle \nabla_h \phi_i, \nabla_h \phi_j \rangle_{\mathbb{R}^3} \, \mathrm{d}a$$

with $T_k = T(f_k) = (X_i, X_j, X_k)$ and $T_l = T(f_l) = (X_l, X_j, X_i)$. Since $\nabla_h \phi_i$ and $\nabla_h \phi_j$ are constant on T_k we get with (3.9)

$$\int_{T_k} \langle \nabla_h \phi_i, \nabla_h \phi_j \rangle_{\mathbb{R}^3} \, \mathrm{d}a = a_k \cdot \frac{(X_k - X_j)^\perp}{2a_k} \cdot \frac{(X_i - X_k)^\perp}{2a_k} = -\frac{\cos \gamma_k}{4a_k} \cdot \|X_k - X_j\| \, \|X_i - X_k\| = -\frac{1}{2} \cot \gamma_k \,,$$

where γ_k denotes the inner triangle angle (wrt. f_k) at vertex v_k and we have used

$$a_k = \frac{1}{2} \sin \gamma_k \, \|X_k - X_i\| \, \|X_k - X_j\| \,.$$

Likewise we get

$$\int_{T_l} \langle \nabla_h \phi_i, \nabla_h \phi_j \rangle_{\mathbb{R}^3} \, \mathrm{d}a = -\frac{1}{2} \cot \gamma_l \,,$$

where γ_l denotes the inner triangle angle (wrt. f_l) at vertex v_l. Altogether, we have shown that for $i \neq j$ we get

$$L_{ij} = -\frac{1}{2}(\cot \alpha_{ij} + \cot \beta_{ij}) \,. \tag{3.13}$$

Using (3.10) we finally get

$$L_{ii} = \sum_{f \in \mathcal{F}} \int_{T(f)} \langle \nabla_h \phi_i, \nabla_h \phi_i \rangle_{\mathbb{R}^3} \, \mathrm{d}a = -\sum_{f \in \mathcal{F}} \int_{T(f)} \langle \nabla_h \phi_i, (\nabla_h \phi_j + \nabla_h \phi_k) \rangle_{\mathbb{R}^3} \, \mathrm{d}a = -\sum_{i \neq j} L_{ij} \,, \tag{3.14}$$

and by (3.12) we compute

$$\langle \Delta_h u | \phi_i \rangle = -\sum_{k=1}^{n} L_{ik} u_k = \frac{1}{2} \sum_{v_j \in N(v_i)} (\cot \alpha_{ij} + \cot \beta_{ij})(u_j - u_i) \,. \tag{3.15}$$

Remark: The representation (3.13) resp. (3.14) is the well-known *cotan formula* [Dzi88, PP93, DMSB99].

Using the paradigm of *spatial averaging* one can formally write down a vertex-wise evaluation of the discrete Laplace-Beltrami. Note that the support of a basis function ϕ_i is given exactly by the 1-ring of faces at vertex v_i, denoted here by A_i. Using

$$m_i := \int_{\mathcal{M}_h} \phi_i \, \mathrm{d}a = \int_{A_i} \phi_i \, \mathrm{d}a = \frac{1}{3} \, |A_i| \,,$$

we might define

$$(\Delta_h u)_i := \Delta_h u(X_i) := \frac{1}{m_i} \int_{A_i} \Delta_h u \, \phi_i \, \mathrm{d}a = \frac{1}{2m_i} \sum_{v_j \in N(v_i)} (\cot \alpha_{ij} + \cot \beta_{ij})(u_j - u_i) \,. \tag{3.16}$$

Remark: The *lumped mass matrix* is given by the diagonal matrix $M = \mathrm{diag}(m_1, \ldots, m_n)$. Then in the standard FEM notation one obtains $(\Delta_h u)_i = -(M^{-1} L \bar{u})_i$, where $\bar{u} = (u_1, \ldots, u_n)^T$.

Alternative derivation & local definition. In the following we present a (geometric) derivation of a weak notion of a Laplace-Beltrami operator. In particular, a local version is defined. Let $v_i \in \mathcal{V}$ be an arbitrary but fixed vertex of $\mathcal{M}_h$, and let A_i be some area associated with v_i. We postulate that the (usually piecewise linear) boundary ∂A_i intersects each adjacent edge of v_i at its midpoint. Usually, one considers barycentric cells, Voronoi cells or mixed Voronoi cells [BKP+10, MDSB02]. As in the definition of a weak Laplace-Beltrami operator in (3.7) we set for $u \in H^1(\mathcal{M}_h)$ and some basis function $\phi_j \in H^1(\mathcal{M}_h)$:

$$\int_{A_i} \Delta_h u \cdot \phi_j \, \mathrm{d}a := -\int_{A_i} \langle \nabla_h u, \, \phi_j \rangle_{\mathbb{R}^3} \, \mathrm{d}a + \int_{\partial A_i} \phi_j \, \langle \nabla_h u, N_s \rangle_{\mathbb{R}^3} \, \mathrm{d}s \, .$$

Summing over all basis functions yields:

$$\begin{aligned}
\int_{A_i} \Delta_h u \, \mathrm{d}a &= \sum_{j=1}^{n} \int_{A_i} \Delta_h u \, \phi_j \, \mathrm{d}a \\
&= \sum_{j=1}^{n} \sum_{f : v_i \in f} \Big(-\int_{A_i \cap T(f)} \langle \nabla_h u, \, \nabla_h \phi_j \rangle_{\mathbb{R}^3} \, \mathrm{d}a + \int_{\partial (A_i \cap T(f))} \phi_j \, \langle \nabla_h u, N_s \rangle_{\mathbb{R}^3} \, \mathrm{d}s \Big) \\
&= \sum_{f : v_i \in f} \int_{\partial A_i \cap T(f)} \langle \nabla_h u, N_s \rangle_{\mathbb{R}^3} \, \mathrm{d}s \, .
\end{aligned}$$

Now consider one fixed triangle $T(f) = (X_i, X_j, X_k)$. e Let E_{jk} the segment connecting the edge midpoints of (v_i, v_j) and (v_i, v_k), i.e. $E_{jk} = -\frac{1}{2} E_i == \frac{1}{2}(X_j - X_k)$. Since ∂A_i runs through all edge midpoints we have

$$\begin{aligned}
\int_{\partial A_i \cap T} \langle \nabla_h u, N_s \rangle_{\mathbb{R}^3} \, \mathrm{d}s &= -\int_{-E_{jk}} \langle \nabla_h u, N_s \rangle_{\mathbb{R}^3} \, \mathrm{d}s = |E_{jk}| \cdot \langle \nabla_h u \Big|_f, \, \frac{E_{jk}^{\perp}}{|E_{jk}|} \rangle_{\mathbb{R}^3} = \frac{1}{2} \, \langle \nabla_h u \Big|_f, \, (X_j - X_k)^{\perp} \rangle_{\mathbb{R}^3} \\
&= (u_j - u_i) \cdot \frac{\langle (X_i - X_k), (X_j - X_k) \rangle_{\mathbb{R}^3}}{4 a_f} + (u_k - u_i) \cdot \frac{\langle (X_j - X_i), (X_j - X_k) \rangle_{\mathbb{R}^3}}{4 a_f}
\end{aligned}$$

Let γ_j and γ_k denote the inner triangle angles (wrt. f) at vertices v_j and v_k, respectively. Using

$$a_f = \frac{1}{2} \sin \gamma_j \, \|X_j - X_i\| \, \|X_j - X_k\| = \frac{1}{2} \sin \gamma_k \, \|X_k - X_i\| \, \|X_k - X_j\| \, .$$

we get

$$\begin{aligned}
\cos \gamma_j &= \frac{\langle (X_j - X_i), (X_j - X_k) \rangle}{\|X_j - X_i\| \, \|X_j - X_k\|} = \sin \gamma_j \, \frac{\langle (X_j - X_i), (X_j - X_k) \rangle}{2 a_f} \, , \\
\cos \gamma_k &= \frac{\langle (X_k - X_i), (X_k - X_j) \rangle}{\|X_k - X_i\| \, \|X_k - X_j\|} = \sin \gamma_k \frac{\langle (X_k - X_i), (X_k - X_j) \rangle}{2 a_f} \, .
\end{aligned}$$

Finally, due to $\cot \theta = \frac{\cos \theta}{\sin \theta}$ we get

$$\int_{\partial A_i \cap T} \langle \nabla_h u, N_s \rangle_{\mathbb{R}^3} \, \mathrm{d}s = \frac{1}{2} \Big((u_j - u_i) \, \cot \gamma_k + (u_k - u_i) \, \cot \gamma_j \Big) \, ,$$

and summing over all triangles $T(f)$ with $X_i \in T(f)$ gives

$$\int_{A_i} \Delta_h u \, \mathrm{d}a = \frac{1}{2} \sum_{v_j \in N(v_i)} \Big(\cot \alpha_{ij} + \cot \beta_{ij} \Big) \, (u_j - u_i) \, , \tag{3.17}$$

which correponds exactly to (3.15). Using the paradigm of *spatial averaging* one can formally write down a vertex-wise evaluation of the discrete Laplace-Beltrami:

$$(\Delta_h u)_i := \frac{1}{|A_i|} \int_{A_i} \Delta_h u \, \mathrm{d}a = \frac{1}{2|A_i|} \sum_{v_j \in N(v_i)} (\cot \alpha_{ij} + \cot \beta_{ij})(u_j - u_i) \, . \tag{3.18}$$

Remark: Note that the integrated version of the discrete Laplace-Beltrami results in the same formula, *i.e.* (3.15) and (3.17) coincide. The only differences are given in the pointwise representation (3.16) resp. (3.18), depending on the size of the associated area A_i. However, if A_i denotes the barycentric cell, then $|A_i|$ is given by one third of the sum of the triangle areas in the 1-ring of v_i, hence (3.16) equals (3.18). Meyer *et al.* [MDSB02] discuss the impact of the specific choice of A_i based on numerical experiments.

Mean curvature functional and function. Using the identity (2.8) one gains a weak notion of an *integrated* mean curvature vector $\overrightarrow{H}_h \in (\mathcal{X}_h')^3$ associated with vertex $v = v_i$ by the vector-valued expression

$$\langle \overrightarrow{H}_h | \phi_i \rangle := -\int_{\mathcal{M}_h} \Delta_h \mathrm{id}\, \phi_i \, \mathrm{d}a = -\sum_{v_j \in N(v_i)} L_{ij} \, (X_j - X_i) = -\frac{1}{2} \sum_{v_j \in N(v_i)} \Big(\cot \alpha_{ij} + \cot \beta_{ij} \Big) \, (X_j - X_i) \, . \tag{3.19}$$

Moreover, the paradigm of *spatial averaging* yields a pointwise mean curvature vector

$$(\overrightarrow{H}_h)(v_i) := \sum_{v_j \in N(v_i)} M^{ij} \langle \overrightarrow{H}_h | \phi_j \rangle = -\frac{1}{2m_i} \sum_{v_j \in N(v_i)} \Big(\cot \alpha_{ij} + \cot \beta_{ij} \Big) \, (X_j - X_i) \, . \tag{3.20}$$

In the terminology used by Wardetzky *et al*. [War06, HPW06, War08] the representation (3.19) is referred to as *mean curvature functional* whereas (3.20) is denoted as *mean curvature function*.

Different Laplace-Beltrami operators used in GP and CG Above, we have derived the *cotan* formula representing a (weak) notion of a discrete Laplace-Beltrami operator. However, there exist also different notions of discrete Laplace-Beltrami operators in Geometry Processing or Computer Graphics, usually starting with a generic representation of the weak notion, *i.e*.

$$(Lu)_i = \sum_j \omega_{ij} (u_j - u_i) \, ,$$

where ω_{ij} are the *weights* associated with the discrete operator. Here one assumes

$$(Lu)_i \approx \int_{\mathcal{M}_h} \Delta_h u \, \varphi_i \, \mathrm{d}a = \langle \Delta_h u | \varphi_i \rangle \, ,$$

for some (basis) function $\varphi_i : \mathcal{M}_h \to \mathbb{R}$ with local support in the vicinity of the ith vertex, *e.g*. $\varphi_i = \phi_i$. The simplest choice, for example, is given by Taubin's operator [Tau95] by setting $\omega_{ij} = 1$. A detailed discussion is given by Wardetzky et al. [WMKG07], who derive an axiomatic approach based on characteristic properties of the *smooth* Laplace-Beltrami operator. In detail, they list a number of properties that a discrete Laplace-Beltrami operator should have, e.g. symmetry wrt. L^2 scalar product, positve weights ($\rightsquigarrow$ maximum principle), local support. Their main result is that *none* of the standard discrete Laplace-Beltrami operators used in GP or CG satisfies all of the desired properties on general meshes. Moreover, the different operators have complementary strenghts, hence it often depends on the application which one is appropiate.
For example, the *cotan Laplace* presented here violates the axiom of positive weights on general meshes. Furthermore, it is not purely intrinsic, that means, its evaluation can lead to different results even for two isometric surfaces with different triangulations. On the other hand, the cotan representation has been proven to converge to the smooth Laplace-Beltrami in a weak formulation [HPW06], as it will be discussed in Sec. 3.3.

Further references [PP93, DMSB99, MDSB02, War08, Tau95, WMKG07]

3.3 Convergence of discrete mean curvature

Wardetzky *et al*. [War06, HPW06, War08] investigated the convergence properties of the mean curvature functional (3.19) as well as the mean curvature function (3.20). In this section we summarize partial results of their convergence analysis—for the full results we refer to the original papers.

In particular, the following question is considered: consider a sequence of discrete surfaces $\mathcal{M}_h$ converging (in Hausdorff-measure) to a smooth embedded surface $\mathcal{S}$. What are the measures and conditions that geometric objects on $\mathcal{M}_h$ converge to the corresponding objects on $\mathcal{S}$? The lantern of Schwartz constitutes an example of what can go wrong: pointwise convergence without convergence of normal fields.

Example: Schwarz lantern Consider a straight smooth cylinder $C \subset \mathbb{R}^3$ with unit radius and unit height. Divide this cylinder into $m \in \mathbb{N}$ evenly spaced circles, and divide each of these circles into $n \in \mathbb{N}$ equal segments, thus obtaining a $m \times n$ grid of points on C which can be connected by flat triangles. Now twist every other horizontal ring by π/n to generate an alternating grid of points. All triangles of the so obtained discrete cylinder $C_{m,n}$ are congruent. Now let m and n approach infinity. The main observation is that the normals of the triangles of the discrete cylinders $C_{m,n}$ will approach the normals of C if and only if

$$\frac{m}{n^2} \to 0\,.$$

One cannot expect convergence of geometric properties from pointwise convergence alone. One of the main results of Wardetzky *et al*. [War06, HPW06, War08] reads: If $\mathcal{M}_h \to \mathcal{S}$ in Hausdorff distance, then convergence of normal fields is equivalent to convergence of metric tensors resp. area resp. Laplace-Beltrami operators. Furthermore, it is shown that in order to prove the convergence of geometric properties it often suffices to additionally require convergence of normals. In particular, it is shown that convergence can in general only be obtained *distributinally*, *i.e*. in a weak/integrated sense. For polyhedral surfaces approximating smooth surfaces one cannot expect pointwise convergence of curvatures but only distributinal convergence.

Shortest distance map & geometric splitting. Let us consider the following setup. Let $\mathcal{S} \subset \mathbb{R}^3$ be a regular embedded surface, and let $\mathcal{M}_h$ be a sequence of meshes (with $h \to 0$) that approximates $\mathcal{S}$. The convergence analysis of Wardetzky is based on the construction of a bi-Lipschatz map between $\mathcal{M}_h$ and $\mathcal{S}$ such that the metric distortion induced by this mapping is bounded by Hausdorff distance and derivation of normals (and the shape operator). In the following, we shall make this precice.

Definition 3.6 (Medial axis and reach)**.** Let $A \subset \mathbb{R}^3$ be a closed subset. The *medial axis* of A is the set of those points in $\mathbb{R}^3$ which do not have a unique closest neighbor in A. The *reach* of A is the distance of A to its medial axis.

If $\mathcal{S} \subset \mathbb{R}^3$ is a smoothly embedded surface then its medial axis corresponds to the locus of centers of spheres tangentially touching $\mathcal{S}$ in at least two points without intersecting $\mathcal{S}$ and the reach of $\mathcal{S}$ is the infimum over the radii of such spheres.

Remark: The reach of a smooth surface $\mathcal{S}$ is bounded above by the radii of osculating spheres of $\mathcal{S}$:

$$\operatorname{reach}(\mathcal{S}) \leq \inf_{p \in \mathcal{S}} \frac{1}{\max(|\kappa_1(p)|, |\kappa_2(p)|)}\,. \tag{3.21}$$

Note that a compact and smoothly embedded surface $\mathcal{S}$ always has positive reach (but a polyhedron does not).

Definition 3.7 (Normal graph, shortest distance map)**.** A discrete surface $\mathcal{M}_h$ is a *normal graph* over the smooth surface $\mathcal{S}$ if it is within the reach of $\mathcal{S}$ and the map which maps each point on $\mathcal{M}_h$ to its closest point on $\mathcal{S}$ is a bijection $\Psi : \mathcal{M}_h \to \mathcal{S}$. The inverse map $\Phi = \Psi^{-1} : \mathcal{S} \to \mathcal{M}_h$ which takes $p \in \mathcal{S}$ to the intersection point $\Phi(p) \in \mathcal{M}_h$ of the normal line through p with the discrete surface $\mathcal{M}_h$ is denoted *shortest distance map*.

The shortest distance map Φ naturally splits into a tangential and a normal component:

$$\Phi(p) = \mathrm{id}_{\mathcal{S}}(p) + \phi(p) \cdot n(p)\,,$$

where $\mathrm{id}_{\mathcal{S}}$ is the embedding of $\mathcal{S}$ into $\mathbb{R}^3$ and ϕ is the scalar-valued (signed) distance function.

The shortest distance map Φ induces a metric on $\mathcal{S}$ which allows to compare the spaces $\mathcal{M}_h$ and $\mathcal{S}$ as metric spaces:

$$(U, V) \mapsto \langle d\Phi(U),\, d\Phi(V)\rangle_{\mathbb{R}^3} \quad \text{a.e.}\,. \tag{3.22}$$

Definition 3.8 (Metric distortion tensor)**.** There exists a symmetric positive definite 2×2 matrix field on $\mathcal{S}$ which represents a linear mapping $A(p) : T_p\mathcal{S} \to T_p\mathcal{S}$ such that for a.e. $p \in \mathcal{S}$

$$g_A(U, V) := \langle A(p)U,\, V\rangle_{\mathbb{R}^3} = \langle d\Phi(U),\, d\Phi(V)\rangle_{\mathbb{R}^3}\,, \quad \forall U, V \in T_p\mathcal{S}\,. \tag{3.23}$$

The linear operator A is smooth on the pre-image of the interior of triangles of $\mathcal{M}_h$ and denoted by *metric distortion tensor*.

The next theorem shows that A only depends on the distance between the surfaces $\mathcal{S}$ and $\mathcal{M}_h$, the angle between their normals and the curvature of the smooth surface $\mathcal{S}$.

Theorem 3.9 (Geometric splitting of metric distortion tensor [War06])**.** *Let $\mathcal{M}_h$ be a closed polyhedral surface with normal field N which is a normal graph over an embedded, closed, smooth surface $\mathcal{S}$ with normal field n. Then the metric distortion tensor A satisfies the decompostion property*

$$A = P \circ Q^{-1} \circ P \quad \textit{a.e. on } \mathcal{S}\,. \tag{3.24}$$

The linear operators P and Q, respectively, can be represented by symmetric positive definite matrices which can be diagonalized (possibly in different ON-frames) to take the form

$$P \sim \begin{pmatrix} 1 + \phi\,\kappa_1 & 0 \\ 0 & 1 + \phi\,\kappa_2 \end{pmatrix}\,, \quad Q \sim \begin{pmatrix} \langle n, N \circ \Phi\rangle^2 & 0 \\ 0 & 1 \end{pmatrix}\,. \tag{3.25}$$

where κ_1 and κ_2 denote the principal curvatures of the smooth manifold $\mathcal{S}$.

Remark:The matrix representing P is positive definite by the assumption that $\mathcal{M}_h$ is in the reach of $\mathcal{S}$, *i.e.* $\phi < \mathrm{reach}(\mathcal{S})$ and hence $1 + \phi \cdot \kappa_i > 0$ by (3.21).

Proof: Consider some fixed triangle $T \in \mathcal{M}_h$ and let $\Psi : T \to \mathcal{S}$. Since $\Psi = \Phi^{-1}$ we get for some $p_h \in T$

$$\Psi(p_h) = p_h - (\phi \circ \Psi)(p_h) \cdot (n \circ \Psi)(p_h)\,.$$

The differential $d_{p_h}\Psi : T_{p_h}\mathcal{M}_h \to T_p\mathcal{S}$, with $p = \Psi(p_h)$, is given for $V \in T_{p_h}\mathcal{M}_h$ by

$$d_{p_h}\Psi(V) = V - (n \circ \Psi) \cdot (d_p\phi(d_{p_h}\Psi(V))) - (\phi \circ \Psi) \cdot (d_p n(d_{p_h}\Psi(V)))\,, \tag{3.26}$$

where $d\phi$ is a linear form on $T_p\mathcal{S}$. Since $\tilde{V} = d_{p_h}\Psi(V) \in T_p\mathcal{S}$ we get

$$0 = \langle d_{p_h}\Psi(V), n \circ \Psi\rangle = \langle V, n \circ \Psi\rangle - d_p\phi(\tilde{V}) \cdot \underbrace{\langle n \circ \Psi, n \circ \Psi\rangle}_{=1} - (\phi \circ \Psi) \cdot \underbrace{\langle d_p n(\tilde{V}), n \circ \Psi\rangle}_{=0}$$

and hence we get $d_p\phi(\tilde{V}) = \langle V, n \circ \Psi\rangle$. This can be plugged into (3.26) and we get with $d_p n = S_p$

$$d_{p_h}\Psi(V) = V - (n \circ \Psi) \cdot \langle V, n \circ \Psi\rangle - (\phi \circ \Psi) \cdot (S_p(d_{p_h}\Psi(V)))\,,$$

and a re-ordering yields

$$\Big(\mathrm{Id} + (\phi \circ \Psi) \cdot S_p\Big)\, d_{p_h}\Psi(V) = V - \langle V, n \circ \Psi\rangle\,(n \circ \Psi)$$

where $\mathrm{Id} : T_p\mathcal{S} \to T_p\mathcal{S}$ is the identity mapping. Hence we define

$$\begin{aligned} P :& T_p\mathcal{S} \to T_p\mathcal{S}\,, \quad P(W) := W + \phi \cdot S_p(W)\,, \\ \tilde{Q} :& T_{p_h}\mathcal{M}_h \to T_p\mathcal{S}\,, \quad \tilde{Q}(V) = V - \langle V, n \circ \Psi\rangle\,(n \circ \Psi)\,, \end{aligned}$$

where P is a symmetric endomorphism on $T_p\mathcal{S}$, $\tilde{Q}$ a projection from $T_{p_h}\mathcal{M}_h$ onto $T_p\mathcal{S}$. This representation yields $Pd_{p_h}\Psi(V) = \tilde{Q}$, *i.e.* $d_{p_h}\Psi(V) = P^{-1} \circ \tilde{Q}$ and hence $d\Phi = d\Psi^{-1} = \tilde{Q}^{-1} \circ P$. If we define a linear mapping $Q^{-1} : T_p\mathcal{S} \to T_p\mathcal{S}$ via

$$\langle Q^{-1}(W_1), W_2\rangle = \langle \tilde{Q}^{-1}(W_1), \tilde{Q}^{-1}(W_2)\rangle\,,$$

we get

$$\begin{aligned}\langle A(W_1), W_2\rangle &= \langle d\Phi(W_1), d\Phi(W_2)\rangle = \langle (\tilde{Q}^{-1} \circ P)(W_1), (\tilde{Q}^{-1} \circ P)(W_2)\rangle \\ &= \langle (Q^{-1} \circ P)(W_1), P(W_2)\rangle = \langle (P \circ Q^{-1} \circ P)(W_1), W_2\rangle\,.\end{aligned}$$

This finishes the proof since S_p has eigenvalues κ_1, κ_2 and $\tilde{Q}$, as the projection from $T_{p_h}\mathcal{M}_h = N^\perp$ onto $T_p\mathcal{S} = n^\perp$, has eigenvalues 0, $\langle n, N \circ \Phi\rangle$ and 1. □

Definition 3.10 (Hausdorff distance)**.** Let $A, B \subset \mathbb{R}^3$ be non-empty subsets. Then the Hausdorff distance between A and B is defined as

$$\begin{aligned}d_H(A,B) &= \max\Big\{\sup_{x\in A}\inf_{y\in B} d(x,y), \sup_{y\in B}\inf_{x\in A} d(x,y)\Big\} \\ &= \inf\{\epsilon > 0 \,|\, A \subset U_\epsilon(B) \text{ and } B \subset U_\epsilon(A)\}\,,\end{aligned}$$

where $U_\epsilon(Y) = \{x \in \mathbb{R}^3 \,|\, \exists y \in Y : d(x,y) < \epsilon\}$.

In the following, we will often assume that a sequence of polyhedral surfaces $(\mathcal{M}_{h_n})_n$ converges in Hausdorff distance to a smooth surface $\mathcal{S}$ if $n \to \infty$ resp. $h_n \to 0$. To ease notation we write $\mathcal{M}_n := \mathcal{M}_{h_n}$ in the following, where one might think of n as being the number of nodes of $\mathcal{M}_n$.

Definition 3.11 (Totally normal convergence)**.** Let $\mathcal{S} \subset \mathbb{R}^3$ be a smooth surface and $(\mathcal{M}_n)_n$ a sequence of polyhedra with shortest distance maps $\Phi_n : \mathcal{S} \to \mathcal{M}_n$ and normal fields $(N_n)_n$. Then $(\mathcal{M}_n)_n$ is said to converge normally to $\mathcal{S}$ if $\|N_n \circ \Phi_n - n\|_\infty \to 0$. Normal convergence is called totally normal if the Hausdorff distances $d_H(\mathcal{S}, \mathcal{M}_n)$ also go to zero.

Each element $\mathcal{M}_n$ in the approximating sequence induces a metric on the smooth reference surface $\mathcal{S}$ determined by the respective distortion tensor A_n. For almost every $p \in \mathcal{S}$, $A_n(p)$ is an endomorphism of $T_p\mathcal{S}$. Let $\|A_n\|_\infty = \operatorname{ess\,sup}_{p\in\mathcal{S}} \|A_n(p)\|$. Then convergence of metric tensors means $\|A_n - \mathbb{1}\|_\infty \to 0$.

Wardetzky *et al*. [War06, HPW06, War08] have shown that under the assumption of convergence in Hausdorff distance of a sequence of polyhedral surfaces to a smooth surface, the following conditions areequivalent: (i) convergence of normals, (ii) convergence of the metric distortion tensors, (iii) convergence of area, and (iv) convergence of the Laplace-Beltrami operators (in operator norm). The proof is based on translating these geometric conditions into algebraic properties of the metric distortion tensor. The equivalence of such algebraic conditions, in turn, is then derived from the splitting of the metric distortion tensor into a product of symmetric operators, *cf*. Thm.3.9. However, we will only consider the equivalence of totally normal convergence and convergence of metric tensors here.

Theorem 3.12 (Equivalent conditions for convergence [War06])**.** *Let $\mathcal{S} \subset \mathbb{R}^3$ be a compact smooth surface, and let $\mathcal{M}_n$ be a sequence of polyhedral surfaces which are normal graphs over $\mathcal{S}$ and which converge to $\mathcal{S}$ in Hausdorff distance. Then the following conditions are equivalent:*

$$\|N_n \circ \Phi_n - n\|_\infty \to 0 \quad \Longleftrightarrow \quad \|A_n - \mathbb{1}\|_\infty \to 0\,. \tag{3.27}$$

Proof: Let A_n be the sequence of metric distortion tensors induced by $\mathcal{M}_n$ and let $A_n = P_n Q_n^{-1} P_n$ be the geometric splitting given by Thm. 3.9. Then Hausdorff convergence $\mathcal{M}_n \to \mathcal{S}$ implies $\|P_n - \mathbb{1}\|_\infty \to 0$ and normal convergence in L^∞ is equivalent to $\langle n, N \circ \Phi\rangle \to 1$. □

Convergence of mean curvature functional For a function $u : \mathcal{S} \to \mathbb{R}$ we define a surface gradient $\nabla_A u$ based on the metric g_A, *i.e.*

$$\forall V \in T\mathcal{S}: \quad g_A(\nabla_A u, V) := \frac{d}{dt} u(. + tV)\Big|_{t=0} = \langle \nabla_{\mathcal{S}} u, V\rangle_{\mathbb{R}^3}\,, \quad \Rightarrow \quad \nabla_A u = A^{-1}\nabla_{\mathcal{S}} u\,.$$

Next, we define two (weak) Laplace-Beltrami operators $\Delta_{\mathcal{S}}, \Delta_n : H_0^1(\mathcal{S}) \to H_0^{-1}(\mathcal{S})$: One corresponds to Def. 3.4 whereas the other one is based on the shortest distance map resp. on the metric g_{A_n}.

$$\begin{aligned}
\langle \Delta_{\mathcal{S}} u | v\rangle &= -\int_{\mathcal{S}} g(\nabla_{\mathcal{S}} u, \nabla_{\mathcal{S}} v)\,\mathrm{d}a = -\int_{\mathcal{S}} \langle \nabla_{\mathcal{S}} u, \nabla_{\mathcal{S}} v\rangle_{\mathbb{R}^3}\,\mathrm{d}a\,,\\
\langle \Delta_n u | v\rangle &= -\int_{\mathcal{S}} g_{A_n}(\nabla_{A_n} u,\, \nabla_{A_n} v)\sqrt{\det A_n}\,\mathrm{d}a = -\int_{\mathcal{S}} \langle {A_n}^{-1}\nabla_{\mathcal{S}} u, \nabla_{\mathcal{S}} v\rangle_{\mathbb{R}^3}\sqrt{\det A_n}\,\mathrm{d}a\,,
\end{aligned}$$

The definition of the Laplace-Beltrami operator Δ_n is based on the pullback of the polyhedral metric to the smooth surface via (3.22). On the other hand, one can define an intrinsic Laplace-Beltrami operator directly on the polyhedral surface $\mathcal{M}_h$ itself, *cf*. (3.12). The main technical difficulty is to rigorously define the Sobolev space $H_0^1(\mathcal{M}_h)$ on a polyhedral surface. A very general scheme for defining H_0^1 is based on a version of Rademacher's theorem which assures that weak differentiability is preserved under bi-Lipschitz maps, then $H_0^1(\mathcal{M}_h)$ is identifies with $H_0^1(\mathcal{S})$ via Φ. Finally, one can show that Δ_n is equal to the pullback of the intrinsically defined Laplace-Beltrami operator on $\mathcal{M}_h$. For a more detailed discussion on this issue we refer to [War06] and state only one result here:

Theorem 3.13 (Consistency with polyhedral theory, (Lemma 3.2.2 in [War06]))**.** *Let $\mathcal{M}_h$ be a polyhedral surface which is a normal graph over the smooth surface $\mathcal{S}$ with corresponding shortest distance map Φ. Then $u \in L^2(\Phi(\mathcal{S}))$ if and only if $u \circ \Phi \in L^2(\mathcal{S})$. Similarly, $u \in H_0^1(\Phi(\mathcal{S}))$ if and only if $u \circ \Phi \in H_0^1(\mathcal{S})$.*

In the spirit of Thm. 2.11 the notion of a (weak) Laplace-Beltrami leads to the following definition:

Definition 3.14 (Discrete mean curvature functional/ Weak mean curvature)**.** Let $\mathrm{id}_{\mathcal{S}} : \mathcal{S} \to \mathbb{R}^3$ and $\mathrm{id}_{\mathcal{M}_n} : \mathcal{M}_n \to \mathbb{R}^3$ be the embeddings of $\mathcal{S}$ and $\mathcal{M}_n$, respectively, and let $\mathrm{id}_n^* = \mathrm{id}_{\mathcal{M}_n} \circ \Phi : \mathcal{S} \to \mathbb{R}^3$. Then we define a (discrete) mean curvature functional by

$$\begin{aligned}
\overrightarrow{H} &= -\Delta_{\mathcal{S}}\mathrm{id}_{\mathcal{S}} \in (H_0^{-1}(\mathcal{S}))^3\\
\overrightarrow{H}_n &= -\Delta_n \mathrm{id}_n^* \in (H_0^{-1}(\mathcal{S}))^3
\end{aligned}$$

Theorem 3.15 (Connection with cotangent formula)**.** *The discrete mean curvature functional, when restricted to the subspace spanned by nodal basis functions, can be expressed using the cotangent formula,* i.e.

$$\langle \overrightarrow{H}_n | \phi_i\rangle = -\frac{1}{2}\sum_{v_j \in N(v_i)} (\cot\alpha_{ij} + \cot\beta_{ij})\,(X_j - X_i)\,.$$

Convergence of the mean curvature functionals is to be understood in the operator norm of linear bounded maps between the spaces $(H_0^1(\mathcal{S}))^d$ and $(H_0^{-1}(\mathcal{S}))^d$, *i.e.* for $F \in (H_0^{-1}(\mathcal{S}))^d$:

$$\|F\|_{H_0^{-1}(\mathcal{S})} := \sup_{\substack{u \in H_0^1(\mathcal{S})\\ u \neq 0}} \frac{\|\langle F|u\rangle\|_{\mathbb{R}^d}}{\|u\|_{H_0^1(\mathcal{S})}}\,.$$

Theorem 3.16 (Convergence of weak mean curvature, [War06])**.** *Let $\mathcal{M}_n$ be a normal graph over the smooth surface $\mathcal{S}$. Then*

$$\|\overrightarrow{H} - \overrightarrow{H}_n\|_{H_0^{-1}(\mathcal{S})} \leq \sqrt{|\mathcal{S}|}\left(\|\sqrt{\det A_n}A_n^{-1} - \mathbb{1}\|_\infty + \|\sqrt{\det A_n}A_n^{-1}\|_\infty\,\|\mathrm{Id} - d\Phi_n\|_\infty\right), \tag{3.28}$$

where $\|\mathrm{Id} - d\Phi_n\|_\infty := \operatorname{ess\,sup}_{p\in\mathcal{S}} \|(\mathrm{Id} - d\Phi_n)_p\|$ with $(\mathrm{Id} - d\Phi_n)_p : T_p\mathcal{S} \to \mathbb{R}^3$. In particular, if a sequence of polyhedral surfaces $(\mathcal{M}_n)_n$ converges totally normal to the smooth surface $\mathcal{S}$, then the corresponding mean curvature functionals converge in $H_0^{-1}(\mathcal{S})$.

Proof: We consider the triangle inequality

$$\overrightarrow{H} - \overrightarrow{H}_n = \Delta_{\mathcal{S}}\mathrm{id} - \Delta_n \mathrm{id}_n^* = (\Delta \mathrm{id} - \Delta_n \mathrm{id}) + (\Delta_n \mathrm{id} - \Delta_n \mathrm{id}_n^*)\,. \tag{3.29}$$

Since $\langle \nabla_{\mathcal{S}} \mathrm{id}, V\rangle = V$ and $\langle \nabla_{\mathcal{S}}(\mathrm{id}_{\mathcal{M}} \circ \Phi), V\rangle = d\Phi(V)$ for any vector field V on $\mathcal{S}$, we get with Hölder's inequality for $u \in H_0^1(\mathcal{S})$

$$\|\langle \Delta_{\mathcal{S}}\mathrm{id} - \Delta_n \mathrm{id} | u\rangle\|_{\mathbb{R}^3} = \left\| \int_{\mathcal{S}} (\sqrt{\det A_n} A_n^{-1} - \mathbb{1})\, \nabla_{\mathcal{S}} u \,\mathrm{d}a \right\|_{\mathbb{R}^3} \leq \sqrt{|\mathcal{S}|}\, \|\sqrt{\det A_n} A_n^{-1} - \mathbb{1}\|_\infty \, \|u\|_{H_0^1(\mathcal{S})}$$

and

$$\begin{aligned}
\|\langle \Delta_n \mathrm{id} - \Delta_n \mathrm{id}_n^* | u\rangle\|_{\mathbb{R}^3} &= \left\| \int_{\mathcal{S}} \langle (\nabla_{\mathcal{S}}\mathrm{id} - \nabla_{\mathcal{S}}\mathrm{id}_n^*), \sqrt{\det A_n} A_n^{-1}\, \nabla_{\mathcal{S}} u\rangle \,\mathrm{d}a \right\|_{\mathbb{R}^3} \\
&= \left\| \int_{\mathcal{S}} (\mathrm{Id} - d\Phi_n)\, (\sqrt{\det A_n} A_n^{-1})\, \nabla_{\mathcal{S}} u \,\mathrm{d}a \right\|_{\mathbb{R}^3} \\
&\leq \sqrt{|\mathcal{S}|}\, \|\sqrt{\det A_n} A_n^{-1}\|_\infty \, \|\mathrm{Id} - d\Phi_n\|_\infty \, \|u\|_{H_0^1(\mathcal{S})}\,.
\end{aligned}$$

Under totally normal convergence we get $\|A_n - \mathbb{1}\|_\infty \to 0$, *i.e.* $\|\sqrt{\det A_n} A_n^{-1} - \mathbb{1}\|_\infty \to 0$. It remains to show $\|\mathrm{Id} - d\Phi_n\|_\infty \to 0$. Consider a single triangle T_n of $\mathcal{M}_n$, let $n \circ \Phi^{-1}$ denote the pull-back of the normal field n on $\mathcal{S}$ to the triangle T_n. From the proof of Thm. 3.9 we know that $d\Phi = \tilde{Q}^{-1} \circ P$, with $\tilde{Q}(V) = V - \langle n \circ \Phi^{-1}, V\rangle\, (n \circ \Phi^{-1})$. Totally normal convergence implies $P \to \mathrm{Id}$ as well as $\tilde{Q} \to \mathrm{Id}$, hence $d\Phi \to \mathrm{Id}$ almost everywhere. □

Counterexample to L^2-convergence [War06]

Definition 3.17 (Discrete mean curvature function)**.** Let $(\phi_i)_i$ the standard hat basis of linear FEM on $\mathcal{M}_h$. Then we define the discrete mean curvature function by

$$\overrightarrow{H}_h(p) = \sum_{i,j=1}^{n} \langle \overrightarrow{H}_h | \phi_i \rangle\, M^{ij} \phi_j(p)\,, \tag{3.30}$$

where $M_{ij} = \int_{\mathcal{M}_h} \phi_i\, \phi_j \,\mathrm{d}a$ resp. $M_{ij} = (\int_{\mathcal{M}_h} \phi_i \,\mathrm{d}a)\, \delta_{ij}$ denotes the (lumped) mass matrix and $\sum_k M_{ik} M^{kj} = \delta_{ij}$.

Denote by $\overrightarrow{H} = H_p n(p)$ the smooth mean curvature vector of the smooth surface $\mathcal{S}$, and let $(\overrightarrow{H}_n)_n$ with $\overrightarrow{H}_n = \overrightarrow{H}_{h_n}$ denote the sequence of discrete mean curvature vectors associated with the sequence of polyhedral surfaces $(\mathcal{M}_n)_n$ with $\mathcal{M}_n = \mathcal{M}_{h_n}$. We show that in general $\|\overrightarrow{H}_n - \overrightarrow{H}\|_{L^2}$ does not converge to zero.

Consider the cylinder $\mathcal{S}$ of height 2π and radius 1. We construct a sequence $(\mathcal{M}_n)_n$ of polyhedral surfaces whose vertices lie on this cylinder and which converges to $\mathcal{S}$ totally normally. Let the cylinder be parameterized as

$$x = \cos u\,, \quad y = \sin u\,, \quad z = v\,.$$

Let the vertices of $\mathcal{M}_n$ be given by

$$\begin{aligned}
u &= \frac{i\pi}{n}\,, \quad i = 0, \dots, 2n-1\,, \\
v &= \begin{cases} 2j \sin\frac{\pi}{2n}, & j < 2n \\ 2\pi, & j = 2n \end{cases}
\end{aligned}$$

This corresponds (up to the uppermost layer) to folding along the vertical lines a regular planar quad-grid of edge length

$$h_n = 2 \sin \frac{\pi}{2n}\,.$$

In other words, all faces of $\mathcal{M}_n$ are rectangular (in fact quadratic except for the uppermost layer). It will now depend on the tessellation pattern of this quad-grid whether there is L^2 -convergence of discrete mean curvature or not. Indeed, consider the regular $4-8$-tessellation scheme (depicted *e.g.* in Figure 7 in [HPW06]). Away from the boundary, there are two kinds of vertices - those of valence 4 and those of valence 8. Call them p_4 and p_8, respectively. Let $\mathcal{V}_k = \{v \in \mathcal{V} |$ valence of v is $k\}$ for $k \in \{4, 8\}$. Using the cotan-formula, it is easy to see that the coefficients of the weak mean curvature satisfy

$$\langle \overrightarrow{H}_n | \phi_v \rangle = \lambda_n \cdot N_v \,, \qquad \lambda_n = 2 \left(1 - \cos \frac{\pi}{n}\right) \,,$$

for all $v \in \mathcal{V}_4$ *and* $v \in \mathcal{V}_8$, where N_v denotes the (radial) outward cylinder normal field at vertex v. Then (away from the boundary) we get with (3.30) based on the lumped mass matrix

$$\overrightarrow{H}_n(p) = \sum_{v \in \mathcal{V}_4} m_v^{-1} \, \lambda_n \cdot \phi_v(p) \cdot N_v(p) + \sum_{v \in \mathcal{V}_8} m_v^{-1} \, \lambda_n \cdot \phi_v(p) \cdot N_v(p) \,,$$

where

$$m_v = \begin{cases} 2/3 \, h_n^{-2}, & v \in \mathcal{V}_4 \\ 4/3 \, h_n^{-2}, & v \in \mathcal{V}_8 \end{cases} .$$

Since $\lambda_n / h_n^2 = 1$ for all $n \in \mathbb{N}$ we get

$$\overrightarrow{H}_n(p_4) = 2 \, \overrightarrow{H}_n(p_8) \,.$$

Note that for all $v \in \mathcal{V}$ we have $\overrightarrow{H}_n(E(v)) \geq c > 0$ for $n \to \infty$. Hence $\overrightarrow{H}_n$ is a family of piecewise affine functions oscillating between different values at vertices with valence 4 and vertices of valence 8 with ever growing frequencies. Such a family does not converge in L^2.

3.4 Notions of discrete curvature measures

In later applications we primarily want to make use of extrinsic curvature measures, i.e. we focus here mainly on a discrete notion of mean curvature and the shape operator.
Having in mind Gauss' Theorema Egregrium, a simple consideration of two triangles glued together at one edge reveals that on a discrete surface:

- mean curvature is concentrated at edges,
- Gaussian curvature is concentrated at vertices.

Hence, a shape operator is also naturally associated with edges. Nevertheless, discrete shape operators are often associated with a triangle by taking into account the bending accross the three edges. Finally, one can also define shape operators on vertices e.g. by averaging over adjacent edges. In the following, after having introduced several concepts of normals on a mesh, we consider vertex-based and edge-based curvature quantities, where the primal focus is on the latter one.

Normals First, we define the weighted face normal $\tilde{N}_f \in \mathbb{R}^3$ resp. the unit face normal $N_f \in S^2$ on a triangle $T(f) = (X_0, X_1, X_2)$ by

$$\tilde{N}(f) = \tilde{N}_f = (X_1 - X_0) \times (X_2 - X_0)\,, \quad N(f) = N_f = \frac{(X_1 - X_0) \times (X_2 - X_0)}{\|(X_1 - X_0) \times (X_2 - X_0)\|}\,.$$

Since extrinsic bending is naturally measured across edges, a normal field associated with edges is a canonical choice. Usually, these edge normals are located at edge midpoints and computed as weighted average of the adjacent triangle normals, i.e. if f_l and f_r are the adjacent faces of some edge E we set

$$N_E = \frac{\alpha_l N_{f_l} + \alpha_r N_{f_r}}{\|\alpha_l N_{f_l} + \alpha_r N_{f_r}\|}\,, \tag{3.31}$$

where the weights might be chosen e.g. as $\alpha_r = \alpha_l = 1/2$. Another ansatz for defining an edge normal is given by postulating $N_E \perp E$ and then parametrizing N_E via the angle e.g. between N_E and $N(f_s)$, where $s \in \{l, r\}$.
Computing vertex normals as spatial averages of face normals (alternatively, of edge normals) in a local 1-ring neighbourhood leads to normalized weighted average of the (constant) face normals, i.e.

$$N(v) = N_v = \frac{\sum_{f \in N_1(v)} \alpha_f N_f}{\|\sum_{f \in N_1(v)} \alpha_f N_f\|}\,.$$

There are numerous alternatives for the weights α_f, e.g. $\alpha_f = 1$ or $\alpha_f = a_f$ or $\alpha_f = \gamma_f$, where γ_f is the interior triangle angle in f at vertex v. For most applications, the latter angle-weighted vertex normal provides a good trade-off between computational efficiency and accurancy.

Vertex-based curvature measures As mentioned above, discrete Gaussian curvature is supposed to be concentrated at vertices. Following the principles of DDG, one defines the discrete Gaussian curvature such that a discrete version of Gauss-Bonnet holds. That means for some area A_v associated with some vertex $v \in \mathcal{V}$ one defines an *integrated* Gaussian curvature by the so-called *angle-defect*, i.e.

$$\int_{A_v} K_h(x)\,\mathrm{d}a := 2\pi - \sum_{f : v \in f} \gamma_f\,, \tag{3.32}$$

where γ_f denotes the interior triangle angle in f at vertex v, and verifies immediately

$$\int_{\mathcal{M}_h} K_h(x)\,\mathrm{d}a = \sum_{v \in \mathcal{V}} \int_{A_v} K_h(x)\,\mathrm{d}a = 2\pi|\mathcal{V}| - \sum_{v \in \mathcal{V}} \sum_{f : v \in f} \gamma_f = 2\pi\left(|\mathcal{V}| - \frac{1}{2}|\mathcal{F}|\right) = 2\pi\left(|\mathcal{V}| + |\mathcal{F}| - |\mathcal{E}|\right),$$

where we have used $\sum_{v : v \in f} \gamma_f = \pi$ as well as $3|\mathcal{F}| = 2|\mathcal{E}|$ in the last step. Cohen-Steiner and Morvan [CSM03] prove the convergence of (3.32) to its continuous counterpart (in an integrated sense!), cf. also Sec. 3.3. Following the paradigm of *spatial averaging* one might define Gaussian curvature evaluated at a vertex, i.e.

$$K_h(v) = \frac{\int_{A_v} K_h(x)\,\mathrm{d}a}{|A_v|} = \frac{1}{|A_v|}\Big(2\pi - \sum_{f : v \in f} \gamma_f\Big)\,.$$

Using the identity (2.8) as well as the weak notion of a discrete Laplace-Beltrami operator from Sec. 3.2 one gains an *integrated* mean curvature vector associated with vertex $v = v_i$ resp. the area $A_i = A_{v_i}$ by

$$\int_{A_i} H_h(x)N(x)\,\mathrm{d}a := -\int_{A_i} \Delta_h \mathrm{id}(x)\,\mathrm{d}a = -\frac{1}{2}\sum_{v_j\in N(v_i)} \Big(\cot\alpha_{ij} + \cot\beta_{ij}\Big)\,(X_j - X_i)\,.$$

Moreover, the paradigm of *spatial averaging* yields a pointwise mean curvature vector

$$H_h(v_i)N(v_i) := -\frac{1}{|A_i|}\int_{A_i} \Delta_h \mathrm{id}(x)\,\mathrm{d}a = -\frac{1}{2|A_i|}\sum_{v_j\in N(v_i)} \Big(\cot\alpha_{ij} + \cot\beta_{ij}\Big)\,(X_j - X_i)\,.$$

Finally, one can define a pointwise notion of (the absolute value of) mean curvature by

$$|H|(v_i) = \frac{1}{2|A_i|}\left\|\sum_{v_j\in N(v_i)} \Big(\cot\alpha_{ij} + \cot\beta_{ij}\Big)\,(X_j - X_i)\right\|\,.$$

The convergence of (integrated) mean curvature has been investigated *e.g.* by Wardetzky and co-workers [War06, HPW06, War08] as shwon in Sec. 3.3 as well as by Cohen-Steiner and Morvan [CSM03]. Meyer et al. [MDSB02] discuss the impact of the specific choice of A_v for the approximation properties of vertex-based curvature measures in practice. Finally, we refer to the work of Hildebrandt and Polthier who define a vertex-based shape operator as average of adjacent edge-based shape operators [HP04] and investigate convergence properties of an integrated as well as pointwise defined shape operator [HP11].

Edge-based curvature measures As mentioned above a discrete notion of mean curvature is naturally associated with edges, more precisely, with the bending between two adjacent faces. Intuitively, the isometric bending of two adjacent triangles sharing an edge E is captured by the so-called *dihedral angle* θ_E, i.e.

$$\theta_E := \angle\Big(N(f_l)\times E,\, E\times N(f_r)\Big)\,,\quad E = T(f_r)\cap T(f_l)\,.$$

Hence we have $\theta_E = \pi$ if $N(f_l) \parallel N(f_r)$. Since bending in either direction should be penalized equally (in absolut value) with positive values if $\theta_E > \pi$ and negative if $\theta_E < \pi$, one intuitively expects

$$H_E \sim -2\,\cos\frac{\theta_E}{2}\,. \tag{3.33}$$

Note that sometimes the quantity $\theta_E - \pi$ is refered to as dihedral angle as well, then (3.33) is usually replaced by $H_E \sim 2\,\sin\frac{\theta_E}{2}$. A Taylor expansion of (3.33) about π leads to

$$H_E \sim (\theta_E - \pi) + O(|\theta_E - \pi|^3)\,.$$

Finally, based on H_E one can define an edge-based shape operator $S_E \in \mathbb{R}^{3,3}$ by

$$S_E = \frac{1}{3}\,H_E\,(N_E\times E)\otimes(N_E\times E)\,,$$

which satisfies $S_E E = 0$ (no curvature along the edge), $S_E N_E$ (no bending in normal direction) and $\mathrm{tr}\,S_E = H_E$.

The discrete notion of mean curvature as stated in (3.33) can be found in several approaches, *cf. e.g.* [CSM03, BMF03, GHDS03, HP04, War06, Sul08, Hee16], and will be justified in the following. Note, however, that in most approaches a discrete notion of mean curvature is first derived in an integrated sense, i.e. if d_E denotes an area associated with edge E satisfying $E \subset d_E \subset T(f_r)\cup T(f_l)$, ones sets

$$\int_{d_E} H_E(x)\,\mathrm{d}a := -2\,\cos\frac{\theta_E}{2}\,\|E\|\,.$$

Convergence results by Cohen-Steiner and Morvan [CSM03] Let $V \subset \mathbb{R}^3$ a convex body such that $\mathcal{S} := \partial V$ is a smooth and compact surface. For $\epsilon > 0$ and some area $B \subset \mathcal{S}$ consider the offset

$$V_\epsilon(B) = \{x + \epsilon\, t\, n(x) : x \in B,\, t \in [0,1]\}\,.$$

Then *Steiner's tube formula* reads (*cf*. [CSM03, Sul08])

$$|V_\epsilon(B)| = \epsilon \int_B \mathrm{d}a + \frac{1}{2}\epsilon^2 \int_B H\,\mathrm{d}a + \frac{1}{3}\epsilon^3 \int_B K\,\mathrm{d}a\,, \tag{3.34}$$

which can be re-formulated as

$$\int_B H\,\mathrm{d}a = 2\epsilon^{-2}\Big(|V_\epsilon(B)| - \epsilon\,|B|\Big) + O(\epsilon)\,. \tag{3.35}$$

Now let $B_h \subset \mathcal{M}_h$. For illustrative reasons, we first consider $B_h = T_1 \cup T_2$. If $E = T_1 \cap T_2$, then we postulate $\theta_E > \pi$ since B_h is supposed to be (part of) the boundary of a *convex* body. For some $\epsilon > 0$ we define the offset $V_\epsilon(B_h)$ in a canonical way. If β_E denotes the angle between $N(f_1)$ and $N(f_2)$ we get

$$|V_\epsilon(B_h)| - \epsilon\,|B_h| = \frac{\beta_E}{2\pi} \cdot \epsilon^2\pi \,\cdot \|E\|,$$

which represents a $\beta_E/(2\pi)$-fraction of the volume of a cylinder of height $\|E\|$ and radius ϵ. Using (3.35) with $\beta_E = \theta_E - \pi$ suggests the definition

$$\int_{B_h} H_h\,\mathrm{d}a := (\theta_E - \pi)\,\|E\|\,.$$

For arbitrary $B_h \subset T_1 \cup T_2$ one obtains analogously

$$\int_{B_h} H_h\,\mathrm{d}a := (\theta_E - \pi)\,\|E \cap B_h\|\,,$$

and for arbitrary $B_h \subset \mathcal{M}_h$ one obtains

$$\int_{B_h} H_h\,\mathrm{d}a = \sum_{E \subset B_h} (\theta_E - \pi)\,\|E \cap B_h\| \,+ O(\epsilon),$$

since the cone-like volume $V_\epsilon(B_h)$ sitting at a vertex is given by a fraction of the ball of radius ϵ, hence scales as ϵ^3.

Definition 3.18 (Delaunay triangulation)**.** A Delaunay triangulation for a set of points in $\mathbb{R}^2$ is a triangulation such that no point is inside the circumcircle of any triangle.

Remark: The Delaunay triangulation of a discrete point set P in general position corresponds to the dual graph of the Voronoi diagram for P. The Voronoi region V_p associated with one point $p \in P$ is defined as

$$V_p = \{q \in \mathbb{R}^2 \,|\, \mathrm{dist}(p,q) \le \mathrm{dist}(p',q) \quad \forall p' \in P\}\,.$$

The Voronoi diagram is simply the tuple of cells V_p for all $p \in P$.

Definition 3.19 (ϵ-sample)**.** A point set $P \subset \mathbb{R}^3$ is an ϵ-sample of a regular surface $\mathcal{S} \subset \mathbb{R}^3$ if for all $p \in \mathcal{S}$

$$B_{r(\epsilon,p)}(p) \cap P \neq \varnothing\,,$$

where $r(\epsilon, p) = \epsilon \cdot \mathrm{dist}(p, \mathrm{med}(\mathcal{S}))$, where $\mathrm{med}(\mathcal{S})$ denote the medial axis of $\mathcal{S}$.

Cohen-Steiner and Morvan [CSM03] prove the following convergence result:

Theorem 3.20 (Convergence of weak edge-based mean curvature [CSM03])**.** *Let $\mathcal{S} \subset \mathbb{R}^3$ be a smooth surface, not necessarily the boundary of a convex body, $\mathcal{M}_h = (\mathcal{V}, \mathcal{F}, \mathcal{E})$ an approximating triangle mesh and $\epsilon > 0$ sufficiently small. If the set $\{E(v) | v \in \mathcal{V}\}$ is an ϵ-sample of $\mathcal{S}$ and the triangulation of $\mathcal{M}_h$ is Delaunay, then for any $B_h \subset \mathcal{M}_h$*

$$\left| \sum_{E \subset B_h} (\theta_E - \pi)\,\|E \cap B_h\| \;-\; \int_{\Phi^{-1}(B_h)} H\,\mathrm{d}a \right| = O(\epsilon)\,, \tag{3.36}$$

*where $\Phi : \mathcal{S} \to \mathcal{M}_h$ is the shortest distance map which is a homeomorphism if h is sufficiently small (*cf. *Sec. 3.3).*

Remark: The proof is based on differential 2-forms and geometric measure theory and is beyond the scope of this course. A similar convergence result is shown for the discrete Gaussian curvature as defined in (3.32), as well as some discrete seecond fundamental form.

Non-conforming FEM Using the canonical basis functions set $\{\phi_E\}_E$ of a Crouzeix-Raviart element on $\mathcal{M}_h$, namely $\phi_E(m_F) = \delta_{EF}$ for an edge midpoint $m_F \in \mathbb{R}^3$ of edge F and $\phi_E|_f$ linear on each $f \in \mathcal{F}$, it is easy to verify (cf. Lemma 2.4.5 in [War06]) that

$$\int_{\mathcal{M}_h} \Delta_h u \, \phi_E \, \mathrm{d}a = 2 \sum_{j=1}^{4} \cot\left(\sphericalangle\left(E_j, E\right)\right) \left(u_{E_j} - u_E\right) . \tag{3.37}$$

Here we have used the notation $u(x) = \sum_E u_E \phi_E(x)$ and if $E = T \cap T'$, then $\cup_j E_j = \partial\omega_E$ with $\omega_E = T \cup T'$. Note that (3.37) is the non-conforming analogon to the conforming approach in (3.15). Using the identity (2.8) one gains an *integrated* mean curvature vector associated with an edge E by

$$\int_{\omega_E} H_h N \, \mathrm{d}a := -\int_{\mathcal{M}_h} \Delta_h \mathrm{id} \, \phi_E \, \mathrm{d}a = -2 \cos\frac{\theta_E}{2} \, \|E\| \, N_E \, , \tag{3.38}$$

where N_E denotes the outer angle-bisecting normal to $\mathcal{M}_h$ at edge E and θ_E is the dihedral angle at E. Again, (3.38) is the non-conforming analogon to the conforming approach in (3.19).

Triangle-averaged discrete shape operator We have already derived a matrix representation $G \in \mathbb{R}^{2,2}$ of a discrete first fundamental form that lives in the reference domain. Furthermore, $G = G_f$ is constant on each triangle f. Hence we aim at defining a matrix representation $H = H_f \in \mathbb{R}^{2,2}$ of a discrete second fundamental form that also lives in the reference domain and is elementwise constant. If we make use of (2.3) we can eventually derive a matrix representation $S = S_f \in \mathbb{R}^{2,2}$ of a discrete shape operator by setting $S_f = G_f^{-1} H_f$.

Let $f \in \mathcal{F}$ be an arbitrary triangle of a discrete surface $\mathbf{S}$ with a local parametrization $X = X_f$ as defined in (3.3). Note that we have

$$\frac{\partial X}{\partial \xi_1} = X_1 - X_0 = E_2 \, , \quad \frac{\partial X}{\partial \xi_2} = X_2 - X_0 = -E_1 \, . \tag{3.39}$$

Plugging this into (2.2) yields for the entries of $H = H_f$:

$$\begin{aligned} H_{11} &= \Big\langle dN(E_2), E_2 \Big\rangle_{\mathbb{R}^3} \quad H_{12} = -\Big\langle dN(E_2), E_1 \Big\rangle_{\mathbb{R}^3} \\ H_{21} &= -\Big\langle dN(E_1), E_2 \Big\rangle_{\mathbb{R}^3} \quad H_{22} = \Big\langle dN(E_1), E_1 \Big\rangle_{\mathbb{R}^3} \end{aligned}$$

For an edge $E \in \mathcal{M}_h$ we define an edge normal N_E by (3.31) using uniform weights $\alpha_r = \alpha_l = 1/2$. With normals associated to edge midpoints, the (discrete) 1-form dN acts on line segments connecting these midpoints[1]. For a triangle f with edges E_0, E_1, E_2 we denote the corresponding edge normals by N_0, N_1, N_2 and the connecting line segments by E_{ij}, *i.e.* E_{ij} connects the midpoint of E_i with that of E_j, *cf.* Fig. 1. In particular, we have the vector identity $E_k = -2\, E_{ij}$, where k is the complementary index to i and j in f. Using this notation, the fundamental theorem of calculus implies

$$dN(E_k) = -2\, dN(E_{ij}) = -2 \int_{E_{ij}} dN = -2\left(N_j - N_i\right) = 2\left(N_i - N_j\right) . \tag{3.40}$$

We can use (3.40) to simplify the entries of $H = H_f$ further, *i.e.*

$$\begin{aligned} H_{11} &= \langle dN(E_2), E_2 \rangle = 2\left\langle N_0 - N_1, E_2 \right\rangle = 2\left\langle N_0, E_2 \right\rangle + 2\left\langle N_1, E_0 \right\rangle \\ H_{12} &= -\langle dN(E_2), E_1 \rangle = -2\left\langle N_0 - N_1, E_1 \right\rangle = 2\left\langle N_0, -E_1 \right\rangle = 2\left\langle N_0, E_2 \right\rangle \\ H_{21} &= -\langle dN(E_1), E_2 \rangle = -2\left\langle N_2 - N_0, E_2 \right\rangle = 2\left\langle N_0, E_2 \right\rangle \\ H_{22} &= \langle dN(E_1), E_1 \rangle = 2\left\langle N_2 - N_0, E_1 \right\rangle = 2\left\langle N_0, E_2 \right\rangle + 2\left\langle N_2, E_1 \right\rangle \end{aligned}$$

[1] A continuous 1-form ω on a surface $\mathcal{S}$ is a mapping with $\omega(p) \in T_p^*\mathcal{S}$ for all $p \in \mathcal{S}$, where $T_p^*\mathcal{S}$ is the dual space of $T_p\mathcal{S}$. Continuous 1-forms are naturally evaluated as integrals along piecewise differentiable curves $\gamma : [a, b] \to \mathcal{S}$. An important example is given by $\omega = df$, where $f : \mathcal{S} \to \mathbb{R}$ is a differentiable function, and $\int_\gamma \omega = f(\gamma(b)) - f(\gamma(a))$. The concept of *Discrete Exterior Calculus (DEC)* aims at deriving a consistent theory of discrete forms on discrete manifolds, *i.e.* polygonal surfaces with certain properties. Analogously to the continuous setup, discrete 1-forms (*e.g.* given as a differential of a discrete function on a discrete manifold) are evaluated as integrals along discrete curves, *i.e.* polygonal chains. For further information and a comprehensive introduction on DEC we refer to [Hir03, DHLM05, DKT08].

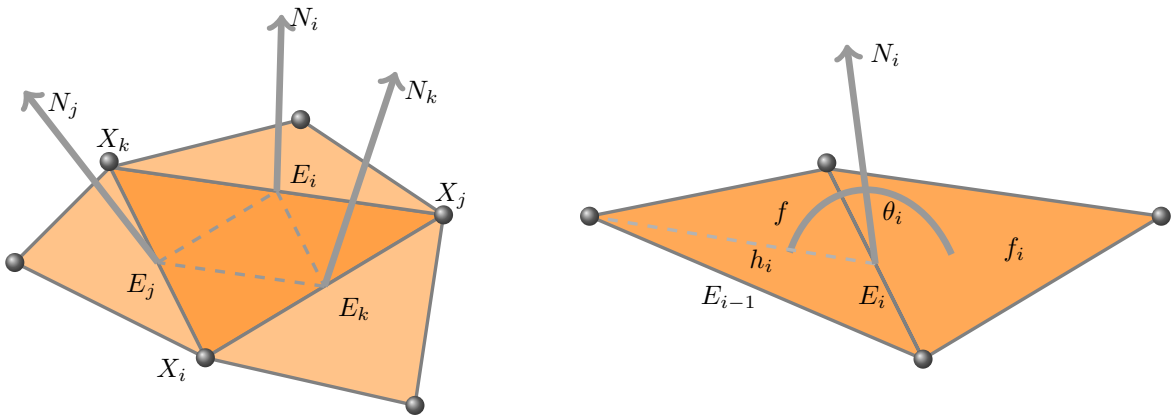

Figure 1: Support of discrete shape operator (left) and geometric interpretation of coefficients (right).

where we have used $\langle N_i, E_i \rangle = 0$ and $E_0 + E_1 + E_2 = 0$. Hence we get the representation

$$H = H_f = 2 \sum_{i=0}^{2} \langle N_i, E_{i-1} \rangle \, M_i \,,$$

with a basis (M_0, M_1, M_2) of symmetric 2×2 - matrices given by

$$M_0 = \begin{pmatrix} 1 & 1 \\ 1 & 1 \end{pmatrix}, \quad M_1 = \begin{pmatrix} 1 & 0 \\ 0 & 0 \end{pmatrix}, \quad M_2 = \begin{pmatrix} 0 & 0 \\ 0 & 1 \end{pmatrix}.$$

In the following, we will interprete the terms $\langle N_i, E_{i-1} \rangle$ geometrically. We refer to the height in f with base E_i by h_i, the neighboring triangle is denoted by f_i, *i.e.* $f \cap f_i = E_i$, *cf.* Fig. 1. Then by definition, the dihedral angle θ_i at E_i between f and f_i is given by two times the angle between h_i and N_i, since N_i is the angle bisector of θ_i by definition. We further use $h_i = -E_{i-1} + \beta E_i$ for some $\beta \in \mathbb{R}$ and obtain

$$\cos \frac{\theta_i}{2} = \langle N_i, \frac{h_i}{|h_i|} \rangle = -\frac{1}{|h_i|} \langle N_i, E_{i-1} \rangle \; + \; \beta \underbrace{\langle N_i, E_i \rangle}_{=0} .$$

Since $a_f := |f| = \frac{1}{2} |h_i| \, \|E_i\|$ we have $\langle N_i, E_{i-1} \rangle = -2 \frac{a_f}{\|E_i\|} \cos \frac{\theta_i}{2}$, hence

$$H_f = -4 \, a_f \sum_{i=0}^{2} \frac{\cos \frac{\theta_i}{2}}{\|E_i\|} \, M_i \,. \tag{3.41}$$

Finally, using (3.5), (3.41) and (2.3), we get a matrix representation of our discrete shape operator

$$S_f = G_f^{-1} H_f \in \mathbb{R}^{2,2} \,. \tag{3.42}$$

Based on the discrete shape operator, we can now derive a representation of discrete mean curvature. Analogously to the continous setting, the discrete mean curvature is defined as $\operatorname{tr} S_f$, hence it is also constant on faces. First, using (3.5) and (3.39) we get

$$G_f^{-1} = \frac{1}{\det G_f} \begin{pmatrix} \|E_1\|^2 & \langle E_1, E_2 \rangle \\ \langle E_1, E_2 \rangle & \|E_2\|^2 \end{pmatrix}$$

and due to (3.6) we have $\det G_f = 4 a_f^2$ and hence one can easily show $\operatorname{tr} (G_f^{-1} M_i) = \frac{\|E_i\|}{4 \, a_f^2}$ for $i = 0, 1, 2$. Finally, this yields

$$\operatorname{tr} S_f = \operatorname{tr} (G_f^{-1} H_f) = -\sum_{i=0}^{2} \frac{\cos \frac{\theta_i}{2}}{a_f} \|E_i\| \,. \tag{3.43}$$

Remark I (Relation to non-conforming FEM): Based on (3.38) one could define an integrated discrete mean curvature on a face $T = T(f)$ by summing over all three edges E_i of f, i.e.

$$\int_T H(x)\,\mathrm{d}a = \frac{1}{2}\sum_{i=0}^{2} -2\cos\frac{\theta_i}{2}\,\|E_i\|\,,$$

where the factor $1/2$ in front accounts for the fact that each edge is counted in both adjacent faces. Then by *spatial averaging* one can derive a discrete mean curvature on faces H_f, i.e.

$$H_f = \frac{1}{|T|}\int_T H(x)\,\mathrm{d}a = -a_f^{-1}\sum_{i=0}^{2}\cos\frac{\theta_i}{2}\,\|E_i\|\,,$$

which correponds exactly to (3.43).

Remark II (Evaluation of embedded discrete shape operator): If we consider the tangent space given by the plane of $T(f)$ the canonical basis is given by (3.39). Then, by definition, the matrix representation of the embedded discrete shape operator wrt. that basis is given by $S_f \in \mathbb{R}^{2,2}$.

Generalization Grinspun *et al*. [GGRZ06] define a discrete shape operators on general meshes similar to the triangle-averaged operator introduced above. However, instead of prescribing an edge normal N_E to be the angle-bisecting normal at edge $E = T(f) \cap T'(f')$ the edge normal is supposed to fulfill $N_E \perp E$ and is parametrized over the angle γ_E between N_E and N_f. The vector $(\gamma_E)_E$ is then considered as another set of degrees of freedom.

Further references: [CSM03, BMF03, GHDS03, HP04, BWH$^+$06, GGRZ06, TW06, War06, HPW06, WBH$^+$07, War08, Sul08, HP11, Hee16, VVP$^+$16]

4 Deformations of discrete shells

Eventually, we want to study deformations and deformation paths of discrete surfaces, *i.e.* triangle meshes. In applications, *e.g.* in animation movies, the mesh represents (the boundary/skin of) a complex character and the deformation path is supposed to describe a natural and non-trivial motion of that character. To obtain intuitive, visually appealing and natural results one needs to have a physically sound model. To this end, we go one step back and start the physical modeling in the continuous setup. Discrete surfaces are approximations of regular surfaces which have the physical interpretation of a *thin shell*. Vice versa, thin shells are three-dimensional solids with a high ratio from width to thickness. Mathematically, they are represented as compact embedded surface describing the midsurface of the material. Finally, this (regular/smooth) midsurface is approximated by a discrete surface.

Usually, one starts with theory of $3D$ elasticity and investigates deformation energies of some solid $\Omega_\delta \subset \mathbb{R}^3$ with δ being a tiny but finite thickness of the material, *i.e.* Ω_δ is a thin shell or plate from the physical point of view. Then on considers $\delta \to 0$ based on a suitable notion of convergence or by further apriori assumptions.

4.1 Elasticity theory

First, we give a survey on the theory of elastic deformations of solid three-dimensional bodies; for further reading we refer to [Cia88, MH94, Bra07b]. Next, we derive a physically sound model for thin plates and shells based on concepts from $3D$ elasticity. This summary is based on the comprehensive and detailed descriptions found in several works by Ciarlet and co-workers [Cia00, Cia05, CM08].

Three-dimensional elasticity. Let $\mathcal{O} \subset \mathbb{R}^3$ be a homogenous[2] and solid object with boundary and $\phi \in W^{1,2}(\mathcal{O}; \mathbb{R}^3)$ a potentially large and nonlinear deformation. Typically, one assumes that ϕ is orientation preserving, *i.e.* $\det D\phi(x) > 0$ for all $x \in \mathcal{O}$, and injective (*i.e.*, no interpenetration of matter occurs). We postulate the existence of an *elastic deformation energy* $\mathcal{W}[\phi, \mathcal{O}]$ associated with the deformation ϕ. By definition, *elastic* means that $\mathcal{W}$ solely depends on the Jacobian $D\phi$ of ϕ. Furthermore, for so-called *hyperelastic* materials, $\mathcal{W}[\phi, \mathcal{O}]$ is the integral of an elastic energy density $W = W(D\phi)$, *i.e.*

$$\mathcal{W}[\phi, \mathcal{O}] = \int_{\mathcal{O}} W(D\phi) \, \mathrm{d}x \,. \tag{4.1}$$

A fundamental axiom of continuum mechanics is *frame indifference*, *i.e.* the invariance of the deformation energy with respect to rigid body motions. Hence, any coordinate transform $x \mapsto Qx + b$ for a rotation $Q \in SO(3)$ and a shift $b \in \mathbb{R}^3$ does not change the energy, *i.e.*

$$W(D\phi) = W(Q^{\mathrm{T}} D\phi Q) \quad \forall Q \in SO(3) \,.$$

A direct consequence is that W only depends on the so-called right Cauchy–Green strain tensor $C[\phi] = D\phi^{\mathrm{T}} D\phi$, which geometrically represents the metric measuring the deformed length in the undeformed reference configuration. The *elastic strain* is then defined by the difference $E[\phi] = \frac{1}{2}(C[\phi] - \mathbb{1})$.

Furthermore, we might assume $\mathcal{O}$ to be an *isotropic* material, *i.e.* a rotation of the material before applying a deformation yields the same energy as before, *i.e.*

$$W(D\phi) = W(D\phi Q) \quad \forall Q \in SO(3) \,.$$

It follows from the Rivlin-Erikson-Theorem [RE55] that the above two conditions lead to the fact that the energy density W only depends on the singular values $\lambda_1, \lambda_2, \lambda_3$ of $D\phi$, the so-called principal stretches. Instead of the principal stretches, one can equivalently describe the local deformation using the so-called invariants of the deformation gradient,

$$\begin{aligned} I_1 &= \|D\phi\|_F = \sqrt{\lambda_1^2 + \lambda_2^2 + \lambda_3^2} \,, \\ I_2 &= \|\mathrm{cof}\, D\phi\|_F = \sqrt{\lambda_1^2\lambda_2^2 + \lambda_1^2\lambda_3^2 + \lambda_2^2\lambda_3^2} \,, \\ I_3 &= \det D\phi = \lambda_1\lambda_2\lambda_3 \,, \end{aligned}$$

[2] This will later result in energy densities that do not depend on $x \in \mathcal{O}$.

where $\|A\|_F = \sqrt{\operatorname{tr}(A^{\mathrm{T}}A)}$ for $A \in \mathbb{R}^{d,d}$ and the cofactor matrix is given by $\operatorname{cof} A = \det A A^{-\mathrm{T}}$ for $A \in GL(d)$. Hence there is a function $\hat{W} : \mathbb{R}^3 \to \mathbb{R}$ with $W(D\phi) = \hat{W}(I_1, I_2, I_3)$, where I_1, I_2, and I_3 can be interpreted as the locally averaged change of an infinitesimal length, area, and volume during the deformation, respectively.

We shall furthermore assume that isometries, *i.e.* deformations with $D\phi^{\mathrm{T}} D\phi = \mathbb{1}$, are local minimizers with $W(D\phi) = 0$. Typical energy densities in this class are given by

$$W(D\phi) = \hat{W}(I_1, I_2, I_3) = a_1 I_1^p + a_2 I_2^q + \Gamma(I_3)\,, \tag{4.2}$$

for $a_1, a_2 > 0$ and a convex function $\Gamma : [0, \infty) \to \mathbb{R}$ with $\Gamma(I_3) \to \infty$ for $I_3 \to 0$ or $I_3 \to \infty$. In this work we focus on $p = q = 2$ which corresponds to the Mooney–Rivlin model [Cia88]. The built-in penalization of volume shrinkage, *i.e.* $\hat{W}(I_1, I_2, I_3) \to \infty$ for $\det D\phi \to 0$, enables us to control local injectivity. Incorporation of such a nonlinear elastic energy allows to describe large deformations with strong material and geometric nonlinearities, which cannot be treated by a linear elastic approach. A particular choice for a nonlinear elastic energy density was introduced in [Wir09] (*cf*. appendix A.1 of [WBRS11]) as

$$W(D\phi) = \frac{\mu}{2}\|D\phi\|_F^2 + \frac{\lambda}{4}(\det D\phi)^2 - \left(\mu + \frac{\lambda}{2}\right)\log\det D\phi - \frac{d\mu}{2} - \frac{\lambda}{4}\,, \qquad d \in \{2, 3\}\,. \tag{4.3}$$

Linear elasticity. If we assume the deformation ϕ to be "small", *i.e.* close to id, a linear approach might be sufficient. Let u be the displacement induced by ϕ, *i.e.* $u(x) = \phi(x) - x$, that means we assume $\|u(x)\|$ to be small for all $x \in \mathcal{O}$. Then the elastic strain $E = E[\phi]$ is linearized *geometrically* as follows:

$$E = \frac{1}{2}(D\phi^T D\phi - \mathbb{1}) = \frac{1}{2}\left(D(u + \mathrm{id})^T D(u + \mathrm{id}) - \mathbb{1}\right) = \frac{1}{2}(Du + Du^T) + O(Du^T Du)\,,$$

where $\epsilon[u] := \frac{1}{2}(Du + Du^T)$ is the linearized elastic strain. A typical energy density in linearized, isotropic elasticity reads

$$W^{\text{lin}}(D\phi) = W^{\text{lin}}(Du) = \frac{1}{2}\sigma : \epsilon[u]\,, \tag{4.4}$$

where $A : B = \operatorname{tr}(A^T B)$ for matrices $A, B \in \mathbb{R}^{d,d}$. Here σ is the so-called *stress-tensor* given by

$$\sigma = \lambda \operatorname{tr}\epsilon[u]\mathbb{1} + 2\mu\epsilon[u] = \frac{E}{1+\nu}\left(\epsilon[u] + \frac{\nu}{1-2\nu}\operatorname{tr}\epsilon[u]\mathbb{1}\right) \tag{4.5}$$

which represents a *linear material law*, *i.e.* the stress σ depends linearly on the (geometrically linearized) strain $\epsilon[u]$. The physical parameters $\lambda, \mu \in \mathbb{R}$ are the *Lamé parameters*, the parameters

$$E = \frac{\mu(3\lambda + 2\mu)}{\mu + \lambda}\,, \quad \nu = \frac{\lambda}{2(\lambda + \mu)}\,,$$

are denoted as *elastic modulus* and *Poisson's ratio*, respectively. The elastic modulus $E > 0$ is a number that measures an object's resistance to being deformed elastically. Poisson's ratio $0 < \nu < 0.5$ is the ratio of transverse contraction strain to longitudinal extension strain in the direction of stretching force. Virtually all common materials become narrower in cross section when they are stretched, hence ν is usually positive. Hence (4.4) can be rewritten as

$$W^{\text{lin}}(D\phi) = W^{\text{lin}}(Du) = \frac{1}{2}\sigma : \epsilon[u] = \frac{\lambda}{2}\left(\operatorname{tr}\epsilon[u]\right)^2 + \mu \operatorname{tr}\left(\epsilon[u]^2\right), \tag{4.6}$$

Notation: Using the so-called *elasticity tensor* $\mathbf{C} : \mathbb{R}^{3,3} \to \mathbb{R}^{3,3}$ the relation (4.5) can be written as $\sigma = \mathbf{C}\epsilon[u]$, *i.e.* (4.6) becomes $W^{\text{lin}}(Du) = \frac{1}{2}\,\mathbf{C}\epsilon[u] : \epsilon[u]$. Often the relation $\sigma = \mathbf{C}\epsilon[u]$ is written in *Voigt notation*:

$$\begin{pmatrix}\sigma_{11}\\ \sigma_{22}\\ \sigma_{33}\\ \sigma_{12}\\ \sigma_{13}\\ \sigma_{23}\end{pmatrix} = \frac{E}{(1+\nu)(1-2\nu)}\begin{pmatrix}1-\nu & \nu & \nu & & & \\ \nu & 1-\nu & \nu & & & \\ \nu & \nu & 1-\nu & & & \\ & & & 1-2\nu & & \\ & & & & 1-2\nu & \\ & & & & & 1-2\nu\end{pmatrix}\begin{pmatrix}\epsilon_{11}\\ \epsilon_{22}\\ \epsilon_{33}\\ \epsilon_{12}\\ \epsilon_{13}\\ \epsilon_{23}\end{pmatrix}$$

Remark I: The nonlinear elastic energy density (4.3) satisfies the following consistency condition:

$$W_{,FF}(\mathbb{1})(G,G) = \lambda(\operatorname{tr} G)^2 + \frac{\mu}{2}\operatorname{tr}\left((G+G^T)^2\right).$$

Remark II: The nonlinear elastic density (4.3) is invariant with respect to rigid body motions, *i.e.* $W(D\phi) = 0$ iff. $\phi(x) = Qx + b$ with $Q \in SO(3)$. However, this is true for the linear elastic density (4.6) only in an infinitesimal sense. In detail, W^{lin} is invariant with respect to linearized rigid body motions, *i.e.* $W^{\text{lin}}(D\phi) = 0$ iff. $\phi(x) = Ax + b$ with $A \in \mathbb{R}^{3,3}$ skew-symmetric.

Variational setup. In elasticity theory one typically considers variational problems as the minimization of

$$\mathcal{E}[\phi] = \int_{\mathcal{O}} W(D\phi)\,\mathrm{d}x - \int_{\mathcal{O}} F(\phi(x))\,\mathrm{d}x - \int_{\Gamma} G(\phi(x))\,\mathrm{d}a\,, \tag{4.7}$$

subject to suitable boundary conditions, where F and G represent body and boundary forces, respectively, and $\Gamma \subset \partial\mathcal{O}$. For linear elasticity one usually uses the representation in terms of the displacement $u = \phi - \mathrm{id}$, *i.e.*

$$\mathcal{E}^{\text{lin}}[u] = \frac{1}{2}\int_{\mathcal{O}} \mathbf{C}\epsilon[u] : \epsilon[u]\,\mathrm{d}x - \int_{\mathcal{O}} f\,u\,\mathrm{d}x - \int_{\Gamma} g\,u\,\mathrm{d}a\,, \tag{4.8}$$

for functions $f : \mathcal{O} \to \mathbb{R}$ and $g : \Gamma \to \mathbb{R}$ and subject to suitable boundary conditions. Existence of a minimzer of (4.8) is obtained by means of Korn's inequality and the Lax-Milgram theorem. A nonlinear existence theory for hyperelastic materials whose corresponding energy density W fulfills certain properties was established by John Ball [Bal77].

However, we will utilize $\mathcal{W}$ to define an elastic *dissimilarity measure* between *shapes*. That means, given two shapes $\mathcal{S}_A$ and $\mathcal{S}_B$ which are supposed to describe two elastic materials $\mathcal{O}_A$ and $\mathcal{O}_B$, we aim at minimizing $\phi \mapsto \mathcal{W}[\phi, \mathcal{S}_A]$ subject to the constraint $\phi(\mathcal{S}_A) = \mathcal{S}_B$. The dissimilarity measure is then given by

$$\mathrm{d}^2_{\text{elast}}(\mathcal{S}_A, \mathcal{S}_B) = \min_{\phi:\phi(\mathcal{S}_A)=\mathcal{S}_B} \int_{\mathcal{S}_A} W(D\phi)\,\mathrm{d}x\,. \tag{4.9}$$

Towards a two-dimensional theory. Physically, a shell is a three-dimensional body which is very thin in one dimension. The main objective of elastic shell theory is to predict the stress and the displacement arising in a thin shell in response to given forces. In a variational setup, this prediction is made by minimizing a suitable energy functional. In the following, we show how a simplification of the variational setup in three-dimensional elasticity (introduced above) leads to a two-dimensional theory. This simplification is done by exploiting the special geometry of the shell, and especially, the assumed "smallness" of the thickness of the shell, denoted by $\delta > 0$, *cf*. Fig. 2. Eventually, this assumption allows to eliminate some of the terms of lesser order of magnitude with respect to the thickness of the shell.

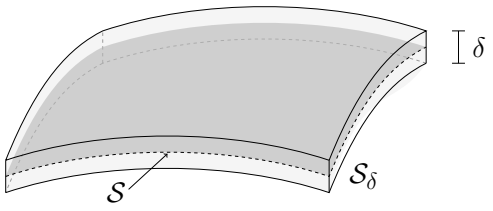

Figure 2: Elastic shell $\mathcal{S}_\delta \subset \mathbb{R}^3$ with finite thickness $\delta > 0$ and midsurface $\mathcal{S}$.

For simplicity, we will first consider *plate theories*, where the undeformed/reference configuration is *flat*. In contrast, in *shell theories*, the undeformed/reference configuration is already curved, *i.e.* given by some material with midsurface $\mathcal{S} \subset \mathbb{R}^3$. Let $\omega \subset \mathbb{R}^2$ be a domain in the plane, $\delta > 0$, and $\Omega_\delta = \omega \times (-\frac{\delta}{2}, \frac{\delta}{2}) \subset \mathbb{R}^3$ be a thickened plate, $p_\delta = (\xi, z) \in \omega \times (-\frac{\delta}{2}, \frac{\delta}{2})$. A deformation $\phi_\delta \in H^1(\Omega_\delta, \mathbb{R}^3)$ of this plate is characterized by a stored energy function $\mathcal{W}$ as in (4.1), *i.e.*

$$\mathcal{W}[\Omega_\delta, \phi_\delta] = \int_{\Omega_\delta} W(D\phi_\delta)\,\mathrm{d}p_\delta\,,$$

and the functional $\mathcal{W}[\Omega_\delta, \phi_\delta]$ is optimized subject to forces and boundary conditions.

In the *two-dimensional approach to shell theory*, the above minimization problem is replaced by a (presumably simpler) two-dimensional problem, which is eventually posed over the middle layer $\omega \subset \mathbb{R}^2$ (resp. middle surface $\mathcal{S} \subset \mathbb{R}^3$) of the plate (resp. shell). The two-dimensional approach to shell theory yields a variety of different shell models, which can be classified into two categories:

(i) The first category of models is obtained from the three-dimensional problem formulation by letting the thickness $\delta > 0$ of the shell go to zero. This can be formulated rigorously by means of Γ-convergence [DGDM83, Bra02]. Depending on the scaling, boundary conditions and applied forces one obtains either a so-called *membrane* shell model [LDR95, LDR96], or a flexual or *bending* shell model [FJM02a, FJM02b, FJMM03].

(ii) The second category of models are obtained from the three-dimensional model by restricting the range of admissible deformations by means of specific a priori assumptions that are supposed to take into account the smallness of the thickness.

In the following, we present the main concepts from these two categories briefly.

4.2 Linear elastic shells: Reissner-Mindlin and Kirchhoff-Love model

Let $\omega \subset \mathbb{R}^2$ bounded and simply connected, $\gamma := \partial\omega$ Lipschitz. In particular, we only consider *plates* here, that means the two-dimensional domain ω is flat and not curved. For $\delta > 0$ we define the reference domain of a *thin plate* by $\Omega_\delta = \omega \times (-\frac{\delta}{2}, \frac{\delta}{2})$. As above, we write $p_\delta = (\xi, z) \in \Omega_\delta$ with $\xi \in \omega$ and $-\frac{\delta}{2} < z < \frac{\delta}{2}$. Let us assume there is a body force $f : \Omega_\delta \to \mathbb{R}^3$ with $f \parallel e_3$ and $f(p_\delta) = f(\xi)$. There are no boundary forces and we make use of *clamped boundary conditions*, that means we postulate $u(x) = u_\partial(x)$ for all $x \in \Gamma_\delta := \gamma \times (-\frac{\delta}{2}, \frac{\delta}{2})$, and $u_\partial : \Gamma_\delta \to \mathbb{R}^3$ a given function. For simplicity we assume that $u_\partial \equiv 0$.
We consider a displacement

$$u = \begin{pmatrix} u_1 \\ u_2 \\ u_3 \end{pmatrix} : \Omega_\delta \to \mathbb{R}^3 ,$$

which is supposed to minimize some elastic energy subject to the body forces and (clamped) boundary conditions.

To derive a two-dimensional elastic model we make use of the following apriori assumptions:

(H1) normal segmets undergo affine transformations

(H2) displacement in vertical direction only depends on ξ, *i.e.* $u_3(p_\delta) = w(\xi)$ for some function $w : \omega \to \mathbb{R}$

(H3) points on $\omega \times \{0\}$ are only deformed in e_3-direction, *i.e.* $u_1(\xi, 0) = u_2(\xi, 0) = 0$ for all $\xi \in \omega$.

Summarizing (H1)-(H3) we get

$$\begin{pmatrix} u_1 \\ u_2 \end{pmatrix}(p_\delta) = -z\,\theta(\xi)$$
$$u_3(p_\delta) = w(\xi)$$

for some mappings $\theta : \omega \to \mathbb{R}^2$ and $w : \omega \to \mathbb{R}$. A fourth hypotheses reads

(H4) normal stress vanishes, *i.e.* $\sigma_{33} = 0$ where $\sigma = \mathbf{C}\epsilon[u]$.

The hypotheses (H1)-(H4) lead to the *Reissner-Mindlin* plate model.

If we add another hypothesis, the so-called *normal hypothesis* or *Kirchhoff-Love hypothesis*, *i.e.*

(H5) deformed normal is again normal to the deformed midsurface

we obtain the *Kirchhoff-Love* plate model.

The deformed tangent vectors resp. the deformed normal of ω are given by the partial derivatives of $\phi = \mathrm{id} + u$ at $(\xi, 0)$:

$$\partial_i \phi(\xi,0) = \begin{pmatrix} e_i \\ \partial_{\xi_i} w(\xi) \end{pmatrix}, \quad i = 1,2, \qquad \partial_3 \phi(\xi,0) = \begin{pmatrix} -\theta(\xi) \\ 1 \end{pmatrix}.$$

Deformed tangent vectors are again tangent to the deformed midsurface, however, this is in general not true for deformed normals. However, (H5) postulates exactly this situation, *i.e.* we have

$$\text{H(5)} \quad \Rightarrow \quad \partial_i \phi(\xi,0) \perp \partial_3 \phi(\xi,0)\,, \quad i = 1,2 \quad \Rightarrow \quad \theta = \nabla_\xi w\,.$$

Next we derive a $2D$ plate model based on linear elasticity and the Reissner-Mindlin assumptions.

$$u = \begin{pmatrix} -z\,\theta(\xi) \\ w(\xi) \end{pmatrix} \quad \Rightarrow \quad Du = \begin{pmatrix} -zD_\xi\theta & -\theta \\ (\nabla_\xi w)^T & 0 \end{pmatrix} \quad \Rightarrow \quad \epsilon[u] = \begin{pmatrix} -z\epsilon[\theta] & \frac{1}{2}(\nabla_\xi w - \theta) \\ \frac{1}{2}(\nabla_\xi w - \theta)^T & 0 \end{pmatrix}$$

In particular, $\epsilon_{33}[u] = 0$. Note that (4.5) and (H4) imply

$$0 = \sigma_{33} = \frac{E}{1+\nu}(\epsilon_{33}[u] + \frac{\nu}{1-2\nu}(\epsilon_{11}[u] + \epsilon_{22}[u] + \epsilon_{33}[u])) \quad \Rightarrow \quad \epsilon_{11}[u] + \epsilon_{22}[u] = 0\,.$$

Hence, since $\operatorname{tr}\epsilon[u] = 0$ we get $\sigma : \epsilon[u] = \frac{E}{1+\nu}(\epsilon[u] : \epsilon[u])$ and hence

$$\begin{aligned}
\mathcal{E}^{\text{lin}}[u] = \mathcal{E}^{\text{lin}}[w,\theta] &= \int_{\Omega_\delta} \frac{1}{2}\sigma : \epsilon[u] - f(x)\,u(x)\,\mathrm{d}x \\
&= \int_\omega \int_{-\frac{\delta}{2}}^{\frac{\delta}{2}} \frac{E}{2(1+\nu)}\Big(z^2\,\epsilon[\theta] : \epsilon[\theta] + 2\cdot\frac{1}{4}|\nabla_\xi w - \theta|^2\Big) - f(\xi)w(\xi)\,\mathrm{d}z\,\mathrm{d}\xi \\
&= \frac{\delta^3 E}{24(1+\nu)}\int_\omega \epsilon[\theta] : \epsilon[\theta]\,\mathrm{d}\xi + \frac{\delta E}{4(1+\nu)}\int_\omega |\nabla_\xi w - \theta|^2\,\mathrm{d}\xi - \delta\int_\omega f\,w\,\mathrm{d}\xi \\
&= \frac{\delta^3}{2}a(\theta,\theta) + \delta\gamma\|\nabla_\xi w - \theta\|_{L^2}^2 - \delta(f,w)_{L^2}\,.
\end{aligned}$$

where we set $\gamma = \frac{E}{4(1+\nu)}$ and

$$a(\theta,\psi) := \frac{E}{12(1+\nu)}\int_\omega \epsilon[\theta] : \epsilon[\psi]\,\mathrm{d}\xi\,.$$

The Euler-Lagrange equation for the corresponding optimization problem reads:
Find $(\theta, w) \in (H_0^1(\omega))^2 \times H_0^1(\omega)$ such that

$$\begin{aligned}
\delta^3 a(\theta,\psi) + 2\delta\gamma(\theta - \nabla_\xi w, \psi)_{L^2} &= 0 \qquad && \forall \psi \in (H_0^1(\omega))^2 \\
2\gamma(\nabla_\xi w, \nabla_\xi \vartheta)_{L^2} &= (f,\vartheta)_{L^2} && \forall \vartheta \in H_0^1(\omega)
\end{aligned}$$

Remark: Note that $0 = \operatorname{tr}\epsilon[u] = -z\operatorname{tr}\epsilon[\theta]$ implies $\operatorname{div}\theta = \operatorname{tr}\epsilon[\theta] = 0$. Since $\vartheta \in H_0^1(\omega)$ we have $(\theta, \nabla_\xi\vartheta)_{L^2} = -(\operatorname{div}\theta, \vartheta)_{L^2} = 0$.

Under the Kirchhoff-Love hypothesis the functional $\mathcal{E}^{\text{lin}}[u]$ simplifies further to

$$\mathcal{E}^{\text{lin}}[u] = \mathcal{E}^{\text{lin}}[w] = \delta^3\frac{E}{24(1+\nu)}\int_\omega |D^2 w|^2\,\mathrm{d}\xi - \delta\int_\omega f\,w\,\mathrm{d}\xi\,. \tag{4.10}$$

Saddle point problem and mixed methods. However, a standard FEM approach to optimize (4.10) requires H^2-conforming elements. Hence one usually makes use of a mixed method based on a saddle point formulation:

$$\text{Minimize } \frac{1}{2}a(\theta,\theta) - (f,w)_{L^2}\,, \qquad \text{subject to the constraint } \theta = \nabla_\xi w\,,$$

where we have set $\delta = 1$ for the ease of notation. This leads to the Lagrange functional $\mathcal{L} : \mathcal{X} \times M \to \mathbb{R}$ with

$$\mathcal{L}(w, \theta; \lambda) = \frac{1}{2} a(\theta, \theta) - (f, w)_{L^2} + (\lambda, \nabla_\xi w - \theta)_{L_2} ,$$

with primal variables $(w, \theta) \in \mathcal{X}$ and the "Lagrange multiplier" $\lambda \in M$. The necessary conditions for a saddle point lead to a *mixed formulation* given by

$$\begin{aligned} \forall (v, \psi) \in \mathcal{X} : \quad & 0 = \partial_{(w,\theta)} \mathcal{L}(w, \theta; \lambda)[(v, \psi)] = a(\theta, \psi) + (\nabla_\xi v - \psi, \lambda)_{L^2} - (f, v)_{L^2} \\ \forall \mu \in M : \quad & 0 = \partial_\lambda \mathcal{L}(w, \theta; \lambda)[\mu] = (\nabla_\xi w - \theta, \mu)_{L^2} \end{aligned}$$

To solve these equations, one can choose different spaces for $\mathcal{X}$ and M, respectively. A canonical choice would be $\mathcal{X} = H_0^2(\omega) \times (H_0^1(\omega))^2$ and $M = H^{-1}(\omega)$. However, to avoid the H^2-regularity for the w component one can also choose $\mathcal{X} = (H_0^1(\omega))^3$ and $M = H(\mathrm{div}\,, \omega) := \{\eta \in H^{-1}(\omega) : \mathrm{div}\, \eta \in H^{-1}(\omega)\}$. Actually, one can show existence of solutions of the necessary conditions in both cases. In practice, the latter choice (with less required regularity!) is often preferred. A well-established discretization of these spaces in the so-called *Discrete Kirchhoff Triangle* (DKT).

4.3 Membrane and bending energies by Γ-convergence

As in the previous section we first study *plate theories* derived from $3D$ elasticity. However, in contrast to the previous section, we here study an ansatz-free approach by means of Γ-convergence. For an introduction to the concepts of Γ-convergence we refer to [DGDM83, Bra02].

Remark: Let us emphasize in particular that we focus on the *qualitative* understanding of the rigorous derivations, *i.e*. we are interested in which objects the limit depends on. These objects will then be used to define a physically sound dissimilarity measure between two thin shells. Hence we neglect *quantitative* aspects, *e.g*. the detailed shape of limit integrands or values of physical constants in the limit, as these will later be chosen individually for different applications.

Let $\omega \subset \mathbb{R}^2$ bounded and simply connected, $\gamma := \partial\omega$ Lipschitz. As, we first only consider *plates* here, that means the two-dimensional domain ω is flat and not curved. For $\delta > 0$ we define the reference domain of a *thin plate* by $\Omega_\delta = \omega \times (-\frac{\delta}{2}, \frac{\delta}{2})$. The starting point is the elastic energy of a deformation $\phi_\delta \in H^1(\Omega_\delta, \mathbb{R}^3)$, *i.e*.

$$\mathcal{W}[\phi_\delta, \Omega_\delta] = \int_{\Omega_\delta} W(D\phi) \, \mathrm{d}p_\delta \tag{4.11}$$

for some frame-indifferent elastic energy density $W : \mathbb{R}^{3,3} \to \mathbb{R}$ which is minimized on $SO(3)$ and fulfills $W(\mathbb{1}) = 0$ and $W(F) = \infty$ if $\det F \leq 0$. Furthermore, one usually assumes some regularity and certain growth conditions. Typical energy densities are for instance

- The distance to the special orthogonal group, *i.e*. $W(F) = \mathrm{dist}^2(F, SO(3)) \approx \frac{1}{4}\|F^T F - \mathbb{1}\|_F^2$.
- A generic isotropic material is described by the *St Venant-Kirchhoff* density given by

  $$W^{\text{StVK}}(F) = \frac{\lambda}{8}(\mathrm{tr}\,(F^T F - \mathbb{1}))^2 + \frac{\mu}{4}\mathrm{tr}\,(F^T F - \mathbb{1})^2 . \tag{4.12}$$

  Note that $W^{\text{StVK}}(D\phi_\delta) = \frac{\lambda}{2}(\mathrm{tr}\, E[\phi_\delta])^2 + \mu \mathrm{tr}\,(E[\phi_\delta]^2)$, with $E[\phi_\delta] = \frac{1}{2}(D\phi_\delta^T D\phi_\delta - \mathbb{1})$, hence W^{StVK} is deduced from W^{lin} in (4.6) by replacing the linearized argument $\epsilon[u]$ by its nonlinear counterpart $E[\phi_\delta]$.
- A general Mooney-Rivlin model:

  $$W(F) = a\|F\|_F^2 + b\|\mathrm{cof}\, F\|_F^2 + c(\det F)^2 - d \log \det F + e ,$$

  with $e \in \mathbb{R}$ s.t. $W(\mathbb{1}) = 0$. Neo-Hooke material: $b = 0$.

In the following we will consider the limit behaviour of (4.11) for $\delta \to 0$.

An excursion in Γ-convergence.

Definition 4.1 (Γ-convergence)**.** Let (X, d) be a metric space, $F_j : X \to \mathbb{R}$ a sequence of functionals and $F : X \to \mathbb{R}$. Then F_j Γ-converges to F with respect to d, *i.e.* $F_j \overset{\Gamma}{\to} F$, if

(i) *liminf condition*. For every sequence $(x_j)_j \subset X$ with $d(x_j, x) \to 0$ for some $x \in X$ we have

$$F[x] \leq \liminf_{j\to\infty} F_j[x_j]\,.$$

(ii) *limsup condition/recovery sequence.* For each $x \in X$ there is a sequence $(x_j)_j \subset X$ with $d(x_j, x) \to 0$ and

$$F[x] \geq \limsup_{j\to\infty} F_j[x_j]\,.$$

Some remarks on Γ-convergence:

(i) If $F_j \overset{\Gamma}{\to} F$ then F is lower semi-continuous (w.r.t. d), *i.e.* if $d(x_j, x) \to 0$ then $F[x] \leq \liminf_{j\to\infty} F[x_j]$.

(ii) If $F_j \overset{\Gamma}{\to} F$ and G is continuous, then $F_j + G \overset{\Gamma}{\to} F + G$.

(iii) But, if $F_j \overset{\Gamma}{\to} F$ and $G_j \overset{\Gamma}{\to} G$ then *not* necessarily $F_j + G_j \overset{\Gamma}{\to} F + G$.

(iv) If $F_j = F$ for all j, then *not* necessarily $F_j \overset{\Gamma}{\to} F$. (Limit has to be lsc.!)

Note the importance of lsc. functions: The *direct method of Calculus of Variations* states that if X is a reflexive Banach space, F is weakly lower semi-continuous and coercive, then F attains its minimum on X.

Example: $X = \mathbb{R}$ with $d(x, y) = \|x - y\|$, $F_j(x) = \sin(jx)$ and $F(x) \equiv -1$. Then $F_j \overset{\Gamma}{\to} F$. The *liminf condition* is trivial. Let $x \in \mathbb{R}$. Define $x_j \in \mathbb{R}$ s.t. $d(x, x_j) = \min\{d(x, y) : \sin(jy) = -1\}$. Then $d(x, x_j) \to 0$ and $-1 \geq F_j(x_j)$, which proves the *limsup condition*.

A function F is said to be coercive if the following holds: If $F[x_j]$ is bounded, then $(x_j)_j$ is precompact in X, *i.e.* has a converging subsequence. A function F is mildly coercive if $\inf_{x\in X} F[x] = \inf_{x\in K} F[x]$ for some compact set $K \subset X$. A sequence $(F_j)_j$ is said to be *equi-coercive* if the following holds: If $F_j(x_j)$ is bounded then $(x_j)_j$ is precompact in X. A sequence $(F_j)_j$ is said to be *equi-mildly coercive* if there is some compact set $K \subset X$ such that $\inf_{x_j\in X} F_j[x_j] = \inf_{x_j\in K} F_j[x_j]$ for all j. If F is coercive, then it is mildly coercive.

Some properties related to the existence/computation of minimizers:

(i) Let $F_j \overset{\Gamma}{\to} F$, x_j minimizer of F_j and $x_j \to x$. Then x is minimizer of F and $F_j[x_j] \to F[x]$.

(ii) Let $F_j \overset{\Gamma}{\to} F$, $(F_j)_j$ equi-mildly coercive, then thre is a minimizer x of F with $F[x] = \lim_{j\to\infty} \inf_{x_j\in X} F_j[x_j]$. Moreover, if $(x_j)_j$ is minimizing sequence, then every accumulation point is a minimum point of F.

Proof (i): Let us assume there is $x' \in X$ with $F[x'] < F[x]$. Then there is a sequence $x'_j \to x'$ with

$$F[x'] \underset{\text{Def.}4.1(ii)}{\geq} \limsup_{j\to\infty} F_j[x'_j] \geq \liminf_{j\to\infty} F_j[x'_j] \underset{x_j \text{ min. of } F_j}{\geq} \liminf_{j\to\infty} F_j[x_j] \underset{\text{Def.}4.1(i)}{\geq} F[x] \quad \lightning$$

Remark I: A minimizing sequence $(x_j)_j$ fulfills $\lim_j F_j[x_j] = \lim_j \inf_{x\in X} F_j[x]$ which is *not* necessarily a sequence of minimizers (which might not exist!).
Remark II: Note that (i) requires existence of minimizers of F_j *and* convergence of minimizers, whereas (ii) provides existance of minimizers without these two conditions.

Applications of Γ-convergence are for instance phase transitions or dimension reductions. In the latter case we consider the functional (4.11) depending on a small parameter $\delta > 0$ with $\delta \to 0$. However, for each $\delta > 0$ the

functional is defined on a different function space, *i.e.* $H^1(\Omega_\delta, \mathbb{R}^3)$. Hence one considers the variable transformation $p_\delta = (\xi, z) \in \Omega_\delta \mapsto p = (\xi, \delta z) \in \Omega_1$ and the corresponding gradient transformation $D_\delta = (D_\xi, \frac{1}{\delta}\partial_z)$, and defines a rescaled functional by

$$\mathcal{W}^*[\phi_\delta, \Omega_1] = \delta \int_{\Omega_1} W(D_\delta \phi_\delta(p))\,\mathrm{d}p \tag{4.13}$$

where $p = (\xi, z)$. Note that still $\mathcal{W}^*[\phi_\delta, \Omega_1] = \mathcal{W}[\phi_\delta, \Omega_\delta]$.

Depending on the boundary conditions a characteristic scaling of the elastic energy (4.11) resp. (4.13) is observed. If the boundary conditions induce a stretching of the midplane ω, *e.g.* by

$$\Omega_\delta = (-1,1)^2 \times (-\frac{\delta}{2}, \frac{\delta}{2}), \quad \phi_\delta(p_\delta)\Big|_{\xi_1=\pm 1} = p_\delta \pm (a,0,0),$$

for some $a > 0$, we observe $\mathcal{W}^*[\phi_\delta, \Omega_1] \sim \mathcal{W}[\phi_\delta, \Omega_\delta] \sim \delta$. If we apply compressive boundary conditions, we have

$$\Omega_\delta = (-1,1)^2 \times (-\frac{\delta}{2}, \frac{\delta}{2}), \quad \phi_\delta(p_\delta)\Big|_{\xi_1=\pm 1} = p_\delta \mp (b,0,0), \tag{4.14}$$

for some $b \in (0,1)$, we observe $\mathcal{W}^*[\phi_\delta, \Omega_1] \sim \mathcal{W}[\phi_\delta, \Omega_\delta] \sim \delta^3$. In particular, the plate will accommodate the boundary conditions by bending while keeping its midsurface unstretched. This leads to the investigation of two different types of models. First, a *membrane limit theory* is derived by studying the Γ-convergence of the rescaled functional $\delta^{-1}\,\mathcal{W}^*[\phi_\delta, \Omega_1]$ for $\delta \to 0$. Second, a *bending limit theory* is derived by studying the Γ-convergence of the rescaled functional $\delta^{-3}\,\mathcal{W}^*[\phi_\delta, \Omega_1]$ for $\delta \to 0$.

Γ-limit for the membrane model. We assume the following growth condition

$$c_1\|F\|^2 - c_2 \le W(F) \le c_3\|F\|^2 + c_4\,, \tag{4.15}$$

for real numbers $c_i \ge 0$ and define rescaled functional

$$\mathcal{W}^\delta_{\text{mem}}[\phi_\delta, \Omega_\delta] := \frac{1}{\delta}\mathcal{W}^*[\phi_\delta, \Omega_1] = \int_{\Omega_1} W(D_\delta \phi(p))\,\mathrm{d}p\,.$$

Theorem 4.2 (Membrane Γ-limit, [LDR95, LDR96])**.** *The sequence $(\mathcal{W}^\delta_{mem})_\delta$ is uniformly coercive in H^1 and $\mathcal{W}^\delta_{mem} \xrightarrow{\Gamma} \mathcal{W}_{mem}$ w.r.t. the weak H^1-topology with*

$$\mathcal{W}_{mem}[\phi, \omega] = \int_\omega QW_{2D}(D\phi)\,\mathrm{d}\xi\,, \quad \phi \in H^1(\omega, \mathbb{R}^3)\,,$$

where $QW_{2D} : \mathbb{R}^{3,2} \to \mathbb{R}$ arises from a double relaxation process:

(1) For $F \in \mathbb{R}^{3,2}$ define $W_{2D}(F) = \min_{b\in\mathbb{R}^3} W(F|b)$

(2) Computation of quasi-convex envelope, i.e. $QW_{2D}(F) = \inf\{\fint_\omega W_{2D}(F + D\phi(x))\,\mathrm{d}x : \phi \in W^{1,\infty}_0\}$

If W fulfills the growth condition (4.15), then the relaxation of $\int_\Omega W(D\phi)\,\mathrm{d}x$ is given by $\int_\Omega QW(D\phi)\,\mathrm{d}x$ (w.r.t. the weak H^1-topology). The relaxation $\mathrm{rel}\,F$ of some functional F is given by $\mathrm{rel}\,F = \sup_G\{G \text{ lsc. } : G \le F\}$.

Some remarks:

- Thm.4.2 holds in $W^{1,p}$ for $p \in (1,\infty)$ if (4.15) is replaced by a corresponding p-growth condition.
- A corresponding result holds for a curved reference domain, *i.e.* ω is replaced by some compact and smooth surface $\mathcal{S} \subset \mathbb{R}^3$.
- For general elastic densities W the computation of QW_{2D} can be very complex.

The growth conditions (4.15) are fulfilled by typical energy densities representing isotropic materials, *e.g.* by (4.12). Furthermore, if the original density W was frame-indifferent, then the limit density is also frame-indifferent and depends on the metric of the deformed middle surface only [LDR96]. If additionally $W(F) \ge W(\mathbb{1})$ for all $F \in \mathbb{R}^{3,3}$, which is always the case in our examples as we assume $W(\mathbb{1}) = 0$ and $W \ge 0$, the corresponding membrane shell energy is constant under compression, *i.e.* the shell offers no resistance to crumpling [LDR96].

Qualitative properties of membrane limit. For frame-indifferent and isotropic densities the limit membrane energy can be written as an integral over the midsurface $\mathcal{S}$ whose integrand depends on the principal invariants of the right Cauchy-Green strain tensor $C[\phi] = D\phi^T D\phi$ only (*cf*. Sec. 4.1), where $\phi : \mathcal{S} \to \mathbb{R}^3$ is a deformation of the midsurface $\mathcal{S}$ to $\mathcal{S}^\phi = \phi(\mathcal{S})$. In detail, the pointwise linear operator $C[\phi]$ measures the distortion of tangent vectors which are mapped from $T_p\mathcal{S}$ to $T_{\phi(p)}\mathcal{S}^\phi$ for some arbitrary point $p \in \mathcal{S}$, *i.e.*

$$g_p(C[\phi]V, W) = g_{\phi(p)}(D\phi\, V, D\phi\, W)\,, \quad V, W \in T_p\mathcal{S}\,. \tag{4.16}$$

If we assume that a local neighborhood of p and $\phi(p)$, respectively, are parametrized over the same domain $\omega \subset \mathbb{R}^2$ by immersions $x, x^\phi : \omega \to \mathbb{R}^3$, we can formally write $\phi = x^\phi \circ x^{-1}$. This concatenation property has been used in [CLR04, LDRS05] to derive a two-dimensional representation of $C[\phi] \in \mathbb{R}^{3,3}$ by a distortion tensor $\mathcal{G}[\phi] \in \mathbb{R}^{2,2}$; we refer to [Hee11] for details. In particular, we can write

$$\mathcal{G}[\phi] = g^{-1} g_\phi \tag{4.17}$$

with $g = Dx^T Dx$ and $g_\phi = (Dx^\phi)^T (Dx^\phi)$ denoting the first fundamental form of the undeformed and deformed configuration, respectively. Note that $\mathcal{G}[\phi]$ as well as g and g_ϕ are defined pointwise.
From the considerations above we deduce a membrane shell energy $\mathcal{W}_{\text{mem}}$ which is supposed to measure the dissimilarity in terms of tangential stretching and shearing induced by a deformation ϕ of the undeformed (reference) shell $\mathcal{S}$, *i.e.*

$$\mathcal{W}_{\text{mem}}[\mathcal{S}, \phi] = \int_{\mathcal{S}} W_{\text{mem}}(\mathcal{G}[\phi])\, \mathrm{d}a\,. \tag{4.18}$$

We shall make use of the density defined in (4.3) with $d = 2$. In particular, we have $W_{\text{mem}}(F) = W_{\text{mem}}(\operatorname{tr} F, \det F)$ as well as $W_{\text{mem}}(\mathbb{1}) = 0$ and $\partial_F W_{\text{mem}}(\mathbb{1}) = 0$.

Γ-limit for the bending model (for plates). We have seen that the elastic energy (4.11) resp. (4.13) scales like δ^3 if we apply compressive boundary conditions (4.14). In particular, the plate accommodates the boundary conditions by bending while keeping its midsurface unstretched. However, as the volume of $\mathcal{S}_\delta$ scales like δ the integrand $W(D\phi_\delta)$ approaches zero much faster. That means, since W is assumed to be minimized exactly on $SO(3)$, the Jacobian $D\phi_\delta \in \mathbb{R}^{3,3}$ tends in a certain sense to $SO(3)$. Friesecke, James and Müller [FJM02b] came up with a rigorous derivation of the thin-plate limit of three-dimensional nonlinear elasticity theory, not just under the special compressive boundary conditions considered above but under any boundary condition that does not induce tangential distortion of the midsurface. As for the derivation of the membrane model, the mathematical setting in which these results are formulated is that of Γ-convergence. However, due to the scaling mentioned above, for the derivation of the bending model the limit process of

$$\mathcal{W}^\delta_{\text{bend}}[\phi_\delta, \Omega_\delta] := \frac{1}{\delta^3} \int_{\Omega_\delta} W(D\phi_\delta)\ \mathrm{d}p_\delta = \frac{1}{\delta^2} \int_{\Omega_1} W(D_\delta \phi_\delta)\ \mathrm{d}p \tag{4.19}$$

is considered for $\delta \to 0$. Although the approaches are similar, the bending model is more difficult to derive since the limit functional contains higher derivatives and one is thus dealing with a singular perturbation problem.

Let $W : R^{3,3} \to \mathbb{R}$ be a continuous and frame-indifferent energy density fulfilling the growth condition $W(F) \geq c\,\mathrm{dist}^2(F, SO(3))$ as well as $W(F) = 0$ if $F \in SO(3)$. For simplicity, we further assume that W represents an *isotropic* material which satisfies the consistency relation

$$W_{,FF}(\mathbb{1})(G, G) = \lambda(\operatorname{tr} G)^2 + \frac{\mu}{2} \operatorname{tr}\left((G + G^T)^2\right). \tag{4.20}$$

For example, W describes a St Venant-Kirchhoff material as in (4.12).

Theorem 4.3 (Bending Γ-limit for plates, [FJM02a, FJM02b])**.** *Under the assumptions on W stated above, the following convergence holds in the H^1-topology for $\delta \to 0$:*

$$\mathcal{W}^\delta_{\textit{bend}}[\phi_\delta, \Omega_\delta] \quad \xrightarrow{\Gamma} \quad \mathcal{W}^0_{\textit{plate}}[\phi, \omega]\,,$$

where $\mathcal{W}^\delta_{\textit{bend}}[\phi_\delta, \Omega_\delta]$ as in (4.19) *and*

$$\mathcal{W}^0_{\textit{plate}}[\phi, \omega] = \begin{cases} \frac{1}{24} \int_\omega \left(2\mu \operatorname{tr}\left(h[\phi]^2\right) + \frac{\lambda\mu}{\mu + \lambda/2} (\operatorname{tr} h[\phi])^2\right) \mathrm{d}\xi & ,\textit{on isometries } \phi : \omega \to \mathbb{R}^3 \\ +\infty & ,\textit{otherwise} \end{cases}.$$

Remark: The limiting energy thus depends on the second fundamental form $h[\phi] = Dn^T D\phi$, where ϕ can be thought of being a parametrization of the deformed plate $\phi(\omega)$, *i.e.* $n \parallel (\phi_{,1} \times \phi_{,2})$. Note that $\phi : \omega \to \mathbb{R}^3$ is an isometry iff. $(g_\phi)_{ij} = \phi_{,i} \cdot \phi_{,j} = \delta_{ij}$, *i.e.* in particular $\det g_\phi = 1$.

*Idea of recovery sequence (*cf. *[Bar15]).* For simplicity, we consider a St.Venant-Kirchhoff material (4.12) with $\lambda = 0$ and $\mu = 1$, *i.e.* $W(F) = \frac{1}{4}\|F^T F - \mathbb{1}\|^2$. Furthermore, we consider the representation (4.13), *i.e.* $\mathcal{W}^\delta_{\text{bend}}[\phi_\delta, \Omega_\delta] = \delta \int_{\Omega_1} W(D_\delta \phi_\delta)\, \mathrm{d}p_\delta$, with $D_\delta = (D_\xi, \frac{1}{\delta}\partial_z)$. Let $\phi : \omega \to \mathbb{R}^3$ a deformation of the middle plate that we seek to *recover*. We assume the sequence of deformations $\phi_\delta : \Omega_1 \to \mathbb{R}^3$ is of the form

$$\phi_\delta(\xi, z) = \phi(\xi) + \delta z n(\xi)\,,$$

where n is the unit normal to the surface parametrized by ϕ, *i.e.* $\langle \partial_k \phi(\xi),\, n(\xi)\rangle = 0$ for $k = 1, 2$. This means, segments normal to ω are mapped to straight lines that are normal to the deformed surface (*cf*. Kirchhoff-Love hypothesis). We consider the splitting

$$D_\delta \phi_\delta = [D_\xi \phi, n] + \delta z [D_\xi n, 0]\,.$$

Since the second fundamental form $h = h[\phi] = (D_\xi \phi)^T D_\xi n$ is symmetric and $(D_\xi n)^T n = 0$ we get

$$\begin{aligned} D_\delta \phi_\delta^T D_\delta \phi_\delta &= \begin{bmatrix} (D_\xi\phi)^T D_\xi \phi & 0 \\ 0 & |n|^2 \end{bmatrix} + \delta z \begin{bmatrix} 2D_\xi \phi^T D_\xi n & (D_\xi n)^T n \\ n^T D_\xi n & 0 \end{bmatrix} + \delta^2 z^2 \begin{bmatrix} (D_\xi n)^T D_\xi n & 0 \\ 0 & 0 \end{bmatrix} \\ &= \begin{bmatrix} g + 2\delta z h + \delta^2 z^2 r & 0 \\ 0 & 1 \end{bmatrix} \end{aligned}$$

where $g = g[\phi] = (D_\xi \phi)^T D_\xi \phi$ is the first fundamental form and $r := (D_\xi n)^T D_\xi n$. Hence

$$\begin{aligned} \mathcal{W}^\delta_{\text{bend}}[\phi_\delta, \Omega_\delta] &= \frac{1}{\delta^3} \cdot \delta \int_{\Omega_1} \frac{1}{4} \|D_\delta \phi_\delta^T D_\delta \phi_\delta - \mathbb{1}\|^2 \,\mathrm{d}p = \frac{1}{4\delta^2} \int_\omega \int_{-\frac{1}{2}}^{\frac{1}{2}} \|(g - \mathbb{1}) + 2\delta z h + \delta^2 z^2 r\|^2 \,\mathrm{d}z\,\mathrm{d}\xi \\ &= \frac{1}{4\delta^2} \int_\omega \int_{-\frac{1}{2}}^{\frac{1}{2}} \|g - \mathbb{1}\|^2 + 4\delta z (g - \mathbb{1}) : h + 2\delta^2 z^2 (g - \mathbb{1}) : r + 4\delta^2 z^2 \|h\|^2 + 4\delta^3 z^3 h : r + \delta^4 z^4 \|r\|^2 \,\mathrm{d}z\,\mathrm{d}\xi \\ &= \int_\omega \frac{1}{4\delta^2} \|g - \mathbb{1}\|^2 + \frac{1}{24}(g - \mathbb{1}) : r + \frac{1}{12}\|h\|^2 + \frac{\delta^2}{20}\|r\|^2 \,\mathrm{d}\xi \\ &\xrightarrow{\delta \to 0} \begin{cases} \frac{1}{12} \int_\omega \|h\|^2 \,\mathrm{d}\xi & , \|g - \mathbb{1}\|^2 = 0 \\ +\infty & , \text{otherwise} \end{cases}, \end{aligned}$$

which correponds to $\mathcal{W}^0_{\text{plate}}[\phi, \omega]$ in Thm.4.3 with $\lambda = 0$ and $\mu = 1$.

***Convergence of minimizers.** A direct consequence of Γ-convergence is the convergence of minimizers of the corresponding optimization problem (subject to forces and boundary conditions). Assume we have body forces $f_\delta : \Omega_\delta \to \mathbb{R}^3$ and rescaled body forces $\tilde{f}_\delta : \Omega_1 \to \mathbb{R}^3$ with $\tilde{f}_\delta(\xi, z) = f_\delta(\xi, \delta z)$ such that $\delta^{-2}\tilde{f}_\delta \to f$ in $L^2(\Omega_1, \mathbb{R}^3)$ for some function f with $f(\xi, z) = f(\xi)$.

Let $(\phi_\delta)_{\delta > 0} \subset H^1(\Omega_\delta, \mathbb{R}^3)$ be a sequence of minimizers of

$$\mathcal{W}^\delta_{\text{bend}}[\phi_\delta, \Omega_\delta] - \int_{\Omega_\delta} f_\delta \cdot \phi_\delta \,\mathrm{d}p_\delta$$

subject to suitable boundary conditions. Then $(\phi_\delta)_\delta$ converges for $\delta \to 0$ in $H^1(\Omega_1, \mathbb{R}^3)$ to a function $\phi \in H^1(\Omega_1, \mathbb{R}^3)$. This limit function is independent of z, defines a parametrized surface $\mathcal{S} = \phi(\omega \times \{0\})$ with first fundamental form $g = (\nabla_\xi \phi)^T \nabla_\xi \phi = \mathbb{1}_2$ and satisfies $\phi \in H^2(\Omega_1, \mathbb{R}^3)$. Moreover, it minimizes

$$\mathcal{W}_{\text{plate}}[\phi, \omega] - \int_\omega f \cdot \phi \,\mathrm{d}a\,,$$

among all functions $\psi \in H^1(\Omega_1, \mathbb{R}^3)$ that are independent of z, satisfy $(\nabla_\xi \psi)^T \nabla_\xi \psi = \mathbb{1}$ and have the same boundary conditions.

Γ-limit for the bending model (for shells). More general, the two-dimensional midsurface of the reference configuration is already curved. Instead of $\omega \subset \mathbb{R}^2$ and $\Omega_\delta = \omega \times (-\delta/2, \delta/2)$, respectively, we consider a smooth and compact surface $\mathcal{S} \subset \mathbb{R}^3$ and

$$\mathcal{S}_\delta = \left\{ x + z\, n(x) \,\middle|\, x \in \mathcal{S}, z \in \left(-\frac{\delta}{2}, \frac{\delta}{2}\right) \right\} .$$

Theorem 4.4 (Bending Γ-limit for shells, [FJMM03])**.** *Under similar assumptions as in Thm.4.3 the scaled energy*

$$\mathcal{W}^\delta_{\text{bend}}[\phi_\delta, \mathcal{S}_\delta] = \frac{1}{\delta^3} \int_{\mathcal{S}_\delta} W(D\phi_\delta)\, \mathrm{d}p_\delta$$

Γ-converges w.r.t the H^1-topology to a two-dimensional limit functional given by

$$\mathcal{W}^0_{\text{shell}}[\phi, \mathcal{S}] = \begin{cases} \frac{1}{24} \int_{\mathcal{S}} \min_{v \in \mathbb{R}^3} Q(S^{\text{rel}}_\phi(p) + v \otimes n(p))\, \mathrm{d}a & , \phi \in \mathcal{A} \\ +\infty & , \text{otherwise} \end{cases} ,$$

with the quadratic form $Q(G) = W_{,FF}(\mathbb{1})(G, G)$ and the admissible set of isometric deformations

$$\mathcal{A} = \{ \phi \in W^{2,2}(\mathcal{S}, \mathbb{R}^3) \,|\, (D_{\text{tan}}\phi)^T (D_{\text{tan}}\phi) = \mathbb{1} \text{ a.e. on } \mathcal{S} \} .$$

Here the tangential derivative $D_{\text{tan}}\phi \in \mathbb{R}^{3,2}$ can be extended to a proper rotation $Q(p) = Q[\phi](p) \in SO(3)$ if ϕ is isometric. The two-dimensional limit energy density depends on the *relative shape operator* $S^{\text{rel}}_\phi(p) : T_p\mathcal{S} \to T_p\mathcal{S}$ as it has been defined in Def. 2.9. Note that the limit bending energy $\mathcal{W}^0_{\text{shell}}[\phi, \mathcal{S}]$ is only finite for deformations $\phi \in \mathcal{A}$, hence we will assume in the remainder of this paragraph that we are dealing with isometric deformations.

Remark: In Sec. 2.2 the relative shape oeprator has been defined via the pulled-back shape operator, *cf*. Def. 2.8. A different (but equivalent) derivation is given by the pointwise definition

$$S^{\text{rel}}_\phi(p) = S(p) - Q(p)^T\, S_\phi(\phi(p))\, Q(p) , \quad p \in \mathcal{S}, \tag{4.21}$$

where $S(p) : T_p\mathcal{S} \to T_p\mathcal{S}$ and $S_\phi(q) : T_q\mathcal{S}^\phi \to T_q\mathcal{S}^\phi$ are the shape operators on the undeformed and deformed configuration, respectively. Here we have used the notation $\mathcal{S}^\phi = \phi(\mathcal{S})$ and $q = \phi(p)$ for $p \in \mathcal{S}$. The relative shape operator is supposed to measure the (pointwise) difference between the shape operators on $\mathcal{S}$ and $\mathcal{S}^\phi$, respectively. However, as these operators live on different tangent spaces, *i.e*. rotated planes in $\mathbb{R}^3$, we must include proper rotations to ensure well-definedness of the pointwise difference. Hence $Q(p)$ and $Q(p)^T$ denote the linear mappings between the two different tangent spaces, as illustrated in the following diagram:

$$\begin{array}{ccc} T_p\mathcal{S} & \xrightarrow{\quad S(p) \quad} & T_p\mathcal{S} \\ {\scriptstyle Q(p)}\downarrow & & \uparrow{\scriptstyle Q(p)^T} \\ T_{\phi(p)}\phi(\mathcal{S}) & \xrightarrow[\quad S_\phi(\phi(p)) \quad]{} & T_{\phi(p)}\phi(\mathcal{S}) \end{array}$$

We have $Q(p) = D\phi(p) \in SO(3)$ and $D\phi(p)n(p) = n^\phi(\phi(p))$, where n^ϕ denotes the normal on the deformed surface. To this end, we can think of $Q^T(S_\phi \circ \phi)Q$ as being a *pulled-back* representation S^*_ϕ of the shape operator S_ϕ on the deformed configuration. The linear operator $S^*_\phi : T_p\mathcal{S} \to T_p\mathcal{S}$ is then implicitly defined as in Def. 2.8.

As for the membrane shell energy we use the analytic results presented above to extract a generic bending shell energy by setting

$$\mathcal{W}_{\text{bend}}[\mathcal{S}, \phi] = \int_{\mathcal{S}} W_{\text{bend}}(S^{\text{rel}}_\phi)\, \mathrm{d}a . \tag{4.22}$$

In general, we make use of the density

$$W_{\text{bend}}(A) = \alpha(\operatorname{tr} A)^2 + (1 - \alpha)\, \|A\|^2_F , \quad \alpha \in \{0, 1\} . \tag{4.23}$$

In particular, for $\alpha = 1$ we recover an adapted form of the Willmore energy measuring differences in mean curvature. Recall that the matrix representation of the relative shape operator in the parameter domain was defined in (2.6)

$$s_\xi^{\text{rel}}[\phi] = s_\xi - s_\xi^*[\phi] = g_\xi^{-1}(h_\xi - \tilde{h}_\xi)\,.$$

It is not difficult to verify that for $\alpha = 0$ we get

$$\mathcal{W}_{\text{bend}}[\mathcal{S}, \phi] = \int_{\mathcal{S}} \|S_\phi^{\text{rel}}\|_F^2 \,\mathrm{d}a = \int_\omega \operatorname{tr}\left(s_\xi^{\text{rel}}[\phi]^2\right)\sqrt{\det g}\,\mathrm{d}\xi\,, \tag{4.24}$$

and for $\alpha = 1$ we get

$$\mathcal{W}_{\text{bend}}[\mathcal{S}, \phi] = \int_{\mathcal{S}} \left(\operatorname{tr} S_\phi^{\text{rel}}\right)^2 \mathrm{d}a = \int_\omega \left(\operatorname{tr} s_\xi^{\text{rel}}[\phi]\right)^2 \sqrt{\det g}\,\mathrm{d}\xi\,. \tag{4.25}$$

Sketch of proof [Hee16]: In the following we drop the specification of the point $p \in \mathcal{S}$ in the notation. We have

$$\|S_\phi^{\text{rel}}\|_F^2 = \|S - S_\phi^*\|_F^2 = \sum_{i,j=1}^2 \left[\langle e_i, Se_j\rangle_{\mathbb{R}^3} - \langle e_i, S_\phi^* e_j\rangle_{\mathbb{R}^3}\right]^2,$$

$$\operatorname{tr} S_\phi^{\text{rel}} = \operatorname{tr}(S - S_\phi^*) = \sum_{i=1}^2 \left[\langle e_i, Se_i\rangle_{\mathbb{R}^3} - \langle e_i, S_\phi^* e_i\rangle_{\mathbb{R}^3}\right],$$

where (e_1, e_2, e_3) is the canonical basis of $\mathbb{R}^3$. Let us assume that a neighboorhoud of $p \in \mathcal{S}$ is parametrized by some chart $x : \omega \subset \mathbb{R}^2 \to \mathbb{R}^3$. For $\xi \in \omega$ such that $p = x(\xi)$ we have another basis (v_1, v_2, n) with $[v_1|v_2] = Dx(\xi)$ and $n = n(p)$ with

$$e_i = a_{1i}v_1 + a_{2i}v_2 + a_{3i}n\,,\quad a_i := \begin{pmatrix} a_{1i} \\ a_{2i} \\ a_{3i}\end{pmatrix} = [v_1|v_2|n]^{-1}e_i =: Ae_i\,,$$

where $A \in \mathbb{R}^{3,3}$ represents the change of basis. Hence using the linearity of S we can write

$$\langle e_i, Se_j\rangle = \langle a_{1i}v_1 + a_{2i}v_2 + a_{3i}n, a_{1j}Sv_1 + a_{2j}Sv_2 + a_{3j}Sn\rangle = \sum_{k,l=1}^2 a_{ki}a_{lj}g(v_k, Sv_l) = \sum_{k,l=1}^2 a_{ki}a_{lj}h_{kl}\,.$$

An analogous computation for $\langle e_i, S_\phi^* e_j\rangle$ and the identity $(AA^T)_{i,j\le 2} = g^{-1}$ yield the result. □

Full elastic model and dissimilarity measure. Given a surface $\mathcal{S} \subset \mathbb{R}^3$ representing a physical shell with thickness $\delta > 0$ and a deformation $\phi : \mathcal{S} \to \mathbb{R}^3$, a generic elastic deformation energy is given by

$$\int_{\mathcal{S}} \delta\, W_{\text{mem}}(\mathcal{G}[\phi]) + \delta^3\, W_{\text{bend}}(S_\phi^{\text{rel}})\,\mathrm{d}a\,, \tag{4.26}$$

with $W_{\text{mem}}(A) = W_{\text{mem}}(\operatorname{tr} A, \det A)$ as defined in (4.3) for $d = 2$ and W_{bend} as defined in (4.23). Nevertheless, for convenience we shall consider in the following a rescaled version of (4.26), namely

$$\mathcal{W}_{\mathcal{S}}[\phi] = \int_{\mathcal{S}} W_{\text{mem}}(\mathcal{G}[\phi]) + \eta\, W_{\text{bend}}(S_\phi^{\text{rel}})\,\mathrm{d}a\,, \tag{4.27}$$

where the bending weight η represents the squared thickness of the shell. Note that (4.27) is invariant with respect to rigid body motions by construction, *i.e.* $\mathcal{W}_{\mathcal{S}}[\phi] = 0$ and $d\mathcal{W}_{\mathcal{S}}[\phi] = 0$ if $\phi(x) = Qx + b$ with $Q \in SO(3)$ and $b \in \mathbb{R}^3$. In particular, we have

$$\mathcal{W}_{\mathcal{S}}[\mathrm{id}] = 0, \quad d\mathcal{W}_{\mathcal{S}}[\mathrm{id}] = 0. \tag{4.28}$$

Similar tp (4.9), we can derive a *dissimilarity measure* for two given shells $\mathcal{S}_A, \mathcal{S}_B \subset \mathbb{R}^3$ by minimizing (4.27) over all deformations satisfying $\phi(\mathcal{S}_A) = \mathcal{S}_B$, *i.e.*

$$\mathrm{d}^2_{\text{shell}}(\mathcal{S}_A, \mathcal{S}_B) = \min_{\phi:\phi(\mathcal{S}_A)=\mathcal{S}_B} \int_{\mathcal{S}} W_{\text{mem}}(\mathcal{G}[\phi]) + \eta\, W_{\text{bend}}(S_\phi^{\text{rel}})\,\mathrm{d}a\,. \tag{4.29}$$

However, we do not discuss whether this definition is actually well-defined, *i.e*. if there exists such a minimizer. Physically, one might regard the second shell $\mathcal{S}_B$ as a deformed version of the first shell $\mathcal{S}_A$, *i.e*., the corresponding material of $\mathcal{S}_B$ is just in a deformed configuration compared to its configuration in $\mathcal{S}_A$. Since every material point has a well-defined position, one can view this correspondence as *a priori* information. In this setup, one can then assume the dissimilarity measure to be well-defined. However, we will see in the next section that the well-posedness of the corresponding discrete dissimilarity measure is trivial by construction of the discrete shell space.

Remark: Note the relation between the dissimilarity measure (4.29) and Thm. 2.7: $\mathrm{d}^2_{\text{shell}}(\mathcal{S}_A, \mathcal{S}_B) = 0$ iff. $\mathcal{S}_A$ and $\mathcal{S}_B$ are congruent, *i.e*. they differ only by a rigid body motion.

Theorem 4.5 (Properties of isometries)**.** *Let $\mathcal{S} \subset \mathbb{R}^3$ be a surface parameterized by an isometric mapping $x : \Omega \to \mathbb{R}^3$,* i.e. *$g = \mathbb{1}$. Then we have $K = 0$, $\partial_i\partial_j x \cdot \partial_k x = 0$,* i.e. *$\partial_i\partial_j x = h_{ij} n$, and*

$$\|D^2 x\|_F = |\Delta x| = \|h\|_F = |H|\,.$$

Proof: We have $K = 0$ due to Gauß' Theorema Egregrium. Since $1 = g_{jj} = \partial_j x \cdot \partial_j x$ we have $0 = \partial_i(\partial_j x \cdot \partial_j x) = 2\partial_i\partial_j x \cdot \partial_j x$. Analogously, since $0 = g_{ij} = \partial_i x \cdot \partial_j x$ we have $0 = \partial_i(\partial_i x \cdot \partial_j x) = \partial_i^2 x \cdot \partial_j x + \partial_i x \cdot \partial_i\partial_j x = \partial_i^2 x \cdot \partial_j$. Hence $\partial_i\partial_j x \cdot \partial_k x = 0$. Since $\partial_i\partial_j x = \sum_k \Gamma^k_{ij}\partial_k x + h_{ij} n$ we have $\Gamma^k_{ij} = 0$ and $\partial_i\partial_j x = h_{ij} n$. In particular, Δx has no tangential component, *i.e*. $\Delta x = \beta n$. Since $(\Delta x) \cdot n = \operatorname{tr}(h) = \operatorname{tr}(s) = H$, we have $\beta = H$. The vectors $(\partial_1 x, \partial_2 x, n)$ form an orthonormal basis of $\mathbb{R}^3$ for every $\xi \in \Omega$, so that $|\partial_i\partial_j x| = |\partial_i\partial_j x \cdot n| = |h_{ij}|$ and hence

$$\|D^2 x\|_F^2 = \sum_{i,j=1}^{2} |\partial_i\partial_j x|^2 = \sum_{i,j=1}^{2} |\partial_i\partial_j x \cdot n|^2 = \|h\|^2\,.$$

Finally, we have $\|h\|_F^2 = \|s\|_F^2 = (\operatorname{tr} s)^2 - 2\det s = H^2 - 2K = H^2$. □

4.4 Discrete shells and discrete deformation energies

According to Def. 3.1, a *discrete surface* is a triangular mesh $\mathcal{M}_h = (\mathcal{V}, \mathcal{F})$ along with an injective embedding $E : \mathcal{V} \to \mathbb{R}^3$, such that $\mathcal{M}_h$ is a discrete 2-manifold which is orientable. In particular, a discrete surface is uniquely determined by its geometry and connectivity. We assume that $\mathcal{M}_h$ is a polyhedral approximation of the midsurface $\mathcal{S}$ of a thin elastic shell. Hence we will denote $\mathbf{S} := \mathcal{M}_h$ as a *discrete shell*.

In the following we consider (discrete) deformations between different discrete shells. Alternatively, we assume a designated *reference shell* to be given which prescribes the connectivity/topology encoded in the sets $\mathcal{V}$ and $\mathcal{F}$. Then different shells a given by different embeddings of the topologically identical mesh.

Definition 4.6 (Dense correspondence and discrete deformation)**.** We say that two discrete shells resp. triangular meshes are in *dense correspondence* or in 1-to-1-correspondence if they share the same connectivity/topology. Given two discrete shells $\mathbf{S}$ and $\tilde{\mathbf{S}}$ with embeddings $E : \mathcal{V} \to \mathbb{R}^3$ and $\tilde{E} : \mathcal{V} \to \mathbb{R}^3$, respectively, which are in dense correspondence. A discrete deformation $\Phi : \mathbf{S} \to \tilde{\mathbf{S}}$ is the unique piecewise affine mapping defined by its nodal values $\Phi(E(v_i)) := \tilde{E}(v_i)$ for $i = 1, \dots, |\mathcal{V}|$.

That means, if $X = (1-\xi_1-\xi_2)X_i + \xi_1 X_j + \xi_2 X_k \in T(f)$, where $T(f) = \{X_i, X_j, X_k\} \subset \mathbf{S}$ and $\xi_1, \xi_2 \in [0,1]$ barycentric coordinates, we have $\Phi(X) = (1-\xi_1-\xi_2)\tilde{X}_i + \xi_1\tilde{X}_j + \xi_2\tilde{X}_k$ with $\tilde{T}(f) = \{\tilde{X}_i, \tilde{X}_j, \tilde{X}_k\} \subset \tilde{\mathbf{S}}$.

Remark: The (pairwise) dense correspondence will guarantee the well-definedness of a dissimilarity measure on the space of discrete shells (*cf*. eq. (4.29)).

In the following we will consider families of discrete shells which are pairwise in dense correspondence. Actually, dense correspondence defines an equivalence relation, *i.e*. we consider a fixed equivalence class. This means, all discrete shells are based on the same sets of indices $\mathcal{V}$ and $\mathcal{F}$, respectively. Nevertheless, for two discrete shells $\mathbf{S}$ and $\tilde{\mathbf{S}}$ we will often denote the corresponding sets by $\mathcal{V}, \mathcal{F}$ and $\tilde{\mathcal{V}}, \tilde{\mathcal{F}}$, respectively. This convention simp[lifies the notation, *e.g*. a_f refers to the area of face f in $\mathbf{S}$, whereas $a_{\tilde{f}} := \tilde{a}_f$ denotes the area of face f in $\tilde{\mathbf{S}}$. Here we have to keep in mind that for $f_i \in \mathcal{F}$ and $\tilde{f}_i \in \tilde{\mathcal{F}}$ we actually have $f_i = \tilde{f}_i$ but $T(f_i) \neq \tilde{T}(\tilde{f}_i)$, since $\mathbf{S}$ and $\tilde{\mathbf{S}}$ have different embeddings.

Discrete membrane model. Let $\mathbf{S}$ and $\tilde{\mathbf{S}}$ two discrete shells that are in dense correspondence. We have elementwise constant first fundamental forms and a unique correspondence between all faces. Furthermore, we want to make use of the membrane model derived in Sec. 4.3 and in particular of the representation of the distortion tensor (4.17). Hence to describe membrane distortions induced by a discrete deformation $\Phi : \mathbf{S} \to \tilde{\mathbf{S}}$ we arrive at an elementwise constant, discrete distortion tensor

$$\mathcal{G}[\Phi]|_f = (G_f)^{-1}\, G_{f_\Phi} \in \mathbb{R}^{2,2}\,, \quad f \in \mathcal{F}, \quad f_\Phi = \tilde{f} \in \tilde{\mathcal{F}}\,. \tag{4.30}$$

Again using the continuous membrane model in Sec. 4.3 and in particular the generic membrane energy in (4.18) we define the *discrete membrane energy* by

$$\mathbf{W}_{\text{mem}}[\mathbf{S}, \tilde{\mathbf{S}}] = \int_{\mathbf{S}} W_{\text{mem}}(\mathcal{G}[\Phi])\,\mathrm{d}a = \sum_{f\in\mathcal{F}} a_f \cdot W_{\text{mem}}(\mathcal{G}[\Phi]|_f)\,, \quad \tilde{\mathbf{S}} = \Phi(\mathbf{S})\,. \tag{4.31}$$

Note that a one point quadrature is sufficient as we are dealing with an elementwise constant discrete distortion tensor. Different from (4.18), the discrete membrane energy directly depends on the undeformed and deformed discrete shell. For the membrane energy density W_{mem} we can use exactly the same density as in (4.18), *i.e.*

$$W_{\text{mem}}(\mathcal{G}[\Phi]|_f) = \frac{\mu}{2}\mathrm{tr}\,\mathcal{G}[\Phi]|_f + \frac{\lambda}{4}\det\mathcal{G}[\Phi]|_f - \left(\frac{\mu}{2}+\frac{\lambda}{4}\right)\log\det\mathcal{G}[\Phi]|_f - \mu - \frac{\lambda}{4}\,.$$

Note that $\mathrm{tr}\,\mathcal{G}[\Phi]|_f$ controls the local change of length, *i.e.* the change of edge lengths, whereas $\det\mathcal{G}[\Phi]|_f$ controls the local change of volume, *i.e.* the change of triangle volumes. In particular, the density grows quadratically for $\det\mathcal{G}[\Phi]|_f \to \infty$ but due to the log-term it grows even faster for $\det\mathcal{G}[\Phi]|_f \to 0$. This prevents a local interpenetration of matter, *i.e.* the degeneration of triangles. Finally, we have $W_{\text{mem}}(\mathbb{1}) = 0$ and $dW_{\text{mem}}(\mathbb{1}) = 0$.

Discrete bending model. Having a notion of a discrete shape operator given by (3.42) at hand, we can translate the general representation of a bending energy given in (4.22) (with the density (4.23) and $\alpha \in \{0, 1\}$) directly into the discrete setup. Setting $\alpha = 0$, as in (4.24), we can define a discrete bending energy via

$$\mathbf{W}_{\text{bend}}[\mathbf{S}, \tilde{\mathbf{S}}] = \sum_{f\in\mathcal{F}} a_f \cdot \mathrm{tr}\left((S_f - S_{f_\Phi})^2\right), \quad \tilde{\mathbf{S}} = \Phi(\mathbf{S})\,, \tag{4.32}$$

with $a_f = |T(f)|$ as above. Alternatively, by choosing $\alpha = 1$, as in (4.25), we can derive a discrete version of the Willmore energy:

$$\tilde{\mathbf{W}}_{\text{bend}}[\mathbf{S}, \tilde{\mathbf{S}}] = \sum_{f\in\mathcal{F}} a_f \cdot \left(\mathrm{tr}\,(S_f - S_{f_\Phi})\right)^2, \quad \tilde{\mathbf{S}} = \Phi(\mathbf{S})\,. \tag{4.33}$$

Note that a one point quadrature is again sufficient as we are integrating over an elementwise constant density.

A simplified discrete bending model. In the remainder of this section we investigate another definition of a discrete Willmore energy and derive a representation that corresponds to a non-conforming FEM approach. Furthermore, after some simplifications, we obtain the *Discrete Shells* bending model [GHDS03] as a special case.

In (3.43), we have computed a triangle-averaged mean curvature, *i.e.*

$$\mathrm{tr}\,S_f = \mathrm{tr}\,(G_f^{-1}H_f) = -\sum_{i=0}^{2}\frac{\cos\frac{\theta_i}{2}}{a_f}|E_i|\,.$$

The discrete mean curvature functional which can be written as a sum over edges:

$$\int_{\mathbf{S}} \mathrm{tr}\,S\,\mathrm{d}a = \sum_{f\in\mathcal{F}} a_f \cdot \mathrm{tr}\,S_f = \sum_{f\in\mathcal{F}}\sum_{i=0}^{2} -\cos\frac{\theta_i}{2}\,|E_i| = -2\sum_{E\in\mathcal{E}}\cos\frac{\theta_E}{2}\,|E|\,.$$

We introduce an area $d_E \in \mathbb{R}$ corresponding to an edge E, such that $|\mathbf{S}| = \sum_{E\in\mathcal{E}} d_E$ and $|d_E \cap d_{E'}| = 0$; a suitable choice (for closed meshes) is given *e.g.* by $d_E = \frac{1}{3}(a_f + a_{f'})$ if $E = T(f) \cap T(f')$, *cf.* Fig. 3. Furthermore, we

make use of the notation $l_E = |E|$. Then we rewrite the discrete mean curvature functional by introducing a mean curvature density at edges:

$$\int_{\mathbf{S}} \operatorname{tr} S \, \mathrm{d}a = \sum_{E \in \mathcal{E}} d_E \cdot \left(\frac{-2 \cos \frac{\theta_E}{2}}{d_E} \, l_E \right) .$$

In the spirit of [MDSB02] an approximative discrete Willmore energy can be deduced by squaring the mean curvature edge density, *i.e.*

$$\int_{\mathbf{S}} (\operatorname{tr} S)^2 \, \mathrm{d}a \approx \sum_{E \in \mathcal{E}} d_E \cdot \left(\frac{-2 \cos \frac{\theta_E}{2}}{d_E} \, l_E \right)^2 = \sum_{E \in \mathcal{E}} \frac{4 \cos^2(\frac{\theta_E}{2})}{d_E} \, l_E^2 \, . \tag{4.34}$$

Remark: Wardetzky *et al*. [WBH$^+$07] present a discretization of the Willmore functional using the non-conforming Crouzeix-Raviart element. The corresponding discrete Willmore energy (*i.e*. eq. (7) in [WBH$^+$07]) coincides exactly with the right hand side of (4.34). This underlines the fact that models derived by principles of *Discrete Differential Geometry* often correspond to non-conforming FEM approaches.

Now we further simplify (4.34) to derive the *Discrete Shells* bending model proposed in [GHDS03]. A Taylor expansion of the function $f(\theta) = -2 \cos \frac{\theta}{2}$ about $\theta = \pi$ yields $f(\theta) = (\theta - \pi) + O(|\theta - \pi|^3)$. Let $\mathbf{S}$ be a reference shell, *i.e*. the undeformed configuration. If we assume that we have an isometric[3] deformation $\Phi : \mathbf{S} \to \mathbb{R}^3$, *i.e*. $l_{\Phi(E)} = l_E$ and $d_{\Phi(E)} = d_E$, we obtain up to higher order terms

$$\int_{\mathbf{S}} \operatorname{tr} \left(S - S_\Phi \circ \Phi \right) \mathrm{d}a = \sum_{E \in \mathcal{E}} d_E \left(\frac{\theta_E - \theta_{\Phi(E)}}{d_E} \, l_E \right) .$$

Again in the spirit of [MDSB02], one arrives at the *Discrete Shells* bending model by squaring the discrete density, *i.e*.

$$\mathbf{W}^{\text{DS}}_{\text{bend}}[\mathbf{S}, \tilde{\mathbf{S}}] = \sum_{E \in \mathcal{E}} \frac{(\theta_E - \theta_{\Phi(E)})^2}{d_E} \, l_E^2 \, , \quad \tilde{\mathbf{S}} = \Phi(\mathbf{S}) \, . \tag{4.35}$$

Intuitively, $\mathbf{W}^{\text{DS}}_{\text{bend}}$ can be considered as a simplification of (4.33). Although (4.35) coincides exactly with the *Discrete Shells* bending energy introduced in [GHDS03], the authors in [GHDS03] derive their discrete bending energy by using results from [CSM03].

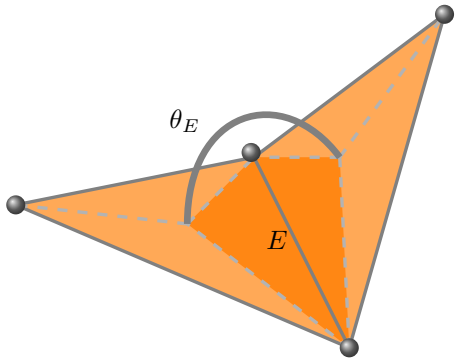

Figure 3: Support of the *Discrete Shells* bending energy [GHDS03]; the dihedral angle $\theta_E = \alpha_E - \pi$ at an edge E is defined as the angle between adjacent triangle normals, where α_E is the angle between the two faces. The darker region represents the area d_E associated with E.

[3]When deriving (discrete) bending models, one typically assumes to deal with *inextensible* materials which are characterized by mostly isometric deformations, *cf*. *e.g*. [GHDS03, BWH$^+$06]. This corresponds to the analytic results presented in Sec. 4.3, where bending modes are of higher order and hence only decisive when the present deformation is (almost) isometric.

A discrete dissimilarity measure. Finally, we are able to define a dissimilarity measure on the space of discrete shells, given by a discrete deformation energy:

Definition 4.7 (Discrete dissimilarity measure)**.** Given two discrete shells $\mathbf{S} = (\mathcal{N}, \mathcal{F}, \mathcal{E})$ and $\tilde{\mathbf{S}} = (\tilde{\mathcal{N}}, \tilde{\mathcal{F}}, \tilde{\mathcal{E}})$ that are in dense correspondence, *i.e.* there is a unique affine deformation Φ with $\tilde{\mathbf{S}} = \Phi(\mathbf{S})$. The *discrete deformation energy* $\mathbf{W} = \mathbf{W}_{\mathbf{S}}[\Phi] = \mathbf{W}[\mathbf{S}, \tilde{\mathbf{S}}]$ is defined by

$$\mathbf{W}[\mathbf{S}, \tilde{\mathbf{S}}] = \mathbf{W}_{\text{mem}}[\mathbf{S}, \tilde{\mathbf{S}}] + \eta\, \mathbf{W}_{\text{bend}}[\mathbf{S}, \tilde{\mathbf{S}}]\,,$$

where the *bending weight* $\eta = \delta^2$ represents the squared thickness of the shell. The *discrete membrane energy* and the *discrete bending energy*, respectively, are given by

$$\begin{aligned}
\mathbf{W}_{\text{mem}}[\mathbf{S}, \tilde{\mathbf{S}}] &= \sum_{f \in \mathcal{F}} a_f \cdot W_{\text{mem}}(\mathcal{G}[\Phi]|_f)\,, \\
\mathbf{W}_{\text{bend}}[\mathbf{S}, \tilde{\mathbf{S}}] &= \sum_{f \in \mathcal{F}} a_f \cdot W_{\text{bend}}(S_f - S_{\Phi(f)})\,,
\end{aligned}$$

where $\mathcal{G}[\Phi] \in \mathbb{R}^{2,2}$ denotes the discrete distortion tensor defined in (4.30) and $S \in \mathbb{R}^{2,2}$ the matrix representation of the discrete shape operator defined in (3.42). The membrane density W_{mem} and the bending density W_{bend}, respectively, are defined as

$$\begin{aligned}
W_{\text{mem}}(A) &= \frac{\mu}{2} \operatorname{tr} A + \frac{\lambda}{4} \det A - \left(\mu + \frac{\lambda}{2}\right) \log \det A - \mu - \frac{\lambda}{4}\,, \\
W_{\text{bend}}(A) &= \alpha (\operatorname{tr} A)^2 + (1 - \alpha) \operatorname{tr}(A^2)\,, \quad \alpha \in \{0, 1\}\,.
\end{aligned}$$

For $\alpha = 1$, a simplification leads to the *Discrete Shells* bending energy [GHDS03], *i.e.*

$$\mathbf{W}^{\text{DS}}_{\text{bend}}[\mathbf{S}, \tilde{\mathbf{S}}] = \sum_{E \in \mathcal{E}} \frac{(\theta_E - \theta_{\Phi(E)})^2}{d_E}\, l_E^2\,.$$

5 The shape space of discrete shells

It is due to Kendall [Ken84] that complex shapes, *e.g.* curves, images or solid materials, are considered as individual elements or points in a high or even infinite dimensional space, *i.e.* the *shape space*. Initially, this space is just a collection of shapes without any mathematical structure. In particular, most shape spaces cannot be considered as linear vector spaces. Nevertheless, one is interested in performing mathematical operations on the set of shapes, for instance, for two given shapes one wants to compute a connecting path (*cf.* Fig. 4). The notion of an optimal or shortest path then induces naturally a distance measure which allows *e.g.* for a statistical analysis. It is a well-established ansatz to consider a given shape space as a *Riemannian manifold*. In a nutshell, a Riemannian manifold can be described as a collection of points that is locally equivalent to the Euclidean space, together with a so-called *Riemannian metric*, *i.e.* an instruction how to measure local variations. On a Riemannian manifold the notion of a connecting path and hence a (locally) shortest path, a so-called *geodesic*, is intrinsically given. Thereby, a geodesic connecting two points can be considered as the solution of the interpolation problem. Similarly, one can extrapolate by extending geodesic paths via the *exponential map* or transport details via the *parallel transport*—both are inherent concepts in Riemannian manifold theory. Hence the mathematical structure of a Riemannian manifold leads to the solution of a couple of problems relevant *e.g.* in computer graphics.

Figure 4: Morphing by means of interpolation (orange) computed between two input shapes (gray).

In this section we shall consider the shape space of discrete shells as a *Riemannian manifold*. We aim at combining a physically sound model of thin shells (as it has been derived in Sec. 4) with a consistent definition of geometric objects in a Riemannian manifold. The key ingredient, as we will see, is the computation of (locally) shortest paths in the manifold, *i.e. geodesic curves*. Hence the collection of geometric objects and corresponding operators in the Riemannian framework is also referred to as *geodesic calculus*.

Continuous geodesics are minimizers of the so-called path energy. One way to approximate geodesic paths connecting two points in a generic manifold is via the minimization of a discretized path energy. Instead of discretizing the underlying flow, the *variational time-discretization* proposed by Rumpf and Wirth [WBRS11] is based on the direct minimization of this discrete path energy subject to the prescribed data given at the initial and the end time. In particular, this approach is built on a local approximation of the squared Riemannian distance, where this approximation can be thought of as a *dissimilarity measure* between shapes. Hence, we shall use the (discrete) dissimilarity measure derived in the previous section to apply the variational time-discretization to the space of discrete shells in order to compute (time-discrete) geodesics.
Building on the variational time-discretization of geodesic paths, Rumpf and Wirth [RW13] developed a comprehensive discrete geodesic calculus on the space of viscous fluidic objects and presented in [RW15] a corresponding complete convergence analysis on general finite- and on certain infinite-dimensional shape spaces with the structure of a Banach manifold. The generic definitions of several discrete geometric objects, such as exponential map, logarithm and parallel transport, are appropiate to be transferred directly to other shape spaces. To this end, we apply exactly this discrete geodesic calculus to the space of discrete shells to obtain useful and robust tools for applications in computer graphics such as extrapolation or detail transfer.

5.1 Geodesic calculus on a Riemannian manifold

Geodesics are usually defined as curves that transport their velocity vector parallely or equivalently, that are solutions of the *geodesic equation*. Both definitions are based on the notion of a *covariant derivative* along a curve. However, we first define geodesics as minimizers of the *path energy*. Later, we will see that this is well-defined as these minimizers indeed satisfy the geodesic equation.

Remark: The geodesic calculus developed by Rumpf and Wirth was designed to work on general, possibly infinite dimensional manifolds. However, the step from finite to infinite dimensions is very delicate hence we try to stick to the finite dimensional setting whenever it is appropiate. This is in particular justified as the discrete shell space is of high but finite dimension. In finite dimensional Riemannian geometry it is convenient to work with coordinates, *i.e.* to consider a (local) parametric representation of the manifold and work in the (Euclidean) parameter domain. On the other hand, it is often useful to derive a *coordinate-free* representation in order to transfer the finite dimensional concepts directly to the infinite dimensional setting. In the following we will often start working with coordinates and derive a corresponding coordinate-free representation afterwards.

References: All concepts based on finite dimensional Riemannian geoemtry are presented according to the well-established textbook by M. doCarmo [dC92]; for further reading on infinite dimensional manifolds we refer to the textbook by S. Lang [Lan95].

We define a *differentiable manifold* $\mathcal{M}$ of dimension $d < \infty$ in the sense of Definition 2.1 in [dC92, chap. 0], *i.e.* there is a family of injective mappings $x_\alpha : \omega_\alpha \subset \mathbb{R}^d \to \mathcal{M}$ with $\cup_\alpha x_\alpha(\omega_\alpha) = \mathcal{M}$, such that $x_\beta^{-1} \circ x_\alpha$ is differentiable for any pair α, β with $x_\alpha(\omega_\alpha) \cap x_\beta(\omega_\beta) \neq \varnothing$. For convenience, we will assume in the following that there is one global parametrization $x : \omega \subset \mathbb{R}^d \to \mathcal{M}$ with $x(\omega) = \mathcal{M}$. In particular, x is twice differentiable, injective and regular in the sense that Dx has full rank. The tangent space $T_p\mathcal{M}$ of $\mathcal{M}$ at $p \in \mathcal{M}$ is defined as

$$T_p\mathcal{M} = \{\dot\gamma(0) \mid \gamma : (-\epsilon, \epsilon) \to \mathcal{M} \text{ is a smooth curve with } \gamma(0) = p,\ \epsilon > 0\}\,.$$

If $x : \omega \to \mathcal{M}$ is a parametrization with $x(\xi) = p$ for some $\xi = (\xi_1, \dots, \xi_d) \in \omega$, the set $(X_1, \dots, X_d)$ with $X_i = X_i(p) = X_i(\xi) = x_{,i}(\xi) = \frac{\partial x}{\partial \xi_i}(\xi)$ is a basis of $T_p\mathcal{M}$, denoted as *canonical basis*. A vector field V on $\mathcal{M}$ is a mapping with $V(p) \in T_p\mathcal{M}$ for all $p \in \mathcal{M}$.

A *Riemannian metric* on $\mathcal{M}$ is a mapping $g : p \mapsto g_p$ such that $g_p : T_p\mathcal{M} \times T_p\mathcal{M} \to \mathbb{R}$ is a bilinear, symmetric and positive-definite form, which varies smoothly in the sense that $\xi \mapsto g_{ij}(\xi) := g_{x(\xi)}(X_i(\xi), X_j(\xi))$ is a differentiable function in ω. A manifold equipped with a Riemannian metric is referred to as Riemannian manifold. As $(g_{ij})_{ij}$ is a regular matrix in $\mathbb{R}^{d,d}$ there is an inverse matrix $g^{-1} \in \mathbb{R}^{d,d}$ which is denoted by $(g^{kl})_{kl}$, *i.e.* $g_{ij}g^{jk} = \delta_{ik}$.

Remark: To avoid confusion, we denote the metric associated with generic Riemannian manifolds by *Riemannian metric* and the metric on a two-dimensional embedded surface by *first fundamental form*, *cf*. Sec. 2.1.

Path energy and geodesics. Given a smooth path $(y(t))_{t\in[0,1]}$ on a Riemannian manifold $(\mathcal{M}, g)$, the length of this path is defined as

$$\mathcal{L}[(y(t))_{t\in[0,1]}] = \int_0^1 \sqrt{g_{y(t)}(\dot y(t), \dot y(t))}\,\mathrm{d}t\,. \tag{5.1}$$

Note that the path length is independent of reparameterization. This geometrically nice property leads to analytical complications when dealing with the existence theory of shortest paths as well as to computational difficulties when optimizing this non-convex functional. The path energy is defined as

$$\mathcal{E}[(y(t))_{t\in[0,1]}] = \int_0^1 g_{y(t)}(\dot y(t), \dot y(t))\,\mathrm{d}t\,. \tag{5.2}$$

In contrast to $\mathcal{L}$, the path energy is *not* independent of reparameterization. A direct application of the Cauchy-Schwarz inequality shows that

$$\mathcal{L}[(y(t))_{t\in[0,1]}] \le \sqrt{\mathcal{E}[(y(t))_{t\in[0,1]}]}$$

and equality holds if and only if $g_{y(t)}(\dot{y}(t), \dot{y}(t)) = \text{const}$. We will see that minimizers of $\mathcal{E}$ will have this *constant speed property*. Thus, to identify shortest paths for fixed boundary data $y(0) = y_A$ and $y(1) = y_B$ with $y_A,\, y_B \in \mathcal{M}$ we will seek for minimizers of the path energy and minimizers will be paths with constant speed.

Definition 5.1 (Geodesic path)**.** For $y_A,\, y_B \in \mathcal{M}$ a minimizer of the path energy among all path $y : [0,1] \to \mathcal{M}$ with $y(0) = y_A$ and $y(1) = y_B$ is denoted as geodesic path connecting y_A and y_B.

Rumpf and Wirth have shown in [RW15] that this variational definition is indeed well-defined, *i.e.* a minimizer of $\mathcal{E}$ exists and is unique under suitable assumptions. In particular, their results holds for general, possibly infinite dimensional manifolds.

***Existence and uniqueness of geodesic paths.** In this paragraph we summarize the theoretical existence and uniqueness results by Rumpf and Wirth [RW15]. In particular, the Riemannian manifold $\mathcal{M}$ does not necessarily be finite dimensional. To this end, we need a precise technical setup. Let $\mathbf{V}$ be a separable, reflexive Banach space that is compactly embedded in a Banach space $\mathbf{Y}$. Let $\mathcal{M}$ be the closure of an open connected subset of $\mathbf{V}$ and hence a Banach manifold, potentially with boundary (in which case we assume the boundary $\partial\mathcal{M}$ to be smooth). We assume $\mathcal{M}$ to be path-connected. Let $g : \mathcal{M} \times \mathbf{V} \times \mathbf{V} \to \mathbb{R}$ be a Riemannian metric, which satisfies the following hypotheses:

(H1)
$$\begin{cases} g \text{ is uniformly bounded and } \mathbf{V}\text{-coercive in the sense } c^*\|v\|_{\mathbf{V}}^2 \le g_y(v,v) \le C^*\|v\|_{\mathbf{V}}^2\,. \\ g \text{ is continuous in the sense } |g_y(v,v) - g_{\tilde{y}}(v,v)| \le \beta(\|y-\tilde{y}\|_{\mathbf{Y}})\|v\|_{\mathbf{V}}^2 \\ \text{for a strictly increasing, continuous function } \beta \text{ with } \beta(0) = 0. \end{cases}$$

Hypothesis (H1) is globally fulfilled only for quite special Riemannian manifolds. However, the setup is also adequate to analyze general, possibly infinite-dimensional manifolds locally, where the linear space $\mathbf{V}$ or its subset $\mathcal{M}$ have to be interpreted as a chart of the considered manifold.

For $y_A,\, y_B \in \mathcal{M}$, the next theorem states the existence of a connecting path with least energy. The key point in the proof is the weak lower semi-continuity of the continuous path energy (5.2) using the compact embedding of $\mathbf{V}$ into $\mathbf{Y}$.

Theorem 5.2 (Existence of continuous geodesics, [RW15])**.** *Let $(\mathcal{M}, g)$ be a Riemannian manifold satisfying assumption* (H1)*. For $y_A,\, y_B \in \mathcal{M}$ there exists a classical geodesic connecting y_A and y_B,* i.e. *a minimizer of $\mathcal{E}$ in the space of all paths $(y(t))_{t\in[0,1]} \in H^1((0,1);\mathcal{M})$ with $y(0) = y_A$ and $y(1) = y_B$. In particular, y is continuous (in the $\mathbf{V}$-topology).*

As in finite-dimensional Riemannian geometry the shortest geodesic between close points is unique as stated in the next theorem (*cf*. also Cor. 5.2 in [Lan95, VIII]).

Theorem 5.3 (Uniqueness of short continuous geodesics, [RW15])**.** *Under the assumptions of Theorem 5.2, for the metric g being $C^2(\mathcal{M}; \mathbf{V}' \otimes \mathbf{V}')$-smooth, classical geodesics are unique locally.*

Once we have existence and uniqueness of geodesics, we can define a Riemannian distance of two points $y_A,\, y_B \in \mathcal{M}$ in the usual way, *i.e.*

$$\operatorname{dist}(y_A, y_B) = \min_{y(0)=y_A, y(1)=y_B} \mathcal{L}[(y(t))_{t\in[0,1]}] = \sqrt{\min_{y(0)=y_A, y(1)=y_B} \mathcal{E}[(y(t))_{t\in[0,1]}]}\,. \tag{5.3}$$

One can verify the axioms of a metric and show that the induced topology is equivalent to the $\mathbf{V}$-topology, *i.e.* $\sqrt{c^*}\|y_B - y_A\|_{\mathbf{V}} \le \operatorname{dist}(y_A, y_B) \le \sqrt{C^*}\|y_B - y_A\|_{\mathbf{V}}$.

Covariant derivative. Next, we will investigate the differentiation of vector fields on manifolds, which will lead us to the notion of the covariant derivative. Finally, we will explore a connection to the Euler-Lagrange equations of geodesic paths. As before, we first consider a finite dimensional Riemannian manifold $\mathcal{M}$ with a parametrization $x : \Omega \subset \mathbb{R}^d \to \mathcal{M}$. This allows us to work with *coordinates*, that means, we can express all quantities in a finite dimensional basis of the tangent space. However, to transfer the following concepts to the infinite dimensional setup, we eventually aim at deriving a *coordinate-free* representation.

The second derivatives $x_{,ij} = \partial_{\xi_i}\partial_{\xi_j} x$ of the parametrization $x : \Omega \subset \mathbb{R}^d \to \mathcal{M}$ decomposes into a normal component and into a tangential component, *i.e.* we obtain

$$x_{,ij} = \sum_{k=1}^{d} \Gamma_{ij}^k X_k + \sum_l \beta_l n_l \,,$$

where Γ_{ij}^k are the Christoffel symbols and $(n_l)_l$ is a basis of the normal space $(T_p\mathcal{M})^\perp$. It follows that

$$x_{,ij} \cdot X_k = \sum_{l=1}^{d} \Gamma_{ij}^l X_l \cdot X_k = \sum_{l=1}^{d} \Gamma_{ij}^l g_{lk} \,. \tag{5.4}$$

From the symmetry of second derivative of the parametrization we immediately obtain the symmetry of the Christoffel symbols, *i.e.* $\Gamma_{ij}^k = \Gamma_{ji}^k$.

Proposition 5.4. *Let $g^{-1} = (g^{ij})_{ij=1,\dots,d}$ be the inverse of g. Then we obtain the following representation of the Christoffel symbols:*

$$\Gamma_{ij}^k = \frac{1}{2} \sum_{l=1}^{d} g^{lk} \left(g_{jl,i} - g_{ij,l} + g_{li,j} \right) . \tag{5.5}$$

Proof: Differentiation of the metric and taking into account (5.4) gives

$$\begin{aligned}
g_{jl,i} &= x_{,ji} \cdot x_{,l} + x_{,j} \cdot x_{,li} = \sum_{m=1}^{d} \Gamma_{ji}^m g_{ml} + \sum_{m=1}^{d} \Gamma_{li}^m g_{mj} \,, \\
g_{ij,l} &= x_{,il} \cdot x_{,j} + x_{,i} \cdot x_{,jl} = \sum_{m=1}^{d} \Gamma_{il}^m g_{mj} + \sum_{m=1}^{d} \Gamma_{jl}^m g_{mi} \,, \\
g_{li,j} &= x_{,lj} \cdot x_{,i} + x_{,l} \cdot x_{,ij} = \sum_{m=1}^{d} \Gamma_{lj}^m g_{mi} + \sum_{m=1}^{d} \Gamma_{ij}^m g_{ml} \,.
\end{aligned}$$

Summing the first and the third equation and substracting the second equation we obtain

$$g_{jl,i} - g_{ij,l} + g_{li,j} = 2 \sum_{m=1}^{d} \Gamma_{ij}^m g_{ml} \,,$$

which after multiplication with g^{-1} (*i.e.* applying $\sum_l g^{lk}(\dots)$ on both sides) verifies the claimed representation. □

To obtain a *coordinate-free* formulation, we define a bilinear operator $\Gamma = \Gamma_p : T_p\mathcal{M} \times T_p\mathcal{M} \to T_p\mathcal{M}$ by

$$\Gamma(X_i, X_j) = \sum_{k=1}^{d} \Gamma_{ij}^k X_k \,,$$

and get for tangent vectors $U = \sum_i u_i X_i$, $V = \sum_j v_j X_j$ and $W = \sum_l w_l X_l$:

$$g_p(\Gamma(U,V), W) = \sum_{i,j,k,l=1}^{d} u_i \, v_j \, w_l \, \Gamma_{ij}^l g_{kl} \,.$$

On the other hand, testing the right-hand side of (5.5) with U, V, W in the metric yields

$$g_p(\Gamma(U,V), W) = \frac{1}{2} \Big(\left(D_p g\right)(V)(U,W) + \left(D_p g\right)(U)(V,W) - \left(D_p g\right)(W)(U,V) \Big) \,.$$

Definition 5.5 (Christoffel operator)**.** For $p \in \mathcal{M}$ the Christoffel operator $\Gamma = \Gamma_p$ is a mapping $\Gamma_p : T_p\mathcal{M} \times T_p\mathcal{M} \to T_p\mathcal{M}$. For $U, V \in T_p\mathcal{M}$ the evaluation $\Gamma_p(U,V)$ is defined implicitly by

$$g_p(\Gamma_p(U,V), W) = \frac{1}{2} \Big(\left(D_p g\right)(V)(U,W) + \left(D_p g\right)(U)(V,W) - \left(D_p g\right)(W)(U,V) \Big) \quad \forall W \in T_p\mathcal{M} \,.$$

Remark: Existence of such an operator is shown in Thm. 4.2 of [Lan95, VIII].

Let $\gamma : I \to \mathcal{M}$ be a curve and W a vector field along the curve, *i.e.* $W(t) = \sum_{l=1}^{d} w_l(t) X_l(\gamma(t))$. Let $\dot{W}(t) := \sum_{l=1}^{d} \dot{w}_l(t) X_l(\gamma(t))$ and let $V(t) = \dot{\gamma}(t)$ with $V(t) = \sum_l v_l(t) X_l(\gamma(t))$, which is also a vector field along γ. The product rule implies

$$\frac{d}{dt} W(t) = \sum_{l=1}^{d} \left(\dot{w}_l(t) X_l(\gamma(t)) + w_l(t) \sum_{k=1}^{d} x_{,lk}(\gamma(t)) v_k(t) \right) .$$

The covariant derivative $\frac{D}{dt} W(t)$ of W along γ is defined as the projection of $\frac{d}{dt} W(t)$ onto the tangent space. Hence we replace $x_{,lk}$ by its tangential part, *i.e.* $\sum_{m=1}^{d} \Gamma_{lk}^{m} X_m = \Gamma_{\gamma(t)}(X_l, X_k)$:

$$\frac{D}{dt} W(t) = \sum_{l=1}^{d} \left(\dot{w}_l(t) X_l(\gamma(t)) + w_l(t) \sum_{k=1}^{d} \Gamma_{\gamma(t)}(X_l, X_k) v_k(t) \right) = \dot{W}(t) + \Gamma_{\gamma(t)}(W(t), V(t)) .$$

This leads to the following (implicit) definition which is also *coordinate-free*:

Definition 5.6 (Covariant derivative)**.** Let $\gamma : I \to \mathcal{M}$ be a curve and $W : I \to T\mathcal{M}$ a vector field along γ. We define the covariant derivative $\frac{D}{dt} W$ of W along γ at $p = \gamma(t)$ for $t \in I$ by

$$g_{\gamma(t)}\Big(\frac{D}{dt} W(t), U\Big) = g_{\gamma(t)}\Big(\dot{W}(t) + \Gamma_p\left(W(t), \dot{\gamma}(t)\right), U\Big) \quad \forall\, U \in T_{\gamma(t)}\mathcal{M} . \tag{5.6}$$

Remark: Due to its coordinate-free formulation, Def. 5.6 is also valid for infinite dimensional manifolds (*cf*. [Lan95]). Since the following concepts are based on this definition they are not restricted to finite dimensional manifolds, either.

With a notion of a covariant derivative along a curve we can define a *parallel transport*, which is indeed well-defined due to Thm. 3.3/3.4 in [Lan95, VIII]:

Proposition 5.7 (Parallel transport)**.** *Let $\gamma : I \to \mathcal{M}$ be a curve. A vector field $V : I \to T\mathcal{M}$ along γ is called* parallel *if $\frac{D}{dt} V(t) = 0$ for all $t \in I$. For $t_0 \in I$, $V_0 \in T_{\gamma(t_0)}\mathcal{M}$, there is a unique parallel vector field $V : I \to T\mathcal{M}$ with $V(t_0) = V_0$. Furthermore, the map $\mathrm{P}_{\gamma(t_0)\to\gamma(t)} : T_{\gamma(t_0)}\mathcal{M} \to T_{\gamma(t)}\mathcal{M}$, $\mathrm{P}_{\gamma(t_0)\to\gamma(t)} V_0 = V(t)$ is a linear isomorphism.*

For a given vector $V_0 \in T_{\gamma(t_0)}\mathcal{M}$ one can solve $\frac{D}{dt} V(t) = 0$ with $V(t_0) = V_0$ as an ordinary differential equation to perform the (unique) parallel transport of V_0 along the path.

As mentioned before, a curve $\gamma : I \to \mathcal{M}$ is usually defined to be *geodesic* if it solves the *geodesic equation*, *i.e.*

$$\frac{D}{dt} \dot{\gamma}(t) = 0 \quad \forall t \in I .$$

This means, that γ transports its own velocity vector parallely. The next theorem states that geodesics as defined in Def. 5.1 are solutions of the geodesic equation:

Theorem 5.8. *If $y : [0,1] \to \mathcal{M}$ is a geodesic connecting $y(0)$ and $y(1)$, then $\frac{D}{dt} \dot{y}(t) = 0$ for all $t \in (0,1)$.*

Proof. Consider the Euler–Lagrange equation of the path energy and apply integration by parts to obtain

$$\begin{aligned} 0 &= \partial_y \mathcal{E}[y](\vartheta) = \int_0^1 (D_y g_y)(\vartheta)(\dot{y}, \dot{y}) + 2 g_y(\dot{y}, \dot{\vartheta})\, \mathrm{d}t \\ &= \int_0^1 (D_y g_y)(\vartheta)(\dot{y}, \dot{y}) - 2(D_y g_y)(\dot{y})(\dot{y}, \vartheta) - 2 g_y(\ddot{y}, \vartheta)\, \mathrm{d}t \end{aligned}$$

for all smooth test vector fields ϑ along the path y. By the fundamental lemma we achieve

$$0 = g_y(\ddot{y}, \vartheta) + (D_y g_y)(\dot{y})(\dot{y}, \vartheta) - \frac{1}{2}(D_y g_y)(\vartheta)(\dot{y}, \dot{y}) = g_y(\ddot{y} + \Gamma(\dot{y}, \dot{y}), \vartheta) = g_y(\frac{D}{\mathrm{d}t}\dot{y}, \vartheta) . \quad \square$$

In particular, minimizers y of the path energy satisfy a *constant speed property*, *i.e.* $g_{y(t)}(\dot{y}(t), \dot{y}(t)) = const.$

If $V : I \to T\mathcal{M}$ is a parallel vector field along a *geodesic* path $y : I \to \mathcal{M}$ the angle $\alpha(t)$ between the velocity field $\dot{y}(t)$ and $V(t)$ is fixed:

$$\frac{\mathrm{d}}{\mathrm{d}t}\cos\alpha(t) \quad = \quad \frac{\mathrm{d}}{\mathrm{d}t}\left(\frac{g_y(V,\dot{y})}{\sqrt{g(V,V)}\sqrt{g(\dot{y},\dot{y})}}\right) = \frac{g_y\left(\frac{D}{\mathrm{d}t}V,\dot{y}\right) + g_y\left(V,\frac{D}{\mathrm{d}t}\dot{y}\right)}{\sqrt{g(V,V)}\sqrt{g(\dot{y},\dot{y})}} = 0\,.$$

Finally, we define the exponential map for a general manifold:

Definition 5.9 (Exponential map)**.** Let $y(t) = y(t,p,V) : I \to \mathcal{M}$, $0 \in I$, be the solution of $\frac{D}{\mathrm{d}t}\dot{y}(t) = 0$ for initial data $y(0) = p$ and $\dot{y}(0) = V$. The (geometric) exponential map $\exp_p : T_p\mathcal{M} \to \mathcal{M}$ is defined as $\exp_p(V) = y(1,p,V)$.

To see that this definition is well-defined we refer to Prop. 4.2 in [Lan95, IV]. Obviously, we have the scaling property $y(t,p,V) = \exp_p(tV)$, which implies that $y(1,p,V)$ is well-defined if $\|V\|$ is sufficiently small. From the local uniqueness of short geodesic paths we deduce that there exists $\delta > 0$, such that $\exp_p : B_\delta(0) \to \exp_p(B_\delta(0))$ is a bijection. In this case, we define $U_p = \exp_p(B_\delta(0))$ to be the *normal neighbourhood* of p. Hence the notion of an inverse mapping is locally well-defined:

Definition 5.10 (Logarithm)**.** The inverse operator of the exponential map is called the (geometric) logarithm $\log_p : U_p \to T_p\mathcal{M}$, where U_p denotes the normal neighbourhood of p.

5.2 Variational time-discretization of geodesics

In a sequence of papers, Rumpf and Wirth [Wir09, WBRS09, RW13, RW15] have introduced a time-discrete analogon of the continuous geodesic calculus presented in the previous section. The resulting time-discrete geodesic calculus has already been applied to several Riemannian manifolds or shape spaces, *e.g.* in [HRWW12, HRS$^+$14, BER15, MRSS15, Per15]. In this section, we provide a survey of the time-discrete geodesic calculus proposed by Rumpf and Wirth and summarize important convergence results that will later be validated numerically on the space of (discrete) shells. As before, we start with a variational formulation of *discrete* geodesics, defined via minimizers of a *discrete* path energy[4]. However, different from the continuous setting, the notion of a discrete geodesic will then serve as the core ingredient of the entire discrete calculus. Hence, the name *geodesic calculus* is in particular justified in the discrete setting.

In the continuous setting the starting point of a geometric calculus on a Riemannian manifold is usually the definition of a Riemannian metric. However, as we will see, the discrete geodesic calculus is solely based on the notion of a (squared) Riemannian distance resp. a local approximation thereof. Obviously, a Riemannian distance is induced by the metric (*cf*. eq. (5.3)). On the other hand, given the Riemannian distance dist, one can recover the Riemannian metric g_p at some point $p \in \mathcal{M}$ by

$$g_p(V,W) = \frac{1}{2}\,\partial_2^2\,\mathrm{dist}^2(p,p)(V,W)\,, \quad V,W \in T_p\mathcal{M}\,. \tag{5.7}$$

For many applications, *e.g.* when dealing with physical shape spaces, it is difficult to define a Riemannian metric a priori. On the other hand, it is often much easier to come up with the notion of a distance, *e.g.* by using a physically sound dissimilarity measure (*cf*. Sec. 4). To account for this circumstance as well as for the fact that Riemannian distances are in practice hard to compute (as they require solving an optimization problem), the discrete geodesic calculus is actually based on an *approximation* of the squared Riemannian distance which is easy to evaluate and consistent with the metric by definition due to (5.7).

Variational time-discretization. In the following, we denote an ordered set of points $Y^K = (y_0, \ldots, y_K)$ in the manifold $\mathcal{M}$ as a time-discrete K-path. Often we interpret this discrete path as a uniform sampling of a smooth curve $y : [0,1] \to \mathcal{M}$, *i.e.* we have $y_k = y(t_k)$ with $t_k = k\tau$ for $k = 0, \ldots, K$ where $\tau = K^{-1}$ and $K \in \mathbb{N}$

[4]We will often omit the prefix "time" when referring to a time-discrete object.

denotes the sample size. Instead of using a straightforward time-discretization of the continuous path energy (5.2) we first consider the following estimates

$$\mathcal{L}[(y(t))_{t\in[0,1]}] \geq \sum_{k=1}^{K} \operatorname{dist}(y_{k-1}, y_k)\,, \qquad \mathcal{E}[(y(t))_{t\in[0,1]}] \geq \frac{1}{\tau}\sum_{k=1}^{K} \operatorname{dist}^2(y_{k-1}, y_k)\,, \tag{5.8}$$

where equality holds for geodesic paths due to the constant speed property. The first estimate is straightforward, and the second estimate follows with the Cauchy-Schwarz inequality, *i.e.*

$$\sum_{k=1}^{K} \operatorname{dist}^2(y_{k-1}, y_k) \leq \sum_{k=1}^{K} \left(\int_{(k-1)\tau}^{k\tau} \sqrt{g_{y(t)}(\dot y(t), \dot y(t))}\ \mathrm{d}t \right)^2 \leq \sum_{k=1}^{K} \tau \int_{(k-1)\tau}^{k\tau} g_{y(t)}(\dot y(t), \dot y(t))\ \mathrm{d}t\,,$$

since the expression on the right hand side is exactly $\tau\ \mathcal{E}[(y(t))_{t\in[0,1]}]$.

The estimate on the path energy in (5.8) suggest that the sum on the right hand side might be a reasonable approximation of $\mathcal{E}$. However, as already mentioned in the beginning, the squared Riemannian distance dist^2 is often difficult to compute in practice. Therefore we assume there is a smooth functional $\mathcal{W} : \mathcal{M} \times \mathcal{M} \to \mathbb{R}$, such that for $y, \tilde y \in \mathcal{M}$

$$\mathcal{W}[y, \tilde y] = \operatorname{dist}^2(y, \tilde y) + O(\operatorname{dist}^3(y, \tilde y))\,. \tag{5.9}$$

Note that $\mathcal{W}$ is not required to be symmetric. For g smooth enough, a valid approximation of dist^2 is *e.g.* given by $\mathcal{W}[y, \tilde y] = \frac{1}{2} g_y(\tilde y - y, \tilde y - y)$. In general, we will see later in Thm. 5.11 that $g_y = \frac{1}{2}\mathcal{W}_{,22}[y, y]$ implies (5.9) for smooth g and $\mathcal{W}$.

Theorem 5.11 (Consistency conditions, [RW15])**.** *Unter hypothesis* (H1)*, if $\mathcal{W}$ is twice Gâteaux - differentiable on $\mathcal{M}\times\mathcal{M}$ with bounded second Gâteaux derivative, then $\mathcal{W}[y, \tilde y] = \operatorname{dist}^2(y, \tilde y) + O(\operatorname{dist}^3(y, \tilde y))$ for $\tilde y$ close to $y \in \mathring{\mathcal{M}}$ implies*

$$\mathcal{W}[y, y] = 0\,, \quad \mathcal{W}_{,2}[y, y](V) = 0\,, \quad \mathcal{W}_{,22}[y, y](V, W) = 2g_y(V, W)$$

for any $V, W \in \mathbf{V}$. Furthermore, $\mathcal{W}_{,1}[y, y](V) = 0$ and

$$\mathcal{W}_{,11}[y, y](V, W) = -\mathcal{W}_{,12}[y, y](V, W) = -\mathcal{W}_{,21}[y, y](V, W) = \mathcal{W}_{,22}[y, y](V, W)\,.$$

If $\mathcal{W}$ is even three times Fréchet-differentiable, the implication becomes an equivalence.

We arrive at the following definition of a *discrete path energy* and a *discrete path length* (see [RW15]):

Definition 5.12 (Discrete length and energy)**.** For a discrete K-path $Y^K = (y_0, \dots, y_K)$ with $y_k \in \mathcal{M}$ for $k = 0, \dots, K$ we define the *discrete length* L^K and the *discrete energy* E^K by

$$L^K[Y^K] = \sum_{k=1}^{K} \sqrt{\mathcal{W}[y_{k-1}, y_k]}\,, \qquad E^K[Y^K] = K\sum_{k=1}^{K} \mathcal{W}[y_{k-1}, y_k]\,. \tag{5.10}$$

Then a *discrete geodesic* (of order K) is defined as a minimizer of $E^K[Y^K]$ for fixed end points y_0, y_K.

Note that discrete minimizers of the discrete path length L^K are in general unrelated to continuous geodesics. Let us consider the case $\mathcal{M} = \mathbb{R}^2 \setminus B_r$, where $B_r = \{x : |x| < r\}$, and $\mathcal{W}[y, \tilde y] = \|y - \tilde y\|^2$, as depicted in Fig. 5. Then a discrete path $(y_0, \dots, y_K)$ connecting $y_A = (-\alpha r, 0)$ and $y_B = (\alpha r, 0)$, $\alpha > 1$, that minimizes the time-discrete path energy tend to distribute uniformly along the connecting curve, as stated in Thm. 5.15. If $r \gg \operatorname{dist}(y_A, y_B)/K$ this is not realizable along a straight line connecting y_A and y_B, *cf*. Fig. 5. However, the distribution of points representing a discrete minimizer of L^K is arbitrary, since moving points along the connecting line does not alter the length.

***Existence and uniqueness of discrete geodesic paths.** In this paragraph we gather important theorems from [RW15], *e.g.* on the existence and uniqueness of discrete geodesics (*cf*. also [**?**]). These results will provide a solid ground for the definition of further discrete geometric objects in the next section, which are based on discrete geodesics.

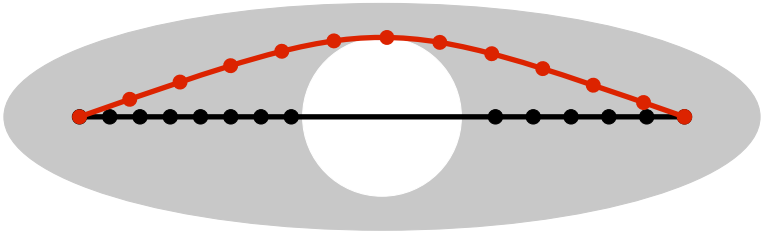

Figure 5: In general, minimizers of the discrete path length do not converge to continuous geodesics.

First of all, one needs to introduce a rigorous functional analytic setup. Let $\mathcal{W} : \mathcal{M} \times \mathcal{M} \to \mathbb{R}$ be a local approximation of the squared Riemannian distance dist^2. In detail, it is supposed that $\mathcal{W}$ is weakly lower semi-continuous and that it satisfies the following hypotheses:

(H2)
$$\begin{cases} \text{There exist } \varepsilon, C > 0 \text{ such that for all } y,\, \tilde{y} \in \mathcal{M}: \\ \mathrm{dist}(y, \tilde{y}) \leq \varepsilon \;\Rightarrow\; |\mathcal{W}[y, \tilde{y}] - \mathrm{dist}^2(y, \tilde{y})| \leq C \mathrm{dist}^3(y, \tilde{y}) \\ \mathcal{W} \text{ is coercive in the sense } \mathcal{W}[y, \tilde{y}] \geq \gamma(\mathrm{dist}(y, \tilde{y})) \\ \text{for a strictly increasing, continuous function } \gamma \text{ with } \gamma(0) = 0 \text{ and } \lim_{d\to\infty} \gamma(d) = \infty. \end{cases}$$

Theorem 5.13 (Existence of discrete geodesics, [RW15])**.** *Given y_A, $y_B \in \mathcal{M}$, there is a discrete geodesic path $(y_0, \ldots, y_K)$ which minimizes the discrete energy E^K over all discrete paths $(\tilde{y}_0, \ldots, \tilde{y}_K)$ with $\tilde{y}_0 = y_A$ and $\tilde{y}_K = y_B$.*

Theorem 5.14 (Convergence of path energy, [RW15])**.** *Under hypothesis* (H2) *there exists $\delta > 0$ such that $\mathrm{dist}(y_A, y_B) < \sqrt{K}\delta$ implies*

$$\Big| \min_{\substack{(y_0,\ldots,y_K) \\ y_0 = y_A, y_K = y_B}} E^K[(y_0, \ldots, y_K)] - \mathrm{dist}^2(y_A, y_B) \Big| = O(\tau)$$

Theorem 5.15 (Equidistribution of points along discrete geodesics, [RW15])**.** *Under hypothesis* (H2) *there exists $\delta > 0$ such that if $\mathrm{dist}(y_A, y_B) < \sqrt{K}\delta$, then discrete geodesics satisfy $\mathrm{dist}(y_{k-1}, y_k) \leq C\tau$ for all $k = 1, \ldots, K$ with the constant $C > 0$ only depending on $\mathrm{dist}(y_A, y_B)$.*

Theorem 5.16 (Uniqueness of discrete geodesics, [RW15])**.** *Let* (H1) *and* (H2) *hold and assume $\mathcal{W}$ to be twice Fréchet-differentiable on $\mathcal{M} \times \mathcal{M}$. For all $y_A \in \mathring{\mathcal{M}}$ and $K \in \mathbb{N}$ there exists $\varepsilon > 0$ such that there exists a unique discrete geodesic $(y_0, \ldots, y_K)$ with $y_0 = y_A$ and $y_K = y_B$ for all y_B with $\|y_A - y_B\|_{\mathbf{V}} < \varepsilon$.*

Application to the discrete shell space. In the following we will consider families of discrete shells which are pairwise in dense correspondence (*cf*. Def. 4.6). Actually, dense correspondence defines an equivalence relation, *i.e*. we consider a fixed equivalence class. This means, all discrete shells are based on the same sets of indices $\mathcal{V}$ and $\mathcal{F}$, respectively.

Definition 5.17 (Shape space of discrete shells)**.** Given some representative *reference shell* $\mathbf{S}$, the shape space of discrete shells $\mathcal{M}[\mathbf{S}]$ is given by the equivalence class of $\mathbf{S}$ where the equivalence relation is given by dense correspondence (as defined in Def. 4.6).

Remark: In the following we assume that we are dealing with an arbitrary but fixed equivalence class $\mathcal{M} = \mathcal{M}[\mathbf{S}]$.

There are two important implications of Def.5.17:

1. The definition of a dissimilarity measure on $\mathcal{M}$ is well-defined, since for two given discrete shells $\mathbf{S}, \tilde{\mathbf{S}}$ having the same connectivity, a piecewise affine deformation $\Phi : \mathbf{S} \to \tilde{\mathbf{S}}$ is uniquely determined.
2. The discrete shell space $\mathcal{M}$ can be identified with $\mathbb{R}^{3n}$, where n is the number of nodes.

Combining Def. 4.7 and Def. 5.12 yields the notion of time-discrete geodesics in the space of discrete shells:

Definition 5.18 (Time-discrete geodesic in the space of discrete shells)**.** Given two discrete shells $\mathbf{S}_A, \mathbf{S}_B \in \mathcal{M} = \mathbb{R}^{3n}$ we refer to the minimizer $(\mathbf{S}_0, \mathbf{S}_1, \dots, \mathbf{S}_K)$ of the *time-discrete path energy*

$$\mathbf{E}^K[\mathbf{S}_0, \dots, \mathbf{S}_K] = K \sum_{k=1}^{K} \mathbf{W}[\mathbf{S}_{k-1}, \mathbf{S}_k]\,, \tag{5.11}$$

with $\mathbf{S}_0 = \mathbf{S}_A$ and $\mathbf{S}_K = \mathbf{S}_B$, as a *time-discrete geodesic*.

The variational formulation of the time-discrete geodesics leads to the following necessary optimality conditions:

$$\begin{aligned} & 0 = \partial_{\mathbf{S}_k} \mathbf{E}^K[\mathbf{S}_0, \dots, \mathbf{S}_K]\,, \quad k = 1, \dots, K-1\,, \\ \iff \quad & 0 = \partial_2 \mathbf{W}[\mathbf{S}_{k-1}, \mathbf{S}_k] + \partial_1 \mathbf{W}[\mathbf{S}_k, \mathbf{S}_{k+1}]\,, \quad k = 1, \dots, K-1\,, \end{aligned} \tag{5.12}$$

where $\partial_i \mathbf{W}$ refers to the variation with respect to the ith argument of $\mathbf{W}$. Note that for a functional $F = F[X]$ we make use of the notation

$$0 = \partial_X F[X] \quad :\Leftrightarrow \quad 0 = \frac{d}{dt}(F[X + tV])\Big|_{t=0} \; \forall\, V \in \mathcal{X}\,,$$

where the test directions V live in a suitable test space $\mathcal{X}$, which is simply $\mathcal{X} = \mathbb{R}^{3n}$ if we consider variations of discrete shell energies. To compute time-discrete geodesics we have to solve the system of nonlinear equations (5.12) simultaneously, where we fix the two end shapes $\mathbf{S}_0$ and $\mathbf{S}_K$.

5.3 Time-discrete geodesic calculus

Let $p, q \in \mathcal{M}$ such that there is a unique geodesic $y : [0,1] \to \mathcal{M}$ with $y(0) = p$ and $y(1) = q$. Then, by Def. 5.10, the logarithm of q with respect to p is the initial velocity $\dot{y}(0) \in T_p\mathcal{M}$, *i.e.* $\log_p(q) = \dot{y}(0)$. The initial velocity $\dot{y}(0)$ can be approximated by a difference quotient in time,

$$\dot{y}(0) = \frac{y(\tau) - y(0)}{\tau} + O(\tau)\,.$$

Thus, we obtain

$$\tau \log_p(q) = y(\tau) - y(0) + O(\tau^2)\,.$$

This gives rise to a consistent definition of a time-discrete logarithm (see [RW15]):

Definition 5.19 (Discrete logarithm)**.** Suppose the discrete geodesic $(y_0, \dots, y_K)$ is the unique minimizer of the discrete path energy (5.10) with $y_0 = p$ and $y_K = q$. Then we define the *discrete logarithm* $\left(\frac{1}{K}\mathrm{LOG}\right)_p(q) = y_1 - y_0$. Note that $\frac{1}{K}$ is part of the symbol and not a factor.

We consider the difference $y_1 - y_0$ as a tangent vector at $p = y_0$. In the special case $K = 1$ we have $\left(\frac{1}{1}\mathrm{LOG}\right)_p(q) = q - p$. As in the continuous case, the discrete logarithm can be considered as a representation of the nonlinear variation q of p in the (linear) tangent space of *displacements*[5] on p.

In the continuous setting, the exponential map $\exp_p$ maps tangent vectors $V \in T_p\mathcal{M}$ onto the end point $y(1)$ of the unique geodesic $(y(t))_{t\in[0,1]}$ with $y(0) = p$ and $\dot{y}(0) = V$. That means, we have $\exp_p(V) = y(1)$ and, via a simple scaling argument, $\exp_p(t_k V) = y(t_k)$, for $k = 0, \dots, K$, where $t_k = k\tau$ and $\tau = K^{-1}$. Let us again consider a discrete geodesic $(y_0, \dots, y_K)$ with $y_0 = p$ and $y_K = q$. Since $V = \left(\frac{1}{K}\mathrm{LOG}\right)_p(q) = y_1 - y_0$ is the discrete logarithm in the tangent space $T_p\mathcal{M}$, we aim at defining a discrete power k exponential map EXP_p^k such that

$$\mathrm{EXP}_p^k(V) = \mathrm{EXP}_p(kV) = y_k\,.$$

This notation is motivated by the observation that $\exp(ks) = \exp^k(s)$ on $\mathbb{R}$ or more general matrix groups. Furthermore, we would like to have the following recursive property, which holds in the continuous setup:

$$y(t_k) = \exp_p(kV) = \exp_{y(t_{k-2})}(2V_{k-1})\,, \quad V_{k-1} := \log_{y(t_{k-2})} y(t_{k-1})\,, \quad k \geq 2\,. \tag{5.13}$$

That means, once we have defined a discrete version EXP_p^2 corresponding to $\exp_p(2\cdot)$, we can use the recursive relation (5.13) to define EXP_p^k for $k \geq 2$ by

$$y_k = \mathrm{EXP}_p^k(V_1) = \mathrm{EXP}_{y_{k-2}}^2(V_{k-1})\,, \quad V_{k-1} = y_{k-1} - y_{k-2}\,, \tag{5.14}$$

for given $y_0 = p$ and $y_1 = y_0 + V_1$, as shown in Fig. 6.

[5] Note that these displacements are indeed well-defined, as we assumed that $\mathcal{M}$ embeds into a Banach space.

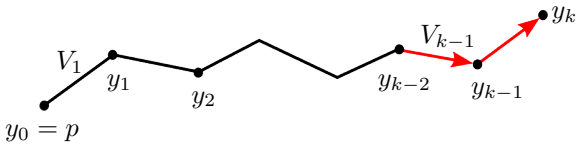

Figure 6: A sketch of the polygonal path associated with the computation of $\mathrm{EXP}_p^k(V_1)$.

Note that the discrete analogon of V_{k-1} is exactly $V_{k-1} = (\frac{1}{1}\mathrm{LOG})_{y_{k-2}} y_{k-1} = y_{k-1} - y_{k-2}$.

It remains to define a discrete version EXP_p^2 corresponding to $\exp_p(2\cdot)$. Formally, we have the identity $\frac{1}{2}\log_p\big(\exp_p(2V)\big) = V$, *i.e.* we can define $\mathrm{EXP}_{y_0}^2(y_1 - y_0)$ as the root of the function

$$z \mapsto (\tfrac{1}{2}\mathrm{LOG})_{y_0}(z) - (y_1 - y_0)$$

for given $y_0, y_1 \in \mathcal{M}$. In fact, we are seeking for a third point $y_2 \in \mathcal{M}$, such that (y_0, y_1, y_2) is a time-discrete geodesic for $K = 2$. Using Def. 5.12, a necessary condition of this is given by

$$0 = \partial_2 \mathcal{W}[y_0, y_1](\psi) + \partial_1 \mathcal{W}[y_1, y_2](\psi) \quad \forall \psi \in \mathbf{V}\,,$$

where $\partial_i \mathcal{W}$ denotes the Gâteaux derivative with respect to the ith argument of $\mathcal{W}$. Hence we define:

Definition 5.20 (Discrete exponential map)**.** For given points $y_0, y_1 \in \mathcal{M}$, $V_1 = y_1 - y_0$, we define $\mathrm{EXP}_{y_0}^2(V_1)$ as the solution of

$$\partial_2 \mathcal{W}[y_0, y_1](\psi) + \partial_1 \mathcal{W}[y_1, y](\psi) = 0 \quad \forall \psi \in \mathbf{V}\,,$$

and hence $\mathrm{EXP}_{y_0}^k(V_1) = \mathrm{EXP}_{y_{k-2}}^2(V_{k-1})$ for $V_{k-1} = y_{k-1} - y_{k-2}$ and $k \geq 2$.

It is straightforward to verify that $\mathrm{EXP}_p^K = (\frac{1}{K}\mathrm{LOG})_p^{-1}$ as long as the discrete logarithm is invertible. In fact, the Euler–Lagrange equations for $(y_0, \dots, y_K)$ being a discrete geodesic with fixed end points y_0 and y_K are given by the $K - 1$ nonlinear equations

$$0 = \partial_2 \mathcal{W}[y_{k-1}, y_k](\psi) + \partial_1 \mathcal{W}[y_k, y_{k+1}](\psi) \quad \forall \psi \in \mathbf{V}\,, \quad k = 1, \dots, K-1\,, \tag{5.15}$$

which have to be solved *simultaneously*. On the other hand, if we compute $\mathrm{EXP}_{y_0}^k(y_1 - y_0)$ for given $y_0, y_1 \in \mathcal{M}$ and $k = 2, \dots, K$, we get exactly the same system (5.15). However, in this case the system can be solved *sequentially*.

Finally, we introduce a time-discrete notion of parallel transport along a discrete path as proposed in [RW15]. In the continuous setting, given a path $y : [0, 1] \to \mathcal{M}$ and a vector $V_0 \in T_{y(0)}\mathcal{M}$, parallel transport $\mathrm{P}_{y(0)\to y(\tau)} V_0$ of V_0 along the path y is defined as the solution of the initial value problem $\frac{D}{dt} V(t) = 0$ for $t \in [0, \tau]$ and $V(0) = V_0$. There is a well-known first-order approximation of parallel transport called Schild's ladder (*cf*. [EPS72, KMN00]), which is based on the construction of a sequence of so-called *geodesic parallelograms*; this method has been used *e.g*. by Lorenzi *et al*. [LAP11] to perform parallel transport of deformations along time series of images (see also [PL11]). We once more use the notation $y_k = y(t_k)$, $t_k = k\tau$, for samples of the path $y : [0, 1] \to \mathcal{M}$. Given a tangent vector $V_{k-1} \in T_{y_{k-1}}\mathcal{M}$, the approximation $V_k \in T_{y_k}\mathcal{M}$ of the parallely transported vector $\mathrm{P}_{y_{k-1}\to y_k} V_{k-1}$ via a geodesic parallelogram is illustrated in Fig. 7.
The scheme in Fig. 7 can be easily transferred to the time-discrete setup by replacing y by a discrete path $(y_0, \dots, y_K)$ and the geodesics that define the geodesic parallelogram by time-discrete geodesics, *e.g*. of length 3. Conceptually, we will again replace tangent or velocity vectors V by displacements ζ of points.
Remark: Let $p_0, p_1, p_2 \in \mathcal{M}$. We define $\hat{p} = \hat{p}(p_0, p_1, p_2)$ such that (p_0, p^c, p_2) and $(p_1, p^c, \hat{p})$ are discrete geodesics for some $p^c \in \mathcal{M}$. Then $(p_0, p_1, p_2, \hat{p})$ defines a *discrete geodesic parallelogram*, p^c is refered to as center point of the parallelogram.

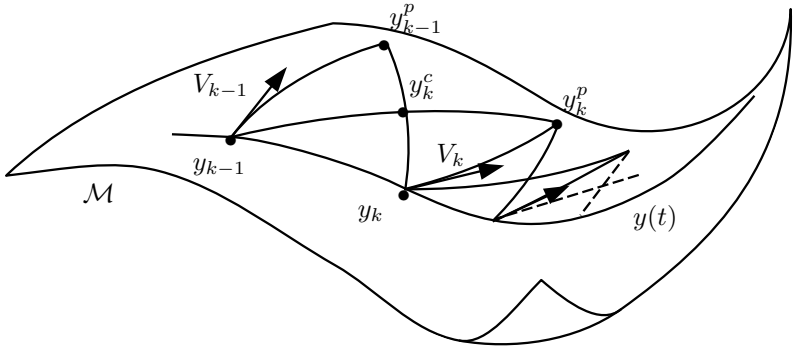

$$y^p_{k-1} = \exp_{y_{k-1}}(V_{k-1})$$

$$y^c_k = \exp_{y^p_{k-1}}\left(\tfrac{1}{2}\log_{y^p_{k-1}}(y_k)\right)$$

$$y^p_k = \exp_{y_{k-1}}\left(2\log_{y_{k-1}}(y^c_k)\right)$$

$$V_k = \log_{y_k}(y^p_k)$$

Figure 7: A sketch of the parallel transport of $V_{k-1} \in T_{y_{k-1}}\mathcal{M}$ from y_{k-1} to y_k along y via Schild's ladder. Here, y^c_k is the midpoint of the two diagonals of the geodesic parallogramm, *i.e.* (y^p_{k-1}, y^c_k, y_k) and (y_{k-1}, y^c_k, y^p_k), which are both geodesic curves.

Definition 5.21 (Discrete parallel transport)**.** Let $(y_0, \dots, y_K)$ be a discrete path in $\mathring{\mathcal{M}}$ with $y_k - y_{k-1}$ sufficiently small for $k = 1, \dots, K$ and ζ_0 a sufficiently small displacement of y_0, given as $y^p_0 = y_0 + \zeta_0$. Then the *discrete parallel transport* of ζ_0 along $(y_0, \dots, y_K)$ is defined for $k = 1, \dots, K$ via the iteration

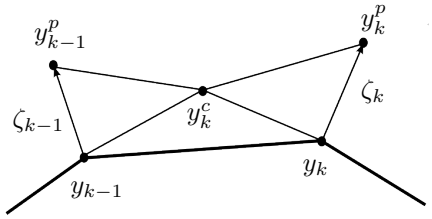

$$y^c_k = y^p_{k-1} + \left((\tfrac{1}{2}\mathrm{LOG})_{y^p_{k-1}}(y_k)\right),$$

$$y^p_k = \mathrm{EXP}^2_{y_{k-1}}\left(y^c_k - y_{k-1}\right),$$

where $\zeta_k = y^p_k - y_k$ is the transported displacement at y_k. We define

$$\mathbf{P}_{y_K,\dots,y_0}(y^p_0 - y_0) = y^p_K - y_K\,.$$

The notation is chosen such that $\mathbf{P}_{y_K,\dots,y_0}\mathbf{P}_{\tilde{y}_K,\dots,\tilde{y}_0} = \mathbf{P}_{y_K,\dots,y_0,\tilde{y}_K,\dots,\tilde{y}_0}$.

In the kth step of the discrete parallel transport the Euler–Lagrange equations to determine y^c_k and $y^p_k = y_k + \zeta_k$ for given $y^p_{k-1} = y_{k-1} + \zeta_{k-1}$ and discrete path $(y_0, \dots, y_K)$ are

$$\begin{aligned}\mathcal{W}_{,2}[y^p_{k-1}, y^c_k](\psi) + \mathcal{W}_{,1}[y^c_k, y_k](\psi) &= 0 \quad \forall \psi \in \mathbf{V}\,,\\ \mathcal{W}_{,2}[y_{k-1}, y^c_k](\psi) + \mathcal{W}_{,1}[y^c_k, y^p_k](\psi) &= 0 \quad \forall \psi \in \mathbf{V}\,.\end{aligned}$$

If $\mathcal{W}$ is symmetric, these conditions are the same as the Euler–Lagrange equations for inverse parallel transport, so that $\mathbf{P}^{-1}_{y_K,\dots,y_0} = \mathbf{P}_{y_0,\dots,y_K}$. However, if $\mathcal{W}$ is not symmetric this is not true in general.

***Convergence analysis of the time-discrete geodesic calculus.** In the remainder of this section we gather important theorems from [RW15], which examine the convergence properties of the discrete geodesic calculus as the time step size $\tau = \frac{1}{K}$ tends to 0.

First, we state that sequences of successively refined discrete geodesic paths converge to a continuous geodesic path. To this end, one considers continuous paths $(y(t))_{t\in[0,1]}$ on $\mathcal{M}$ which are composed of shortest geodesic segments. This means, $(y(t))_{t\in[\frac{k-1}{K},\frac{k}{K}]}$ is a (possibly non-unique) shortest geodesic path connecting $y(\frac{k-1}{K})$ and $y(\frac{k}{K})$ for all $k = 1, \dots, K$. We define an energy $\tilde{E}^K : L^2((0,1);\mathbf{Y}) \to \mathbb{R}$ via

$$\tilde{E}^K[(y(t))_{t\in[0,1]}] = \begin{cases} E^K\left[\left(y(0), y(\frac{1}{K}), \dots, y(\frac{K-1}{K}), y(1)\right)\right], & \text{if } (y(t))_{t\in[0,1]} \text{ is a pw. geodesic path} \\ \infty, & \text{else}\end{cases}.$$

where E^K denotes the discrete path energy in (5.10). Based on these notational preliminaries one obtains the following convergence result:

Theorem 5.22 (Γ-convergence of the discrete energy, [RW15])**.** *Assuming* (H1) *and* (H2)*, the* Γ*-limit of* $\tilde{E}^K$ *for* $K \to \infty$ *in the* $L^2((0,1);\mathbf{Y})$*-topology is* $\mathcal{E}$ *.*

We refer to [DGDM83, Bra02] for an introduction to the concept of Γ-convergence. It is a fundamental implication of the Γ-convergence $\tilde{E}^K \to \mathcal{E}$, that minimizers of $\tilde{E}^K$ converge to minimizers of $\mathcal{E}$, *i.e.* one has actually shown convergence of time-discrete geodesic to continuous geodesics:

Corollary 5.23 (Convergence of discrete geodesics, [RW15])**.** *Under* (H1) *and* (H2)*, any sequence of minimizers of* $\tilde{E}^K$ *contains a* $C^0([0,1];\mathbf{Y})$*-convergent subsequence, and the limit is a minimizer of* $\mathcal{E}$*.*

Taking into account the equivalence of the $\mathbf{V}$ topology and the manifold topology (*cf*. Sec. 5.1), a similar argument can be given for the piecewise linear interpolation of discrete geodesics $(y_0, \dots, y_K)$ instead of piecewise geodesic interpolations.

For convergence of discrete logarithm, exponential map, and parallel transport, the following smoothness hypotheses are required (in addition to (H1) and (H2)):

(H3) The metric g is $C^2(\mathbf{Y}; \mathbf{V}' \otimes \mathbf{V}')$-smooth.

(H4) The energy $\mathcal{W}$ is $C^4(\mathcal{M} \times \mathcal{M}; \mathbb{R})$-smooth with bounded derivatives.

In [RW15] it is shown that under hypotheses (H1) - (H4) one can expect local uniqueness of $(\frac{1}{2}\mathrm{LOG})$ and local existence of (EXP^2). Moreover, Rumpf and Wirth have proven that all time-discrete geometric objects introduced above converge to their continuous counterparts:

Theorem 5.24 (Convergence of discrete logarithm, [RW15])**.** *Given* $y, \tilde{y} \in \mathring{\mathcal{M}}$*, assume that hypotheses* (H1) - (H4) hold, that the continuous and discrete geodesics between $y, \tilde{y}$ are unique, and that the continuous geodesic lies in $\mathring{\mathcal{M}}$. Then $K(\frac{1}{K}\mathrm{LOG})_y \tilde{y} \to \log_y \tilde{y}$ weakly in $\mathbf{V}$ (and thus strongly in $\mathbf{Y}$) as $K \to \infty$.

Theorem 5.25 (Existence and convergence of discrete exponential, [RW15])**.** *Let* $y : [0,1] \to \mathring{\mathcal{M}}$ *be a smooth geodesic. Under the hypotheses* (H1) - (H4), $\mathrm{EXP}^K_{y(0)}(\frac{\dot{y}(0)}{K})$ exists for K large enough, and for $\tau = \frac{1}{K}$ one obtains

$$\left\| \mathrm{EXP}^K_{y(0)}\left(\tfrac{\dot{y}(0)}{K}\right) - y(1) \right\|_{\mathbf{V}} = O(\tau)\,.$$

Theorem 5.26 (Convergence of discrete parallel transport, [RW15])**.** *Let* $y : [0,1] \to \mathcal{M}$ *be a smooth path and* $\zeta : [0,1] \to \mathbf{V}$ *a parallel vector field along* y*. For* $K \in \mathbb{N}$ *and* $\tau = K^{-1}$ *we set* $y_k = y(k\tau)$*,* $k = 0, \dots, K$*. Then under the hypotheses* (H1) - (H4), we have

$$\left\| K\mathbf{P}_{y_K,\dots,y_0}\left(\frac{\zeta(0)}{K}\right) - \zeta(1) \right\|_{\mathbf{V}} = O(\tau)\,.$$

More generally, if the sequence $(y_k)_k$ only satisfies $\|y_k - y(k\tau)\|_{\mathbf{V}} \le \epsilon$, $k = 0, \dots, K$, we still get

$$\left\| K\mathbf{P}_{y_K,\dots,y_0}\left(\frac{\zeta(0)}{K}\right) - \zeta(1) \right\|_{\mathbf{V}} = O(\tau + \epsilon)\,.$$

5.4 *Riemannian splines

For two points $p_0, p_1 \in \mathcal{M}$ a smooth interpolation $y : [0,1] \to \mathcal{M}$ with $y(0) = p_0$ and $y(1) = p_1$ is given by the connecting geodesic path. However, for a sequence $0 = t_1 < t_2 < \ldots < t_J = 1$ and corresponding points $p_1, \ldots, p_J \in \mathcal{M}$, there is in general no geodesic curve $y : [0,1] \to \mathcal{M}$ that fulfills the *interpolation constraints*, *i.e.* $y(t_j) = p_j$ for $j = 1, \ldots, J$. In particular, a curve y satisfying the interpolation constraints does in general not comply with the geodesic equation $\frac{D}{dt}\dot{y} = 0$. For example, a piecewise geodesic curve connecting $p_1, \ldots, p_J$ fulfills $\frac{D}{dt}\dot{y} = 0$ on each segment (t_j, t_{j+1}), $j = 1, \ldots, J-1$, but exhibits discontinuities in $\dot{y}$ at the interpolation points. Nevertheless, if one is interested in a curve that on the one hand satisfies the interpolation constraints *exactly* and on the other hand is *as smooth as possible*, one might consider the geodesic equation as a *penalty term*. This motivation leads to the functional

$$\mathcal{F}[(y(t))_{t\in[0,1]}] = \int_0^1 g_{y(t)}\left(\frac{D}{dt}\dot{y}(t), \frac{D}{dt}\dot{y}(t)\right) \,\mathrm{d}t\,, \tag{5.16}$$

where $\frac{D}{dt}$ denotes the covariant derivative along y as defined by Def. 5.6.

In the finite dimensional Euclidean setting, *i.e.* $\mathcal{M} = \mathbb{R}^d$ and g_p denotes the standard Euclidean product, the covariant derivative of $\dot{y}$ is simply given by the second time derivative $\ddot{y}$, *i.e.* we have

$$\mathcal{F}_{\mathrm{Euc}}[(y(t))_{t\in[0,1]}] = \int_0^1 \|\ddot{y}(t)\|^2 \,\mathrm{d}t\,. \tag{5.17}$$

Consider a discretization of the unit interval $I = [0,1]$ with nodes $I_h = \{0 = z_0 < z_2 < \ldots < z_N = 1\}$. A spline function of degree k on I_h is a function $s \in C^{k-1}(I, \mathbb{R}^d)$ such that s is a polynomial of degree $\leq k$ on each interval $[z_{n-1}, z_n]$, $n = 1, \ldots, N$. The following theorem is often refered to as Schoenberg's theorem although it has been proved first by de Boor[6]:

Theorem 5.27 (de Boor, 1963)**.** *For $0 = t_1 < t_2 < \ldots < t_J = 1$ and $p_1, \ldots, p_J \in \mathbb{R}^d$ there is a unique minimizer $y \in C^2([0,1], \mathbb{R}^d)$ of $\mathcal{F}_{\mathrm{Euc}}$ that satisfies the interpolation constraints $y(t_j) = p_j$ for $j = 1, \ldots, J$ as well as one of the boundary conditions*

$$\begin{aligned}
&\ddot{y}(0) = \ddot{y}(1) = 0\,, && \text{(\textit{natural b.c.})}\\
&\dot{y}(0) = v_0, \quad \dot{y}(1) = v_1 \quad \textit{for given } v_0, v_1 \in \mathbb{R}^d\,, \ \textit{or} && \text{(\textit{Hermite b.c.})}\\
&y(0) = y(1), \quad \dot{y}(0) = \dot{y}(1), \quad \ddot{y}(0) = \ddot{y}(1)\,. && \text{(\textit{periodic b.c.})}
\end{aligned}$$

The minimizer is given by the unique cubic spline, i.e. *a spline of degree 3, satisfying the interpolation constraints and boundary conditions.*

As (5.16) can be seen as a generalization of (5.17) to Riemannian manifolds, we refer to $\mathcal{F}$ as *spline energy* and we denote minimizers of $\mathcal{F}$ as *Riemannian (cubic) splines*.

On general manifolds there may be situations where global minimizers of the spline energy $\mathcal{F}$ do not exist. To ensure well-posedness one can regularize the problem and consider minimizers of the augmented functional $y \mapsto \mathcal{F}[y] + \sigma\mathcal{E}[y]$ with $\sigma > 0$. Here $\mathcal{E}$ denotes the path energy as defined in (5.2). Under certain additional assumptions on $\mathcal{M}$ and g one can then show existence of minimizers of $\mathcal{F} + \sigma\mathcal{E}$ (see [HRS$^+$16, Sec. 9]). Minimizers of a linear combination of path energy and spline energy are often referred to as *splines in tension*, *cf*. *e.g.* [Sch66].

Variational time-discretization. In this section, we derive a consistent time-discretization of the spline energy (5.16) that fits into the framework of time-discrete geodesic calculus presented in Sec. 5.2. As a motivation we start taking a look at the Euclidean setup, *i.e.* $\mathcal{M} = \mathbb{R}^d$. We consider a curve $y : [0,1] \to \mathcal{M}$ and for some stepsize $\tau = K^{-1}$ a uniform sampling $y_k = y(t_k)$ with $t_k = k\tau$ for $k = 0, \ldots, K$. In the following, we focus on the local configuration around some interior point y_k, $0 < k < K$. The continuous spline energy is given by (5.17), *i.e.*

[6] Actually, Schoenberg cites de Boor's paper [dB63] when referring to this result in [Sch64b]. For further reading on this we refer to [Sch73, Sch64a], a simple proof is given *e.g.* in [DH02, 7.4].

the covariant derivative of $\dot{y}$ is simply the second time derivative $\ddot{y}$. Approximating the integrand $\|\ddot{y}(t_k)\|^2$ by a second order finite difference quotient yields

$$\|\ddot{y}(t_k)\|^2 \approx \left\| \frac{2\,y_k - y_{k-1} - y_{k+1}}{\tau^2} \right\|^2 = 4\tau^{-4} \left\| y_k - \frac{y_{k-1} + y_{k+1}}{2} \right\|^2 .$$

The key insight is to interprete the local average $\frac{1}{2}(y_{k-1} + y_{k+1})$ as the midpoint of a geodesic in the Euclidean space connecting y_{k-1} and y_{k+1}, where a geodesic is given by the straight connecting line. Replacing the Euclidean metric by a general Riemannian metric, *i.e.* the squared Euclidean distance $\operatorname{dist}^2_{\text{euc}}(p,q) = \|p-q\|^2$ by the squared Riemannian distance dist^2, and the local average by the midpoint $\tilde{y}_k$ of a short geodesic connecting y_{k-1} and y_{k+1}, one obtains

$$g_{y(t_k)} \left(\frac{D}{dt}\dot{y}(t_k), \frac{D}{dt}\dot{y}(t_k) \right) \approx 4\tau^{-4} \operatorname{dist}^2(y_k, \tilde{y}_k) .$$

If we finally substitute the squared Riemannian distance by the local approximation $\mathcal{W}$, we arrive at

$$g_{y(t_k)} \left(\frac{D}{dt}\dot{y}(t_k), \frac{D}{dt}\dot{y}(t_k) \right) \approx 4\tau^{-4}\, \mathcal{W}[y_k, \tilde{y}_k] , \tag{5.18}$$

$\tilde{y}_k$ is midpoint of the geodesic connecting y_{k-1} and y_{k+1}.

Using the simple numerical quadrature $\int_0^1 f(t)\,\mathrm{d}t \approx \tau \sum_{k=1}^{K-1} f(t_k)$ to integrate (5.18) we arrive at the definition of a *time-discrete spline energy*:

Definition 5.28 (Time-discrete spline energy)**.** For $K \in \mathbb{N}$ let $Y^K = (y_0, \dots, y_K)$ be a discrete K-path in $\mathcal{M}$. We define the time-discrete spline energy by

$$F^K[Y^K] = 4K^3 \sum_{k=1}^{K-1} \mathcal{W}[y_k, \tilde{y}_k] , \tag{5.19}$$

subject to the constraint that $(y_{k-1}, \tilde{y}_k, y_{k+1})$ is a discrete geodesic for $k = 1, \dots, K-1$, *i.e.*

$$\tilde{y}_k = \operatorname*{arg\,min}_{y \in \mathcal{M}} \Big(\mathcal{W}[y_{k-1}, y] + \mathcal{W}[y, y_{k+1}] \Big) , \text{ for } k = 1, \dots, K-1 . \tag{5.20}$$

Boundedness of the discrete spline energy does not necessarily imply boundedness of the discrete path energy in general. Indeed, a discrete geodesic has zero discrete spline energy but positive discrete path energy. As a consequence, minimizing the discrete spline energy might not be a well-posed problem. However, one can consider the functional $F^K + \sigma E^K$ instead. Again, one can show existence of discrete minimizers for every $\sigma > 0$ subject to the interpolation conditions as well as the Γ-convergence of $F^K + \sigma E^K$ to $\mathcal{F}^K + \sigma \mathcal{E}^K$ (*cf.* [**?**]). In what follows, however, we stick to F^K (without adding the path energy) since we never observed numerical instabilities in practice.

Definition 5.29 (Time-discrete spline)**.** For $K \in \mathbb{N}$ let $Y^K = (y_0, \dots, y_K)$ be a discrete K-path in $\mathcal{M}$. Let $0 = i_1 < i_2 < \dots < i_J = K$ be an index set ($J \geq 2$). We say that Y^K is a time-discrete spline interpolating $y_{i_1}, \dots, y_{i_J}$ if it minimizes (5.19) while fixing y_{i_j} for $j = 1, \dots, J$.

If $J = 2$, *i.e.* we only fix y_0 and y_K, the time-discrete spline is precisely the time-discrete geodesic connecting y_0 and y_K.

Boundary conditions. Before proving consistency of the time-discrete spline energy, we will comment on the boundary conditions. In the following, we formulate three types of boundary conditions, analogously to the Euclidean case in Thm. 5.27. Therefore we temporarily consider a generalization of Def. 5.28 by introducing *ghost points* y_{-1} and y_{K+1}, which are supposed to extend the discrete path $(y_0, \dots, y_K)$ in both directions. We derive the boundary conditions in the generalized setting and eventually see that we do not need the ghost points at all, *i.e.* end up with Def. 5.28 again. The generalized time-discrete spline energy is defined by

$$\begin{aligned} \tilde{F}^K[y_0, \dots, y_K] =& F^K[\, y_{-1},\, y_0, \dots, y_K,\, y_{K+1}\,] = 4K^3 \sum_{k=0}^{K} \mathcal{W}[y_k, \tilde{y}_k] , \\ & \text{s.t. } \tilde{y}_k = \operatorname*{arg\,min}_{y \in \mathcal{M}} \Big(\mathcal{W}[y_{k-1}, y] + \mathcal{W}[y, y_{k+1}] \Big) , \text{ for } k = 0, \dots, K . \end{aligned}$$

Different to Def. 5.28 the index in the sum as well as in the constraint equations now runs from $k = 0$ to $k = K$. The constraint equations can be expressed as the following necessary conditions which have to hold for all test functions $\psi \in \mathbf{V}$:

$$\begin{aligned}
[0] \quad 0 &= \partial_2 \mathcal{W}[y_{-1}, \tilde{y}_0](\psi) + \partial_1 \mathcal{W}[\tilde{y}_0, y_1](\psi) \\
[1] \quad 0 &= \partial_2 \mathcal{W}[y_0, \tilde{y}_1](\psi) + \partial_1 \mathcal{W}[\tilde{y}_1, y_2](\psi) \\
&\vdots \\
[K-1] \quad 0 &= \partial_2 \mathcal{W}[y_{K-2}, \tilde{y}_{K-1}](\psi) + \partial_1 \mathcal{W}[\tilde{y}_{K-1}, y_K](\psi) \\
[K] \quad 0 &= \partial_2 \mathcal{W}[y_{K-1}, \tilde{y}_K](\psi) + \partial_1 \mathcal{W}[\tilde{y}_K, y_{K+1}](\psi)
\end{aligned}$$

We distinguish between the following discrete boundary conditions:

- *Natural boundary conditions:* The condition $\ddot{y}(0) = 0$ resp. $\ddot{y}(1) = 0$ is given by enforcing $\tilde{y}_0 := y_0$ resp. $\tilde{y}_K := y_K$, *i.e.* we have $\mathcal{W}[y_0, \tilde{y}_0] = 0$ resp. $\mathcal{W}[y_K, \tilde{y}_K] = 0$. Obviously, the summation in $\tilde{F}^K$ will then run from $k = 1$ to $k = K-1$ again. Furthermore, if we formally define

$$y_{-1} := \mathrm{EXP}^2_{y_1}(y_0 - y_1)\,, \quad y_{K+1} := \mathrm{EXP}^2_{y_{K-1}}(y_K - y_{K-1})\,, \tag{5.21}$$

  condition [0] and [K] are fulfilled by definition, hence we end up with the setting in Def. 5.28.

- *Hermite boundary conditions:* Instead of prescribing first derivatives at $t = 0$ and $t = 1$ we will prescribe y_1 and y_{K-1} (note that y_0 and y_K are always fixed). Again we set $\tilde{y}_0 := y_0$ and $\tilde{y}_K := y_K$ and use (5.21) to get back the setting in Def. 5.28 (fixing at least y_0, y_1 and y_{K-1}, y_K).

- *Periodic boundary conditions:* We set $y_0 = y_K$ to have a closed curve. In order to ensure higher regularity we additionally postulate $y_{K+1} := y_1$ and $y_{-1} := y_{K-1}$. Plugging this into condtion [0] and [K] we see that these two equations coincide, *i.e.* we have $\tilde{y}_K = \tilde{y}_0$. Due to the periodic identification summation runs from $k = 0$ to $k = K-1$ and we end up having K conditions for $\tilde{y}_0, \ldots, \tilde{y}_{K-1}$.

Consistency of the time-discrete spline energy. In this section we prove consistency for the time-discrete spline energy (5.19), which is based on a quantitative consistency error analysis of the approximation in (5.18).
Due to the variational constraint in the definition of F^K, we have to ensure that the objects $\tilde{y}_k$ in (5.20), $k = 1, \ldots, K-1$, are indeed well-defined:

Definition 5.30 (Admissible path)**.** A discrete path $(y_0, \ldots, y_K)$ is admissible, if $\epsilon = 2 \max_k \|y_k - y_{k-1}\|_{\mathbf{V}}$ is small enough, s.t. for each $0 < k < K$ any two points in $B_\epsilon(y_k) = \{y \in \mathcal{M} : \|y - y_k\|_{\mathbf{V}} < \epsilon\}$ can be uniquely connected by a discrete geodesic.

Remark 5.31. Let $y : [0,1] \to \mathcal{M}$ be a curve with $y_k = y(k\tau)$ for $k = 0, \ldots, K$ and $\tau = K^{-1}$. Then we have $\max_k \|y_k - y_{k-1}\| \leq \tau \|\dot{y}\|_\infty$. Hence for any $\epsilon > 0$ there is a $K \in \mathbb{N}$ such that $\max_k \|y_k - y_{k-1}\|_{\mathbf{V}} < \epsilon$. This means that $(y_0, \ldots, y_K)$ is *admissible* if K is large enough.

Furthermore it follows directly from Remark 5.31:

Proposition 5.32. *For $y \in C^1([0,1], \mathcal{M})$, $y_k = y(k\tau)$, $\tau = K^{-1}$ and $K \in \mathbb{N}$ we have*

$$\max_{k=1,\ldots,K} \|y_k - y_{k-1}\|_{\mathbf{V}} = O(\tau)\,.$$

Our main result will be proved at the end of this section:

Theorem 5.33. *We assume* (H1) - (H4) to hold. Let $y : [0,1] \to \mathcal{M}$ be a smooth path with $y_k = y(t_k)$ for $t_k = \tau k$, $\tau = K^{-1}$ and $K \in \mathbb{N}$. We assume that K is large enough such that $(y_0, \ldots, y_K)$ is *admissible* in the sense of Def. 5.30. We define $\tilde{y}_k$ for $k = 1, \ldots, K-1$ such that $(y_{k-1}, \tilde{y}_k, y_{k+1})$ is a discrete geodesic. Then

$$g_{y(t_k)}\Big(\frac{D}{dt}\dot{y}(t_k),\, \frac{D}{dt}\dot{y}(t_k)\Big) = 4K^4\, \mathcal{W}[y_k, \tilde{y}_k] + O(\tau)\,.$$

Using the first order consistency of the numerical quadrature rule $\int_0^1 f(t)\,\mathrm{d}t = \tau \sum_{k=1}^{K-1} f(t_k) + O(\tau)$ then results directly in the consistency of the time-discrete spline energy (5.19):

Theorem 5.34 (Consistency of time-discrete spline energy)**.** *We assume* (H1) - (H4) to hold. Let $y : [0,1] \to \mathcal{M}$ be a path with $y_k = y(t_k)$ for $t_k = \tau k$, $\tau = K^{-1}$ and $K \in \mathbb{N}$. We assume that K is large enough such that $(y_0, \dots, y_K)$ is *admissible* in the sense of Def. 5.30. Then we have for the spline energy $\mathcal{F}$ defined in (5.16) and the discrete spline energy defined in (5.19), respectively:

$$\left| F^K[y_0, \dots, y_K] - \mathcal{F}[(y(t))_{t\in[0,1]}] \right| = O(\tau)\,.$$

Idea of proof: First, one introduces a consistent approximation of the covariant derivative based on the geodesic parallelogram construction shown in Fig. 8. In particular, one shows that the geodesic parallelogram is actually flat, *i.e*. all edge lengths are of order $O(\tau)$, whereas the length of the *short* diagonal connecting y_k and $\hat{y}_k$ is of order $O(\tau^2)$. Afterwards, one proves that the evaluation of the covariant derivative in the metric can be approximated by the (properly scaled) squared distance of y_k and $\hat{y}_k$. Finally, a rather technical calculation reveals that this quantity is proportional to the squared distance of y_k and $\tilde{y}_k$, where the latter is the geodesic midpoint of the geodesic parallelogram. Then the consistency statement in is a direct consequence.

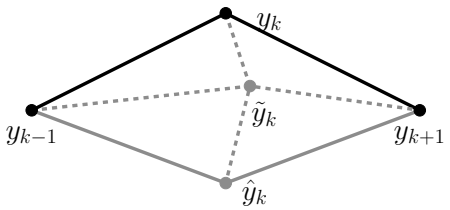

Figure 8: Geodesic parallelogram, *i.e*. $(y_{k-1}, \tilde{y}_k, y_{k+1})$ and $(y_k, \tilde{y}_k, \hat{y}_k)$ are discrete geodesics.

References

[Bal77] John M. Ball. Convexity conditions and existence theorems in nonlinear elasiticity. *Arch. Ration. Mech. Anal.*, 63:337–403, 1977.

[Bär00] Christian Bär. *Elementare Differentialgeometrie*. Walter de Gruyter, 2000.

[Bar15] Sören Bartels. *Numerical Methods for Nonlinear Partial Differential Equations*, volume 47 of *Springer Series in Computational Mathematics*. Springer, 2015.

[BER15] Benjamin Berkels, Alexander Effland, and Martin Rumpf. Time discrete geodesic paths in the space of images. *SIAM J. Imaging Sci.*, 8(3):1457–1488, 2015.

[BKP+10] Mario Botsch, Leif Kobbelt, Mark Pauly, Pierre Alliez, and Bruno Lévy. *Polygon Mesh Processing*. A K Peters, 2010.

[BLZ00] Henning Biermann, Adi Levin, and Denis Zorin. Piecewise smooth subdivision surfaces with normal control. In *Proc. of SIGGRAPH 00*, Annual Conference Series, pages 113–120, 2000.

[BMF03] Robert Bridson, Sebastian Marino, and Ronald Fedkiw. Simulation of clothing with folds and wrinkles. In *Proc. of ACM SIGGRAPH/Eurographics Symposium on Computer Animation*, 2003.

[Bra02] Andrea Braides. Γ-*convergence for beginners*, volume 22 of *Oxford Lecture Series in Mathematics and its Applications*. Oxford University Press, Oxford, 2002.

[Bra07a] Dietrich Braess. *Finite elements*. Cambridge University Press, Cambridge, third edition, 2007. Theory, fast solvers, and applications in elasticity theory, Translated from the German by Larry L. Schumaker.

[Bra07b] Dietrich Braess. *Finite elements*. Cambridge University Press, Cambridge, third edition, 2007. Theory, fast solvers, and applications in elasticity theory, Translated from the German by Larry L. Schumaker.

[BWH+06] Miklos Bergou, Max Wardetzky, David Harmon, Denis Zorin, and Eitan Grinspun. A quadratic bending model for inextensible surfaces. In *Proc. of Eurographics Symposium on Geometry Processing*, 2006.

[Cia88] Philippe G. Ciarlet. *Mathematical elasticity. Vol. I*, volume 20 of *Studies in Mathematics and its Applications*. North-Holland Publishing Co., Amsterdam, 1988. Three-dimensional elasticity.

[Cia00] Philippe G. Ciarlet. *Mathematical elasticity. Vol. III*, volume 29 of *Studies in Mathematics and its Applications*. North-Holland Publishing Co., Amsterdam, 2000. Theory of shells.

[Cia05] Philippe G. Ciarlet. *An Introduction to Differential Geometry with Applications to Elasticity*. Springer, Dordrecht, 2005.

[CL11] Fehmi Cirak and Quan Long. Subdivision shells with exact boundary control and non–manifold geometry. *Internat. J. Numer. Methods Engrg.*, 88(9):897–923, 2011.

[CLR04] Ulrich Clarenz, Nathan Litke, and Martin Rumpf. Axioms and variational problems in surface parameterization. *Comput. Aided Geom. Design*, 21(8):727–749, 2004.

[CM08] Philippe G. Ciarlet and Christinel Mardare. An introduction to shell theory. In *Differential geometry: theory and applications*, volume 9 of *Ser. Contemp. Appl. Math. CAM*, pages 94–184. Higher Ed. Press, Beijing, 2008.

[CO01] Fehmi Cirak and Michael Ortiz. Fully C1–conforming subdivision elements for finite deformation thin–shell analysis. *Internat. J. Numer. Methods Engrg.*, 51(7):813–833, 2001.

[COS00] Fehmi Cirak, Michael Ortiz, and Peter Schröder. Subdivision surfaces: a new paradigm for thin-shell finite–element analysis. *Internat. J. Numer. Methods Engrg.*, 47(12):2039–72, 2000.

[CSA+02] Fehmi Cirak, Michael J. Scott, Erik K. Antonsson, Michael Ortiz, and Peter Schröder. Integrated modeling, finite–element analysis and engineering design for thin–shell structures using subdivision. *Comput.-Aided Des.*, 34(2):137–148, 2002.

[CSM03] David Cohen-Steiner and Jean-Marie Morvan. Restricted Delaunay triangulations and normal cycle. In *Proc. of Symposium on Computational Geometry*, pages 312–321, 2003.

[dB63] Carl de Boor. Best approximation properties of spline functions of odd degree. *J. Math. Mech.*, 12:747–749, 1963.

[dC76] Manfredo P. do Carmo. *Differential geometry of curves and surfaces*. Prentice Hall, 1976. Translated from the Portuguese.

[dC92] Manfredo P. do Carmo. *Riemannian geometry*. Birkhäuser Boston Inc., 1992. Translated from the second Portuguese edition.

[DGDM83] Ennio De Giorgi and Gianni Dal Maso. Γ-convergence and calculus of variations. In *Mathematical theories of optimization (Genova, 1981)*, volume 979 of *Lecture Notes in Math.*, pages 121–143. Springer, Berlin, 1983.

[DGSW08] Mathieu Desbrun, Eitan Grinspun, Peter Schröder, and Max Wardetzky. Discrete differential geometry: An applied introduction. SIGGRAPH Asia 08 Course Notes, 2008.

[DH02] Peter Deuflhard and Andreas Hohmann. *Numerische Mathematik. I.* de Gruyter Lehrbuch. [de Gruyter Textbook]. Walter de Gruyter & Co., Berlin, third edition, 2002. Eine algorithmisch orientierte Einführung. [An algorithmically oriented introduction].

[DHLM05] Mathieu Desbrun, Anil N. Hirani, Melvin Leok, and Jerrold E. Marsden. Discrete exterior calculus, 2005. arXiv:math.DG/0508341 on arxiv.org.

[DKT08] Mathieu Desbrun, Eva Kanso, and Yiying Tong. Discrete differential forms for computational modeling. In *Discrete Differential Geometry*, volume 38 of *Oberwolfach Semin.*, pages 287–324. Birkhäuser, Basel, 2008.

[DMSB99] Mathieu Desbrun, Mark Meyer, Peter Schröder, and Alan Barr. Implicit fairing of irregular meshes using diffusion and curvature flow. In *Proc. of SIGGRAPH 99*, Annual Conference Series, pages 317–324, 1999.

[DSB07] Patrick W. Dondl, Ching-Ping Shen, and Kaushik Bhattacharya. Computational analysis of martensitic thin films using subdivision surfaces. *Internat. J. Numer. Methods Engrg.*, 72(1):72–94, 2007.

[Dzi88] Gerhard Dziuk. Finite elements for the Beltrami operator on arbitrary surfaces. In S. Hildebrandt and R. Leis, editors, *Partial Differential Equations and Calculus of Variations*, volume 1357 of *Lecture Notes in Math.*, pages 142–155. Springer, Berlin, 1988.

[EPS72] Jürgen Ehlers, Felix A. E. Pirani, and Alfred Schild. The geometry of free fall and light propagation. In *General relativity (papers in honour of J. L. Synge)*, pages 63–84. Clarendon Press, Oxford, 1972.

[FJM02a] Gero Friesecke, Richard D. James, and Stefan Müller. Rigorous derivation of nonlinear plate theory and geometric rigidity. *C. R. Math. Acad. Sci. Paris*, 334(2):173–178, 2002.

[FJM02b] Gero Friesecke, Richard D. James, and Stefan Müller. A theorem on geometric rigidity and the derivation of nonlinear plate theory from three-dimensional elasticity. *Comm. Pure Appl. Math.*, 55(11):1461–1506, 2002.

[FJMM03] Gero Friesecke, Richard D. James, Maria Giovanna Mora, and Stefan Müller. Derivation of nonlinear bending theory for shells from three-dimensional nonlinear elasticity by Gamma-convergence. *C. R. Math. Acad. Sci. Paris*, 336(8):697–702, 2003.

[GGRZ06] Eitan Grinspun, Yotam Gingold, Jason Reisman, and Denis Zorin. Computing discrete shape operators on general meshes. *Comput. Graph. Forum*, 25(3):547–556, 2006.

[GHDS03] Eitan Grinspun, Anil N. Hirani, Mathieu Desbrun, and Peter Schröder. Discrete shells. In *Proc. of ACM SIGGRAPH/Eurographics Symposium on Computer animation*, pages 62–67, 2003.

[GKS02] Eitan Grinspun, Petr Krysl, and Peter Schröder. CHARMS: A simple framework for adaptive simulation. *ACM Trans. Graph.*, 21(3):281–290, 2002.

[Hee11] Behrend Heeren. Geodätische im Raum von Schalenformen. diploma thesis, 2011.

[Hee16] Behrend Heeren. *Numerical Methods in Shape Spaces and Optimal Branching Patterns*. PhD thesis, University of Bonn, 2016.

[Hir03] Anil N. Hirani. *Discrete Exterior Calculus*. PhD thesis, California Institute of Technology, 2003.

[HP04] Klaus Hildebrandt and Konrad Polthier. Anisotropic filtering of non-linear surface features. *Comput. Graph. Forum*, 23(3):391–400, 2004.

[HP11] Klaus Hildebrandt and Konrad Polthier. Generalized shape operators on polyhedral surfaces. *Comput. Aided Geom. Design*, 28(5):321–343, 2011.

[HPW06] Klaus Hildebrandt, Konrad Polthier, and Max Wardetzky. On the convergence of metric and geometric properties of polyhedral surfaces. *Geom. Dedicata*, 123:89–112, 2006.

[HRS+14] Behrend Heeren, Martin Rumpf, Peter Schröder, Max Wardetzky, and Benedikt Wirth. Exploring the geometry of the space of shells. *Comput. Graph. Forum*, 33(5):247–256, 2014.

[HRS+16] Behrend Heeren, Martin Rumpf, Peter Schröder, Max Wardetzky, and Benedikt Wirth. Splines in the space of shells. *Comput. Graph. Forum*, 35(5):111–120, 2016.

[HRWW12] Behrend Heeren, Martin Rumpf, Max Wardetzky, and Benedikt Wirth. Time-discrete geodesics in the space of shells. *Comput. Graph. Forum*, 31(5):1755–1764, 2012.

[JMPR16] Bert Jüttler, Angelos Mantzaflaris, Ricardo Perl, and Martin Rumpf. On numerical integration in isogeometric subdivision methods for PDEs on surfaces. *Computer Methods in Applied Mechanics and Engineering*, 302:131–146, 2016.

[Ken84] David G. Kendall. Shape manifolds, Procrustean metrics, and complex projective spaces. *Bull. London Math. Soc.*, 16(2):81–121, 1984.

[KMN00] Arkady Kheyfets, Warner A. Miller, and Gregory A. Newton. Schild's ladder parallel transport procedure for an arbitrary connection. *Internat. J. Theoret. Phys.*, 39(12):2891–2898, 2000.

[Lan95] Serge Lang. *Differential and Riemannian Manifolds*, volume 160 of *Graduate Texts in Mathematics*. Springer-Verlag, New York, third edition, 1995.

[LAP11] Marco Lorenzi, Nicholas Ayache, and Xavier Pennec. Schild's ladder for the parallel transport of deformations in time series of images. In *Proc. of International Conference on Information Processing in Medical Imaging*, volume 6801 of *Lecture Notes in Computer Science*, pages 463–474, 2011.

[LDR95] Hervé Le Dret and Annie Raoult. The nonlinear membrane model as variational limit of nonlinear three-dimensional elasticity. *J. Math. Pures Appl. (9)*, 74(6):549–578, 1995.

[LDR96] Hervé Le Dret and Annie Raoult. The membrane shell model in nonlinear elasticity: a variational asymptotic derivation. *J. Nonlinear Sci.*, 6(1):59–84, 1996.

[LDRS05] Nathan Litke, Mark Droske, Martin Rumpf, and Peter Schröder. An image processing approach to surface matching. In *Proc. of Eurographics Symposium on Geometry Processing*, pages 207–216, 2005.

[MDSB02] Mark Meyer, Mathieu Desbrun, Peter Schröder, and Alan H. Barr. Discrete differential-geometry operators for triangulated 2-manifolds. In *Visualization and Mathematics III*, pages 35–57. Springer Berlin Heidelberg, 2002.

[MH94] Jerrold E. Marsden and Thomas J. R. Hughes. *Mathematical foundations of elasticity*. Dover Publications, Inc., New York, 1994. Corrected reprint of the 1983 original.

[MRSS15] Jan Maas, Martin Rumpf, Carola Schönlieb, and Stefan Simon. A generalized model for optimal transport of images including dissipation and density modulation. *ESAIM Math. Model. Numer. Anal.*, 49(6):1745–1769, 2015.

[Per15] Ricardo Perl. *Isogeometric Approximation of Variational Problems for Shells*. PhD thesis, University of Bonn, 2015.

[PL11] Xavier Pennec and Marco Lorenzi. Which parallel transport for the statistical analysis of longitudinal deformations? In *Proc. of Colloque GRETSI*, September 2011.

[PP93] Ulrich Pinkall and Konrad Polthier. Computing discrete minimal surfaces and their conjugates. *Experimental Mathematics*, 2 (1):15–35, 1993.

[RE55] Ronald Samuel Rivlin and Jerald Laverne Ericksen. Stress-deformation relations for isotropic materials. *J. Rational Mech. Anal.*, 4:323–425, 1955.

[Rei95] Ulrich Reif. A unified approach to subdivision algorithms near extraordinary vertices. *Comput. Aided Geom. Design*, 12(2):153–174, 1995.

[RW13] Martin Rumpf and Benedikt Wirth. Discrete geodesic calculus in shape space and applications in the space of viscous fluidic objects. *SIAM J. Imaging Sci.*, 6(4):2581–2602, 2013.

[RW15] Martin Rumpf and Benedikt Wirth. Variational time discretization of geodesic calculus. *IMA J. Numer. Anal.*, 35(3):1011–1046, 2015.

[Sch64a] Isaac Jacob Schoenberg. On interpolation by spline functions and its minimal properties. In *On Approximation Theory (Proceedings of Conference in Oberwolfach, 1963)*, pages 109–129. Birkhäuser, Basel, 1964.

[Sch64b] Isaac Jacob Schoenberg. Spline interpolation and best quadrature formulae. *Bull. Amer. Math. Soc.*, 70:143–148, 1964.

[Sch66] Daniel G. Schweikert. An interpolation curve using a spline in tension. *J. Math. and Phys.*, 45:312–317, 1966.

[Sch73] Isaac Jacob Schoenberg. *Cardinal spline interpolation*. Society for Industrial and Applied Mathematics, Philadelphia, Pa., 1973. Conference Board of the Mathematical Sciences Regional Conference Series in Applied Mathematics, No. 12.

[Sta99] Jos Stam. Evaluation of Loop subdivision surfaces. SIGGRAPH 99 Course Notes, 1999.

[Sul08] J. M. Sullivan. Curvatures of smooth and discrete surfaces. *Oberwolfach Seminars: Discrete differential geometry*, 38:175–188, 2008.

[SZ00] Peter Schröder and Denis Zorin. Subdivision for modeling and animation. SIGGRAPH 00 Course Notes, 2000.

[Tau95] Gabriel Taubin. A signal processing approach to fair surface design. *Computer Graphics*, pages 351–358, 1995.

[TW06] Bernhard Thomaszewsk and Markus Wacker. Bending models for thin flexible objects. In *Proc. of International Conference on Computer Graphics, Visualization and Computer Vision*, 2006.

[VVP+16] Libor Vása, Petr Vanecek, Martin Prantl, Vera Skorkovská, Petr Martínek, and Ivana Kolingerová. Mesh statistics for robust curvature estimation. *Comput. Graph. Forum*, 35(5), 2016.

[War06] Max Wardetzky. *Discrete Differential Operators on Polyhedral Surfaces - Convergence and Approximation*. PhD thesis, Freie Universität Berlin, 2006.

[War08] Max Wardetzky. Convergence of the cotangent formula: an overview. In *Discrete differential geometry*, volume 38 of *Oberwolfach Semin.*, pages 275–286. Birkhäuser, Basel, 2008.

[WBH+07] Max Wardetzky, Miklós Bergou, David Harmon, Denis Zorin, and Eitan Grinspun. Discrete quadratic curvature energies. *Comput. Aided Geom. Design*, 24(8-9):499–518, 2007.

[WBRS09] Benedikt Wirth, Leah Bar, Martin Rumpf, and Guillermo Sapiro. Geodesics in shape space via variational time discretization. In *Proc. of International Conference on Energy Minimization Methods in Computer Vision and Pattern Recognition*, volume 5681 of *Lecture Notes in Computer Science*, pages 288–302, 2009.

[WBRS11] Benedikt Wirth, Leah Bar, Martin Rumpf, and Guillermo Sapiro. A continuum mechanical approach to geodesics in shape space. *Int. J. Comput. Vis.*, 93(3):293–318, 2011.

[Wir09] Benedikt Wirth. *Variational methods in shape space*. Dissertation, University Bonn, 2009.

[WMKG07] Max Wardetzky, Saurabh Mathur, Felix Kälberer, and Eitan Grinspun. Discrete Laplace operators: No free lunch. *Eurographics Symposium on Geometry Processing*, 2007.